The Pennsylvania State University

The Graduate School

AUTOROTATION PATH PLANNING USING BACKWARDS

REACHABLE SET AND OPTIMAL CONTROL

A Thesis in

Aerospace Engineering

by

Shane Tierney

Submitted in Partial Fulfillment

of the Requirements

for the Degree of

Master of Science

December 2010

The thesis of Shane Tierney was reviewed and approved* by the following:

Jack W. Langelaan
Assistant Professor of Aerospace Engineering
Thesis Advisor

Joseph F. Horn
Associate Professor of Aerospace Engineering

George A. Lesieutre
Professor and Head of Aerospace Engineering

*Signatures are on file in the Graduate School.

Abstract

This paper presents a methodology to compute the backwards reachable set from safe on ground to a trimmed autorotation condition. This backwards reachable set represents the region of the trimmed autorotation state space from which safe paths to touchdown at a specified point are guaranteed to exist. The backwards reachable set is found by computing optimal trajectories from candidate initial states (distance and height above the touchdown point, horizontal speed, descent rate, rotor speed) to the designated touchdown point. In addition, the set of trimmed autorotation conditions which are likely to lead to safe trajectories to ground are computed. As an example, the safe landing set is computed for a generic utility helicopter.

Table of Contents

List of Figures

List of Tables

List of Symbols

Acknowledgments

While I am the author of this thesis, it represents the input and help of a multitude of friends, family, and coworkers. I would first like to thank my parents, who have been the most encouraging, caring, wonderful, self-sacrificing people imaginable for my entire life. Without their support and guidance I would not be anywhere near the quality of person I am today. I would like to thank my brothers for offering support, being able to take a punch, and allowing me to poke around at the insides of their expensive electronics based on the promise that I can "totally fix it." My extended family is also full of amazing, encouraging people and I thank them for their support and encouragement.

My advisor Jack Langelaan is everything I could have possibly hoped for throughout my undergraduate and graduate careers. Jack is one of the most intelligent people I know, but carries no ego. He is able to make even the most complex concepts understandable and does so while treating his students as peers rather than subordinates. Jack is also encouraging and patient, constantly challenging but not overwhelming in his expectations. His guidance has been invaluable in the pursuit of this thesis.

I would like to thank Dr. Joseph Horn for his time and effort in reviewing my thesis. His advice and criticisms were insightful and led to a more informative thesis. I would like to offer him additional thanks for working with me on my constrained time schedule.

My labmates during my graduate student tenure have also been wonderful. Specifically Sean Marlow, Sana Sarfraz, Anjan Chakrabarty, and Nate Depenbusch. All have been wonderful, intelligent, encouraging people the entire time I have worked with them. Each has has helped me on the way to completion of this thesis by helping to debug code, offering advice on solving problems, leading by example (not always successfully but always educationally), and providing much needed stress relief in the form of air cannon wars. I would additionally like to thank the neighboring graduate students in the Rotorcraft Center of Excellence for putting up said air cannon wars.

Dedication

For everyone who has given me help and kindness, so that I may give it give it others.

Chapter 1

Introduction

This thesis describes a method for determining a safe region for an unmanned aerial vehicle(UAV) helicopter during the flare phase of autorotation. The motivation for this work comes from autorotation being an unavoidable, and exceedingly dangerous, risk for rotorcraft, manned or unmanned. Additionally, the flare phase of autorotation occurs so quickly that real-time trajectory planning is not feasible.

Autorotation is the condition a helicopter enters when its engine ceases to provide power to the rotor or rotors. The helicopter enters a descent in which the air flowing upward through the rotor keeps the rotor spinning at level that makes control of the aircraft possible. The spinning rotor also provides some lift, keeping the descent rate within a manageable range for the pilot. Engine failure, entry, descent, and flare are the main pats of autorotation. This thesis focuses on flare and how the helicopter can safely complete this final stage of autorotation. Combined with other controllers that guide entry into autorotation and maneuvers during descent the method described herein for a successful flare maneuver can make autonomous helicopters considerably safer, sparing damage to the helicopter, cargo, or passengers.

Flare, being the final part of autorotation, occurs close to the ground and lasts only a few seconds. In this time, the helicopter must be taken out of a steady descent and brought to an airspeed of as close to zero as possible at the same moment that the helicopter reaches the designated landing zone. This is accomplished by using kinetic energy stored in the rotor to rapidly arrest the descent rate. As a consequence, the rotor slows considerably during flare. Throughout the maneuver

careful control of the main rotor thrust and main rotor tip-path-plane angle are required to bring the helicopter in to a landing while ensuring that the helicopter stays within operable limits while in the air.

This thesis (a)introduces the **Safe Landing Set**, the area of a vehicle's state space which guarantees the possibility of safe flare to landing; (b)describes the problem of performing flare during autorotation and introduces height discretized equations of motion and safe set analysis as a means of performing a safe flare maneuver; (c)presents a method for using optimal path planning as a way of finding the Safe Landing Set and an algorithm for finding the Safe Landing Set itself; and (c)presents computer simulation results verifying the usefulness of this method for finding safe, feasible paths to landing and for finding a set of states for which a safe, feasible path to landing exists.

1.1 Motivation

There is considerable interest in the use of autonomous helicopters for tasks such as reconnaissance, resupply and casualty evacuation. Some manned helicopters also now have the ability to switch to unmanned flight. Further, sensor packages carried by some autonomous rotorcraft (such as the FORESTER radar carried by the A160 Hummingbird) are becoming very complex (and hence expensive). Some of these helicopters are shown in Figure 1.1. Loss of a payload (or worse, a loss of a patient undergoing transport to a medical facility) is thus becoming a critical concern, and safe recovery in the event of vehicle failure is a critical technology. Power loss, in particular, is a vehicle failure which is known to be recoverable through autorotation landing.

However, autorotation is an extremely difficult maneuver and one which often fails because of pilot error. Safety of autorotation continues to be a significant concern to the manned rotorcraft community. The final phase (i.e. flare) of the maneuver is especially difficult, requiring precise control and timing for success, while the consequences of failure include severe damage to the vehicle and injury or death to the pilot or passenger. Practice autorotation thus continues to be a part of the training curriculum for military pilots, but this is a dangerous aspect of training, since a significant number of accidents occur during practice. This

(a) Northrop Grumman Firescout UAV

(b) Lockheed Martin K-MAX Cargo Transport UAV

(c) Being A160 Hummingbird with FORESTER radar

(d) Boeing Littlebird Manned/Unmanned Helicopter

Figure 1.1. Autonomous Helicopters. Image credits: [a]: Northrop Grumman; [b]: Lockheed Martin; [c]:DARPA; [d]:Boeing

is mitigated somewhat in multi-engine aircraft, however unmanned rotorcraft are typically single-engine vehicles.

An automated autorotation system for UAVs, or a cueing system to guide human pilots during autorotation, would greatly reduce the risk of damage or destruction to the aircraft, cargo, and any human pilots or passengers for both manned and unmanned aircraft. It would also reduce the pressure placed on pilots of manned helicopters in case of engine failure. A system of this type would need to successfully enter autorotation, maintain a steady descent, and flare shortly before touchdown. This thesis seeks to solve the problem of producing a safe flare to touchdown maneuver.

1.2 Previous Work

Entry into the descent phase of autorotation and maneuvers during descent are themselves both active areas of research. Research has been presented where optimal path planning is used to find autorotation paths [1–3]. Optimal control has also been used for powered flight maneuver solutions [4] and autorotation pilot cueing [5, 6]. Other methods that have been explored for autorotation solutions are a machine-learning approach by Abbeel at al. [7] and a model-predictive control approach by Dalamagkidis [8].

The Safe Landing Set, mentioned briefly earlier in this chapter, is the backwards reachable set from safe-on-ground: any vehicle which enters the Safe Landing Set is guaranteed to have a safe, feasible path to landing. The use of backwards reachable sets for safe (powered) landing of fixed wing aircraft has been reported [9, 10], but the authors are unaware of backwards reachable set computations for rotorcraft landing (powered or unpowered).

While much progress has been made towards autonomous autorotation, the research and technology are still not to a level where systems can be safely implemented. The flare phase especially is an area that requires more research and experimentation. This is especially true because flare is a very dangerous part of autorotation, taking place close to the ground and having a very small margin for error. In addition, current work does not provide much robustness to wind gusts or steady wind fields, non-flat terrain, or landing at a specific touchdown location. This thesis seeks to deal with this robustness issue.

1.3 Framework for Safe Autorotation

Figure 1.2 shows the whole of the autorotation problem. Typical autorotation follows five steps. First the engine fails. This causes rapid power loss to the main rotor. The pilot must quickly lower the collective pitch input, reducing the angle of attack of the main rotor blades. This enters the helicopter into autorotation, where the air flowing up through the rotor as the helicopter descends spins the rotor. The spinning rotor provides the needed lift for the helicopter to maintain a stable descent. During the steady descent the pilot (or unmanned autopilot) must select

a suitable landing site and direct the helicopter toward it, while still maintaining the integrity of the balance between acceptable descent rate and acceptable main rotor angular speed. During this phase the helicopter may use an estimator along with available sensor data (air data, GPS, Inertial Measurement Unit (IMU), local terrain mapping) and known vehicle dynamics to maintain its steady flight and select a landing location. When the helicopter senses it is near the ground it must initiate flare. During the flare maneuver the cyclic and collective pitch are varied to minimize descent rate and forward speed on the way to the desired touchdown location while ensuring that the helicopter does not pitch excessively and cause a tail strike.

Flare is a very difficult maneuver because of the rapid loss in rotor speed as a result of the increase in collective pitch. Once the energy from the rotor is used to slow the aircraft, it is no longer able to maintain lift. Initiating flare too high leads to a stall and crash, while initiating flare too low does not give sufficient time to correct forward speed, sink rate, or aircraft pitch to safe levels before touchdown and also leads to a crash landing.

'Flare', for the purpose of this thesis, may be thought of as the portion of autorotation descent near the ground and after which the helicopter maneuvers out of trim and the collective pitch (and therefore the thrust and thrust coefficient) increases noticeably. Analysis in later chapters will show this region to be bounded roughly by a height of 500 feet and a distance to touchdown of 800 feet.

Depending on the steady trim condition the helicopter is in when it initiates flare, certain points for flare initiation may or may not allow the helicopter to reach the desired landing site safely. The Safe Landing Set is the paired set of flare initiation points and steady descent conditions from which the helicopter can safely reach the desired landing site.

1.4   The Flare Problem

In [5] Aponso et al. note three important points: first, vehicle parameters such as weight can have a strong influence on the computed trajectory; second, a critical improvement would be the ability to continuously update trajectories to account for performance differences as well as errors in trajectory following; third, optimal
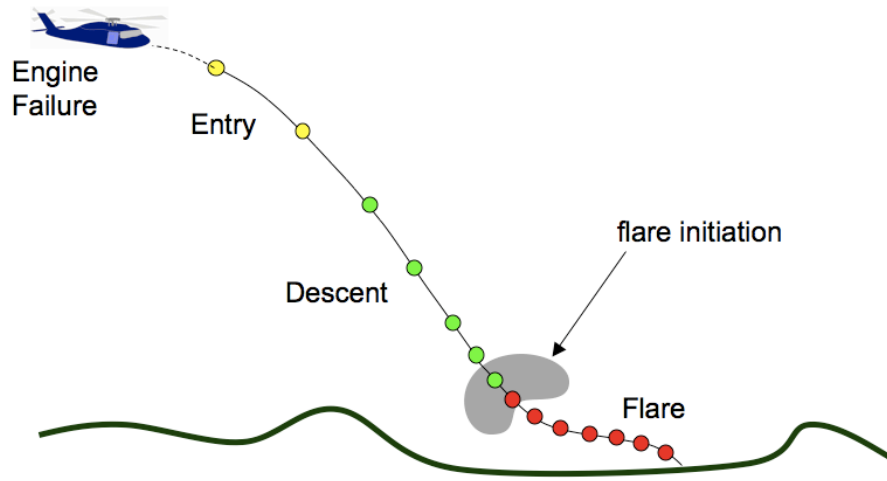
Figure 1.2. Autorotation: engine failure, entry, descent, and flare(beginning with initiation)

trajectory planning can be used to expand the V-h envelope. Further, the previous work on autorotation does not account for disturbances (e.g. gusts, or even steady wind fields) or the effect on non-uniform terrain on autorotation, flare and landing. Thus there is still a need for significant research before the problem of autonomous autorotation can be completely solved. A large amount of that research must be focused on finding a way to safely flare for autorotation touchdown.

Computing a safe, feasible flare trajectory in real time is extremely difficult because of the high dimensionality of the problem, the limited computational resources likely to be available, and the likelihood of external disturbances such as gusts. Moreover, if an incorrect steady descent state is chosen there may not be a safe, feasible flare trajectory to landing.

1.5 Contributions

This section details the contributions of this thesis:

Safe and Probably Safe Sets

The Safe Landing Set and **Probably Safe Set** were created as methods for determining safe flare. These are backwards reachable sets. The Safe Landing Set consists of combined trimmed autorotation conditions and flare initiation points

for which a safe path to touchdown exists. The Probably Safe Set contains only trimmed autorotation conditions for which a path to safe touchdown probably exists (at least one safe flare initiation point exists for that autorotation condition). An algorithm for computing the Safe Landing Set using parameter optimization is developed.

Derivation of Height-Discretized Equations of Motion

The equations of motion for a generic utility helicopter are modified such that height replaces time as the independent variable. These equations create a known end condition for simulation, that being the helicopter touching down.

Trajectory/Parameter Optimization

A trajectory optimization approach is described as a method for solving for a safe path from flare initiation to touchdown. When the height-based equations of motion are introduced, this becomes a parameter optimization approach. This approach uses a two-part cost function, with costs based on the path to touchdown as well as the distance from the desired landing condition.

Autorotation Analysis Using the method described above, flare is analyzed for a generic utility helicopter. Results from this simulation show that certain trimmed autrotation conditions are preferable during descent for a safe flare maneuver. Specifically, conditions with low forward velocity make it easier for the pilot to reach a safe-on-ground condition. Unsafe start conditions are also examined and reasons why these conditions do not lead to safe landing are given.

1.6   Reader's Guide

Chapter Two describes the problem that is solved by this thesis. It also introduces the time-based equations of motion and derives the height based equations of motion. It further describes the Safe and Probably Safe Sets.

Chapter Three describes a method for using trajectory optimization to find safe paths from flare initiation to landing. It also describes the algorithm used to find the Safe Landing Set, which incorporates trajectory optimization.

Chapter Four shows simulation results of the Safe Landing Set finding algorithm presented in Chapter Three.

Chapter Five summarizes results and presents conclusions. It also gives recom-

mendations for future work in this area.

Chapter 2

Flare Problem

The following chapter defines the reachable set problem. The major topics discussed are:

1. Problem Statement: The problem to be solved is presented an outline of the system is discussed.

2. Equations of Motion: Equations of motion described by Aponso are presented. The equations are explained and simplifications made for the flare phase of autorotation are discussed. A similar set of height based equations are proposed and derived.

3. Guaranteed and Probably Safe Sets: The guaranteed and Probably Safe Sets are defined. Optimal path planning is introduced as a method for computing vehicle trajectories.

2.1 Problem Statement

The scenario under consideration is a helicopter entering and proceeding through the flare phase of autorotation to safe-on-ground touchdown. The flare phase begins with flare initiation, a transition from a trimmed autorotation state to the flare maneuver. Flare initiation is characterized by a trimmed autorotation state and a flare initiation point. A trimmed autorotation state includes the helicopter's horizontal and vertical velocities (u and w) and its main rotor angular speed, Ω. The flare initiation point consists of a horizontal distance to and vertical distance above the desired touchdown location. This point is represented by the variables

d and h, respectively. In addition, any residual shaft power from the motor is represented by the variable P_s. Equation (2.1) shows how these values together make up the helicopter's state vector.

$$\mathbf{x} = \begin{bmatrix} u & w & \Omega & d & h & P_s \end{bmatrix}^T \tag{2.1}$$

The desired touchdown location is assumed to be at the origin, (0,0). The desired touchdown state is variable, but generally has low values for both horizontal and vertical velocities (< 5 ft/s) and also includes a desired touchdown vehicle pitch, θ. A schematic of the reachable set problem is given in Figure 2.1.
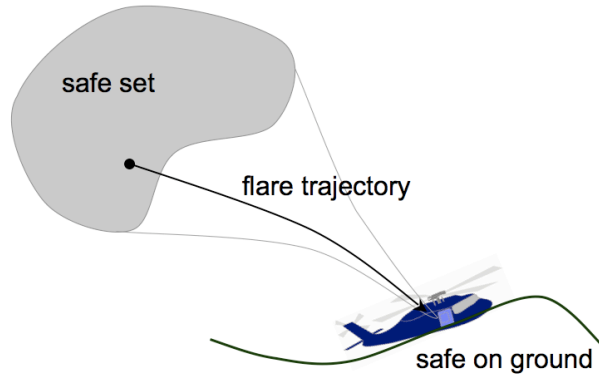
Figure 2.1. Schematic of the guaranteed Safe Set: the set of trimmed autorotation states and initial points that are guaranteed to have a safe, feasible path to landing.

The flare maneuver control inputs are the helicopter thrust coefficient and main rotor tip path plane angle, as seen in equation Equation (2.2).

$$\mathbf{u} = \begin{bmatrix} C_T & \alpha \end{bmatrix}^T \tag{2.2}$$

These are used to influence the main rotor speed, as well as the horizontal and vertical velocities. The velocities, in turn, determine the horizontal and vertical position. Flare ends when the helicopter reaches the ground. The height above touchdown, h, is a relative measure of height. It is defined such that $h = 0$ always indicates touchdown. This means that when $h = 0$, the maneuver has ended.

Thus, the generic trajectory problem is expressed as:

$$\text{minimize } C \tag{2.3}$$

$$\text{subject to } \dot{\mathbf{x}} = f(\mathbf{x}, \mathbf{u}) \tag{2.4}$$

$$g(\mathbf{x}) \leq 0 \tag{2.5}$$

$$\mathbf{x}_{t=0} = \mathbf{x}_0 \tag{2.6}$$

C is some cost function relating to the vehicle's state vectors and landing conditions, $\dot{\mathbf{x}} = f(\mathbf{x}, \mathbf{u})$ are the equations of motion, and $g(\mathbf{x})$ represents state dependent constraints such as structural loads or aircraft performance limits.

2.2 Guaranteed and Probably Safe Sets

A backwards reachable set is a set of start conditions for which a path to a desired end condition exists. In the problem presented here, the Safe Landing Set is a reachable set consisting of all those trimmed autorotation states, $[u \ w \ \Omega]^T$, and flare initiation points, $[h \ d]$, for which a safe path to desired touchdown exists. Along with the trimmed autorotation vehicle state and flare initiation point, the vehicle control inputs throughout the maneuver are also recorded and stored.

The importance of the Safe Landing set is this: if a helicopter is able to enter the Safe Landing Set, it is guaranteed to have a safe, feasible path to the desired touchdown. Thus, a helicopter in the descent phase of autorotation may use the Safe Landing Set as a goal, because once it reaches the Safe Landing Set it is known that the helicopter can reach the desired landing zone safely.

Given the vehicle state

$$\mathbf{x} = \begin{bmatrix} u & w & \Omega & d & h \end{bmatrix}^T \tag{2.7}$$

where $[u \ w \ \Omega]^T$ are taken from the set of all trimmed autorotation conditions

$$\mathcal{A} = \left\{ \mathbf{a}_i | \mathbf{a}_i = [u \ w \ \Omega]^T \right\} \tag{2.8}$$

the *Safe Landing Set* is defined as

$$\mathcal{S} = \left\{ \mathbf{s}_i | \mathbf{s}_i = [d \ t \ u \ w \ \Omega]^T, \ [u \ w \ \Omega]^T \in \mathcal{A} \right\} \tag{2.9}$$

Here $\mathbf{s}_i \in \mathcal{S}$ means that a safe, feasible trajectory to touchdown exists from $\mathbf{s}_i$. Thus any trajectory that guides the helicopter from the moment of engine failure in to $\mathcal{S}$ is guaranteed to end in a safe landing at a particular desired touchdown point.

The set of only vehicle autorotation conditions, $\mathbf{a}_i$, which are likely to result in a safe landing are the Probably Safe Set. The Probably Safe Set is denoted as

$$\tilde{\mathcal{A}} = \{\tilde{\mathbf{a}}_i\} \tag{2.10}$$

This set does not include particular choices of flare initiation position, and thus it cannot guarantee safe landing: a member of $\tilde{\mathcal{A}}$ may have safe paths to landing from some flare initiation points but not others. The set $\tilde{\mathcal{A}}$ is the projection of $\mathcal{S}$ onto $\mathcal{A}$. Any trajectory that guides the helicopter from the moment of engine failure to a point in $\tilde{\mathcal{A}}$ is likely to result in a safe landing somewhere. Note that the touchdown point cannot be specified here: it will be dependent on the particular flare initiation point.

The Probably Safe Set is good for suggesting in which state a helicopter should try to initiate flare.

2.3 Equations of Motion

2.3.1 Time Parameterized Equations of Motion

Aponso [2] describes equations of motion for a helicopter represented by a point mass with a main rotor based on equations presented by Lee, et al. [3] These are repeated without derivation here:

$$\dot{d} = u \tag{2.11}$$

$$\dot{h} = -w \tag{2.12}$$

$$m\dot{u} = \rho(\pi R^2)(\Omega R)^2 C_x - \frac{1}{2}\rho f_e u\sqrt{u^2 + w^2} \tag{2.13}$$

$$m\dot{w} = mg - \rho(\pi R^2)(\Omega R)^2 C_z - \frac{1}{2}\rho f_e w\sqrt{u^2 + w^2} \tag{2.14}$$

$$I_R\Omega\dot{\Omega} = P_s - \frac{1}{\eta}\rho(\pi R^2)(\Omega R)^3 C_P \tag{2.15}$$

$$\dot{P}_s = \frac{1}{\tau_p}(P_{res} - P_s) \tag{2.16}$$

Because the work presented here focuses on the flare phase of the autorotation trajectory, it is assumed that the helicopter has been in autorotation long enough for residual engine power, P_{res}, to decay away. Equation (2.16) then simplifies to the identity $0 = 0$. Also, the helicopter pitch angle, θ, is assumed to be approximately equal to the tip path plane angle, α. Alpha is then used in place of θ in Equation (2.18) - Equation (2.20) and for any constraints on the vehicle pitch at landing.

Coefficients are defined as:

$$C_P = \frac{1}{8}\sigma c_{d_0} + C_T\lambda \tag{2.17}$$

$$C_x = C_T\sin(\alpha) \tag{2.18}$$

$$C_z = C_T\cos(\alpha) \tag{2.19}$$

$$\lambda = \frac{u\sin(\alpha) - w\cos(\alpha) + v}{\Omega R} \tag{2.20}$$

The induced velocity is given as:

$$v = K_{ind}v_h f_I f_G \tag{2.21}$$

where v_h is the reference (hover) induced velocity, f_I is the ratio of actual induced velocity to the reference v_h, and f_G accounts for the decrease in induced velocity due to ground effect:

$$v_h = (\Omega R)\sqrt{\frac{C_T}{2}} \tag{2.22}$$

$$f_I = \begin{cases} 1/\sqrt{b^2 + (a + f_I)^2} & if\,(2a + 3)^2 + b^2 \geq 1 \\ a(.373a^2 + .598b^2 - 1.991) & otherwise \end{cases} \tag{2.23}$$

a and b are given as:

$$a = \frac{u\sin(\alpha) - w\cos(\alpha)}{v_h} \tag{2.24}$$

$$b = \frac{u\cos(\alpha) + w\sin(\alpha)}{v_h} \tag{2.25}$$

$$f_G = 1 - \frac{R^2\cos^2(\theta_W)}{16(h + H_R)} \tag{2.26}$$

$$\cos^2(\theta_w) = \frac{(-wC_T + vC_z)^2}{(-wC_T + vC_z)^2 + (uC_T + vC_x)^2} \tag{2.27}$$

2.3.2   Height Parameterized Equations of Motion

The problem of computing flare trajectories consists of finding the input sequence $\mathbf{u}(t)$ which results in a safe landing without violating operational bounds. One approach is to discretize the problem into finite steps. It is assumed that the input is constant over the interval between these steps. Naturally, this means the intervals must be relatively close together. This discretization will result in a parameter optimization problem. Typically the problem is discretized in time such that $\mathbf{t} = [t_0\ t_1\ t_2 \dots t_k \dots t_{final}]$ is a vector of equally spaced times and the values are known.

For the case considered here, a helicopter in autorotation, the time required to fly a path depends on the inputs. Adjusting C_T or α will change the sink rate. The sink rate together with the starting altitude controls the time to reach the ground. The time of touchdown, t_f, is unknown until it is reached. Due to this, time becomes an additional parameter in the optimization problem. It is therefore more convenient to discretize the problem in height (since the final altitude of the helicopter is specified as $h_f = 0$ regardless of inputs or initial states). In this case inputs are assumed to be constant over an interval Δh (see Figure 2.2).

In Aponso's work the equations of motion are time based. This means that the problem is originally a time discretized problem. Examining these equations, a forward Euler integration can be used to simulate the flight of the helicopter. When comparing the forward Euler method and more computationally expensive but accurate methods, such as a fourth order Runga-Kutta, the forward Euler solution matched the more robust solution for small time steps. The forward
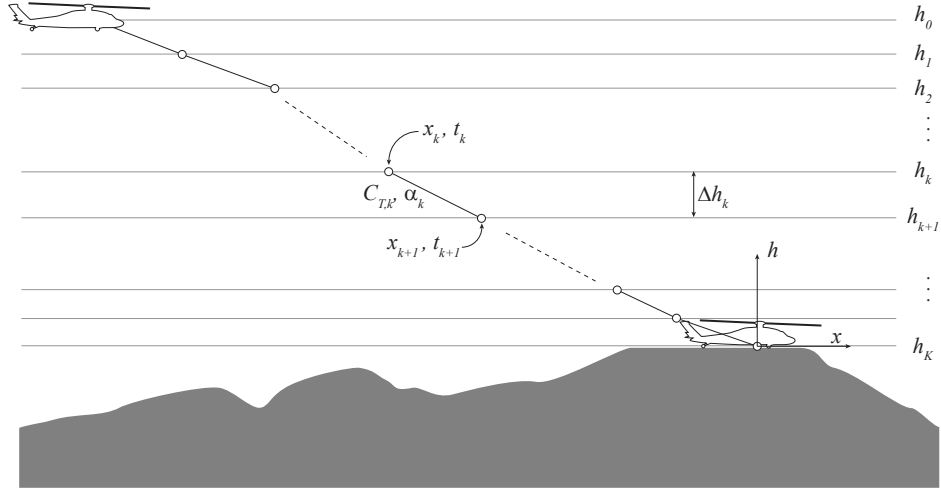
Figure 2.2. Height Discretized Approach to the Equations of Motion

Euler solution also makes it straightforward to re-write the equations of motion in a height discretized form. For these reasons the forward Euler method is used when discretizing the problem.

At time k the state vector, $\mathbf{x}_k$ is assumed to be known. The state derivative, $\dot{\mathbf{x}}_k$, can be calculated from the equations of motion. And the time interval, Δt_k, is selected such that the control input can be assumed constant over each step. Equation (2.28) shows this mathematically.

$$\mathbf{x}_{k+1} = \mathbf{x}_k + \dot{\mathbf{x}}_k \Delta t_k \tag{2.28}$$

In an effort to transition from time-discretized to height-discretized equations of motion the height variable, h, is examined. Δt_k can be found in terms of the altitude interval Δh_k and the descent rate $\dot{h}_k$ over an interval:

$$h_{k+1} = h_k + \dot{h}_k \Delta t_k = h_k + \Delta h_k \tag{2.29}$$

Hence

$$\Delta t_k = \frac{\Delta h_k}{\dot{h}_k} \tag{2.30}$$

Using the equality given in Equation (2.30) the height based values are substituted for the time interval value for all state variables. The system dynamics can now be written as

$$\mathbf{x}_{k+1} = \mathbf{x}_k + \dot{x}_k \frac{\Delta h_k}{\dot{h}_k} \tag{2.31}$$

$$= \mathbf{x}_k + \left(\frac{\dot{\mathbf{x}}_k}{\dot{h}_k}\right) \Delta h_k \tag{2.32}$$

Hence

$$\mathbf{x}_{k+1} = \mathbf{x}_k + \left.\frac{d\mathbf{x}}{dh}\right|_k \Delta h_k \tag{2.33}$$

The discretization is now based on height intervals rather than time intervals. Only the height derivatives remain to be calculated.

Recognizing that $\dot{h}_k = -w_k$ (from vehicle kinematics), because w is positive for downward velocity, and using Aponso's equations of motion, the components of $\left.\frac{d\mathbf{X}}{dh}\right|_k$ are

$$\frac{dd}{dh} = -\frac{u}{w} \tag{2.34}$$

$$\frac{dt}{dh} = -\frac{1}{w} \tag{2.35}$$

$$\frac{du}{dh} = -\frac{1}{mw}\left(\rho(\pi R^2)(\Omega R)^2 C_x - \frac{1}{2}\rho f_e u \sqrt{u^2 + w^2}\right) \tag{2.36}$$

$$\frac{dw}{dh} = -\frac{1}{mw}\left(mg - \rho(\pi R^2)(\Omega R)^2 C_z - \frac{1}{2}\rho f_e w \sqrt{u^2 + w^2}\right) \tag{2.37}$$

$$\frac{d\Omega}{dh} = -\frac{1}{I_R \Omega w}\left(P_s - \frac{1}{\eta}\rho(\pi R^2)(\Omega R)^3 C_P\right) \tag{2.38}$$

The height-index subscript, k, has been dropped for clarity. The height above touchdown is no longer part of the state vector, it has become an independent variable.

Time, conversely, is now a dependent variable. It is assumed that $\Delta t > 0$, which implies $\dot{h} < 0$ and $\Delta h_k < 0$ or $\dot{h} > 0$ and $\Delta h_k > 0$. during autorotation the helicopter is always descending so it must be true that $\dot{h} < 0$ and $\Delta h_k < 0$. Thus

$$\Delta t = \frac{dt}{dh}\Delta h > 0 \tag{2.39}$$

This approach has two implicit assumptions: first, the helicopter is always descending during final approach (i.e. no "swoops"); second, the time interval Δt_k is short enough that changes in descent rate can be ignored.

The state vector is now

$$\mathbf{x} = \begin{bmatrix} u & w & \Omega & d & t \end{bmatrix}^T \tag{2.40}$$

2.4 Summary

Section 2.1 defines the problem. The problem presented is two dimensional control of a helicopter during its flare and landing phases of an autorotation maneuver. Flare is the portion of autorotation where the helicopter makes a series of quick and precise control inputs in order to transfer the helicopter from a steady autorotative descent to the safe on ground condition. The vehicle is modeled as a point mass with a rotor and vehicle state variables are horizontal and vertical distance from touchdown, horizontal and vertical velocity, and main rotor angular speed. Available control inputs are main rotor coefficient of thrust and main rotor tip-path-plane angle. The flare maneuver begins at flare initiation, which is a full vehicle state and accompanying trimmed controls representing steady state autorotation, and ends when the helicopter reaches the ground, $h = 0$

Section 2.2 defines a reachable set and the specific 'Safe Landing Set', $\mathcal{S}$, used in this solution. The backwards reachable set is a set of beginning conditions for which there exists an acceptable path to a desired end condition. The Safe Landing Set is a reachable set consisting of a vehicle state and control setting for which an acceptable path to a desired touchdown condition exists. The vehicle state is comprised of a steady autorotation condition, a distance to touchdown, and time from start of flare. The controls are determined by the autorotation condition, they hold the helicopter in trim. The reachable set is found using optimal path

planning.

Section 2.3 contains a discussion of the equations of motion.

Section 2.3.1 discusses the time-discretized equations of motion. These equations are given by Aponso and modified slightly to fit the specific needs of the flare maneuver. A simplification is the assumption that no residual power exists because the helicopter is in a steady autorotative descent.

Section 2.3.2 derives method with which to transform the time based equations of motion to height based equations of motion. The reason for this: the simulation ends at known height $h = 0$, which occurs at some unknown time. Height based equations of motion eliminate the ambiguity in the model simulation end condition. This transforms the trajectory optimization problem into a parameter optimization problem.

A solution to the reachable set problem presented here is given in Chapter 3. Chapter 4 contains simulation results for application of this method to a generic utility helicopter.

Computing the Safe Landing Set

The following chapter describes how to solve for the Safe Landing Set of an au-
torotating helicopter in the flare phase of flight. The major topics discussed are:

    1. Trajectory Optimization: The parameter optimization problem is briefly
described and its solution is presented.

    2. Safe Set Algorithm: The Safe Landing Set is found by repeatedly solving
the trajectory optimization problem for varied initial conditions.

3.1   Trajectory Optimization

Computing flare trajectories that result in a safe landing is accomplished by al-
tering the control inputs, $\mathbf{u}(t)$. Assuming that the inputs are constant over some
interval leads to a parameter optimization problem. Generally, a time interval is
used for this parameter optimization. In the case presented here time is dependent
on the inputs and becomes an extra, unneeded, parameter. A more elegant solu-
tion is to discretize the problem in height. This is useful because the final height,
h_f is known to be 0 for all cases. The problem is presented as:

$$\text{minimize } C\left(\mathbf{x}_{0...K}, \mathbf{u}_{0...K-1}\right) \tag{3.1}$$

$$\text{subject to } \mathbf{x}_{k+1} = \mathbf{x_k} + \left.\frac{d\mathbf{x}}{dh}\right|_k \Delta h_k \tag{3.2}$$

$$\mathbf{x}_{min} \leq \mathbf{x}_k \leq \mathbf{x}_{max} \tag{3.3}$$

$$g(\mathbf{x}_k) \leq 0 \tag{3.4}$$

$$\mathbf{u}_{min} \leq \mathbf{u}_k \leq \mathbf{u}_{max} \tag{3.5}$$

$$x_0 = [u_0 \ w_0 \ \Omega_0 \ d_0 \ t_0] \tag{3.6}$$

That is, a cost function that depends on the vehicle state and controls at each height step is optimized subject to some constraints. Those constraints are: the vehicle height based equations of motion, state dependent constraints, and vehicle control limits.

The vehicle state constraints simply imply that the vehicle state at height k+1 be determined from the state at height k and the height based equations of motion. State dependent constraints, $g(x)$, include considerations such as structural load limits. The vehicle control limits are selected based on requirements of the vehicle model.

The cost function, $\mathbf{C}(x, u)$, is composed of two parts. These are the touchdown and state costs. The equation for the cost function is:

$$C\left(\mathbf{x}_{0...K}, \mathbf{u}_{0...K-1}\right) = C_{td} + \gamma C_{state} \tag{3.7}$$

where γ is a parameter that can be varied to change the relative weight of the state cost versus the touchdown cost.

3.1.1 State Constraints

State constraints are expressed as a barrier function, shown mathematically in Equation (3.8) and graphically in Figure 3.1.

$$c(x) = \frac{1}{(x - x_{min})^2} + \frac{1}{(x_{max} - x)^2} \tag{3.8}$$

The variables introduced here, x_{min} and x_{max}, are constraints on the minimum and maximum vehicle states, respectively. These limits are given in table Table (3.1)

A state cost is calculated at each point during the path to landing, and the sum
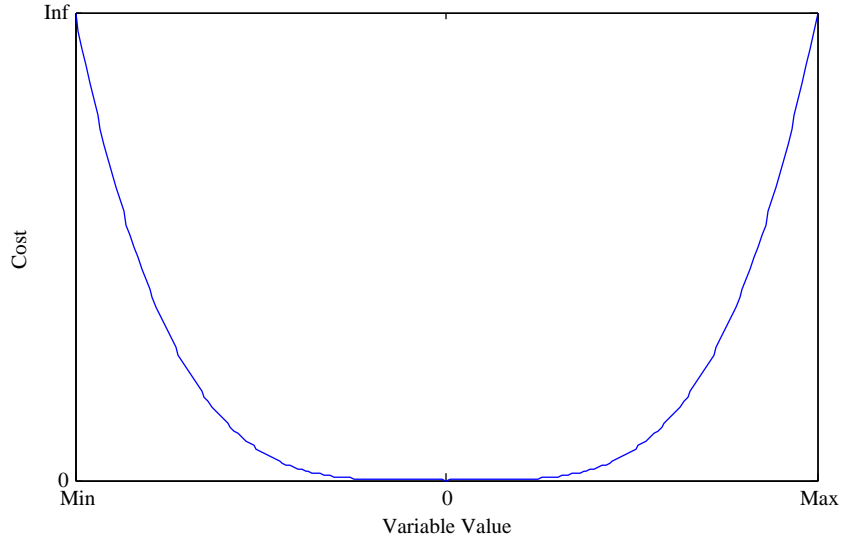
Figure 3.1. An Example Barrier Function: costs rise rapidly as states approach their boundaries

Table 3.1. Touchdown safe conditions. $\theta_{terrain}$ is the terrain slope at the touchdown point ($0°$ here).

state	upper	lower
forward speed	+25 ft/s	-3 ft/s
descent rate	+10 ft/s	-3 ft/s
rotor speed	–	–
x position	+25 ft	-25ft
time	–	–
aircraft pitch angle	$\theta_{terrain} + 10°$	$\theta_{terrain} - 10°$

of these costs is the total state cost (see Equation (3.9)). Hence the total state cost is the sum of the costs of state violations at each height step. Representing the state cost function as a barrier function turns the problem into an interior-point problem.

$$C_{state} = \sum_{k=1}^{K} c(\mathbf{x}_k) \tag{3.9}$$

At altitudes below $50 ft$ the helicopter is assumed to be very close to landing. During this period, the constraint on rotor speed is dropped. The constraint exists

mainly to ensure the helicopter maintains sufficient rotor speed to provide lift. Below 50 ft this is of little concern, the helicopter will touch down before a drop in rotor speed can appreciably degrade the lift.

3.1.2 Touchdown Cost

The touchdown cost, $\mathbf{C}_{td}$ is defined as:

$$C_{td} = \left(\begin{bmatrix} \mathbf{x}_K \\ \mathbf{u}_k \end{bmatrix} - \begin{bmatrix} \mathbf{x}_{des} \\ \mathbf{u}_{des} \end{bmatrix} \right)^T \mathbf{W}_{td} \left(\begin{bmatrix} \mathbf{x}_K \\ \mathbf{u}_k \end{bmatrix} - \begin{bmatrix} \mathbf{x}_{des} \\ \mathbf{u}_{des} \end{bmatrix} \right) \tag{3.10}$$

Here, $\begin{bmatrix} \mathbf{x}_K \\ \mathbf{u}_k \end{bmatrix}$ concatenates the state and control vectors at time k. $\begin{bmatrix} \mathbf{x}_{des} \\ \mathbf{u}_{des} \end{bmatrix}$ is the desired landing condition. $\mathbf{W}_{td}$ is the touchdown weight matrix, given in Equation (3.11).

$$\mathbf{W}_{td} = \mathrm{diag}\left(W_u,\ W_w,\ 0,\ W_d,\ 0,\ 0,\ W_\alpha\right) \tag{3.11}$$

Setting the weights related to time, rotor speed, and thrust coefficient to zero in the touchdown weight matrix implies that the values of these parameters at touchdown are unimportant. Touchdown cost is determined only by the proximity to the desired landing zone, horizontal and vertical speeds at touchdown and the helicopter pitch angle at touchdown.

3.1.3 Gradient Based Optimizer

A gradient descent approach is used to iteratively solve this optimization problem for a particular initial state. The MATLAB function fmincon, which finds the minimum of a constrained nonlinear multivariable function, is used for the gradient based approach. The gradient based approach means that the solution which is found is a local minimum. This solution may or may not be the absolute minimum cost, but so long as the solution satisfies the 'safe' conditions a local minima is acceptable. The solution depends heavily on the initial guess of the control

sequence. This is because a poor initial guess could "trap" the optimizer in an unsuitable local minimum which does not produce a safe solution.

All control inputs are splines based off of a seven-point input, regardless of initial height. Obviously then, initial guesses for the controls, **u** are a spline (Figure 3.2). For the initial guess the thrust coefficient is brought from its trim condition to its maximum and the tip path plane transitions from trim to a high negative value, then down to the terrain angle at touchdown. Construction of the spline may cause the controls to exceed allowed values, even when the seven points the spline is based on do not. To combat this, if the control inputs exceed maximum bounds, the controls are limited to their maximum/minimum values.
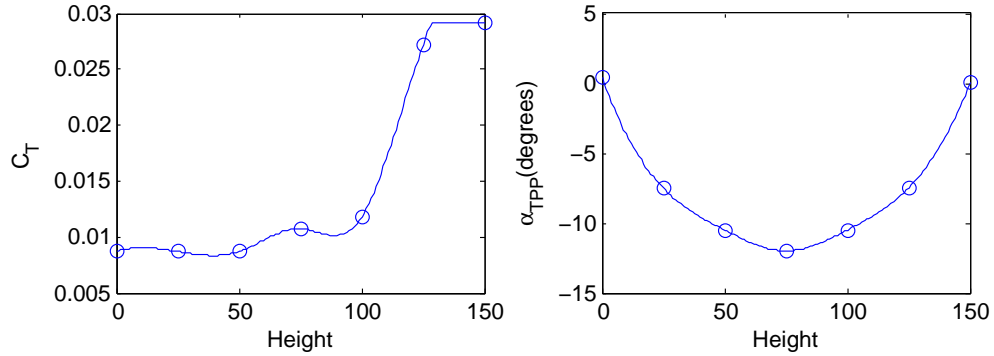
Figure 3.2. Control Spline Initial Guess

If another initial state has already found a solution at an identical or nearby initial position, that solution is used as an initial guess for the new start condition instead of the spline described in the previous paragraph.

The optimization problem can now be described more specifically as:

$$\text{minimize } C_{td} + \gamma C_{state} \tag{3.12}$$

$$\text{subject to } \mathbf{x}_{k+1} = \mathbf{x_k} + \left.\frac{d\mathbf{x}}{dh}\right|_k \Delta h_k \tag{3.13}$$

$$\mathbf{x}_{min} \leq \mathbf{x}_k \leq \mathbf{x}_{max} \tag{3.14}$$

$$g(\mathbf{x}_k) \leq 0 \tag{3.15}$$

$$\mathbf{u}_{min} \leq \mathbf{u}_k \leq \mathbf{u}_{max} \tag{3.16}$$

$$\mathbf{u}_k = spline\,(U) \tag{3.17}$$

$$x_0 = [u_0 \ w_0 \ \Omega_0 \ d_0 \ t_0] \tag{3.18}$$

To find a solution, the first iteration of the gradient approach uses a large value of γ to ensure that a path which does not violate state constraints is found. If a path is found then γ is reduced and the optimization is run again using the previous solution as the initial guess. This is repeated until a path which is both feasible and safe (meaning that touchdown constraints are satisfied) is found. Additionally, if the first iteration finds a solution which touches down successfully but violates state constraints, the value of γ can be raised until a suitable solution is found. Thus the question of the existence of a feasible path has been expressed as an optimization problem: if the optimal path is not feasible, then a feasible path does not exist. An example of this approach is presented in Figure 3.3

3.2 Safe Set Algorithm

The success of the flare maneuver is determined by two components. First, the vehicle state and controls are examined as the helicopter moves towards the ground. If at any point the vehicle states or controls violate constraints, the maneuver is considered a failure. The constraints are set according recommended vehicle state and control limits. Second, the helicopter's final vehicle state at touchdown is examined. If any part of the vehicle state is out of allowable constraints, including the touchdown velocities, the aircraft pitch angle, or if the helicopter does not touch down close enough to the desired landing zone, the maneuver is considered a failure. If the helicopter stays within allowable bounds throughout the maneuver and lands within the desired landing zone with acceptable states at touchdown, the maneuver is considered a success.

Optimal path planning is used to determine the path to ground. The path planner minimizes a cost function, C, which is a function of vehicle states and controls. Constraints on the optimization are the constraints on the allowable control inputs for the helicopter.

The guaranteed safe landing set is found by repeatedly solving the trajectory optimization problem defined in previous section of this chapter for candidate
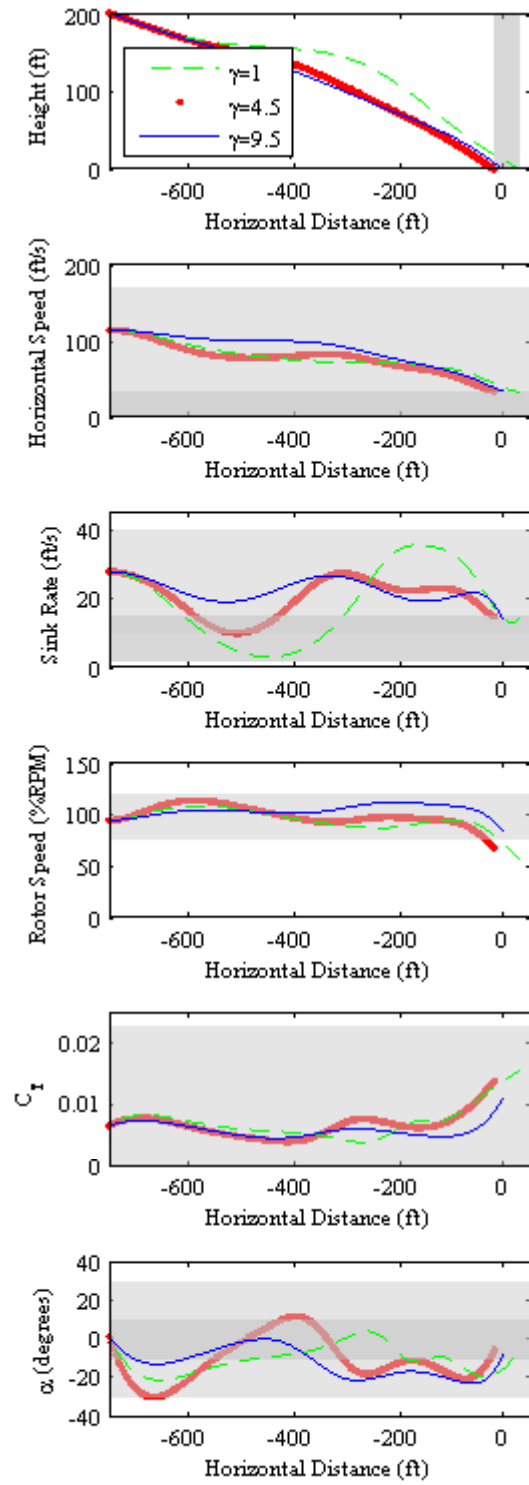
Figure 3.3. Example of γ adjustment to find a safe solution

initial states

$$\hat{\mathbf{s}}_i = \begin{bmatrix} x_{ip} & z_{ip} & \mathbf{a}_i^T \end{bmatrix}^T, \ \mathbf{a}_i \in \mathcal{A} \tag{3.19}$$

Figure 3.4 shows the trim set $\mathcal{A}$ for a generic utility helicopter with parameters given in Table 3.2.
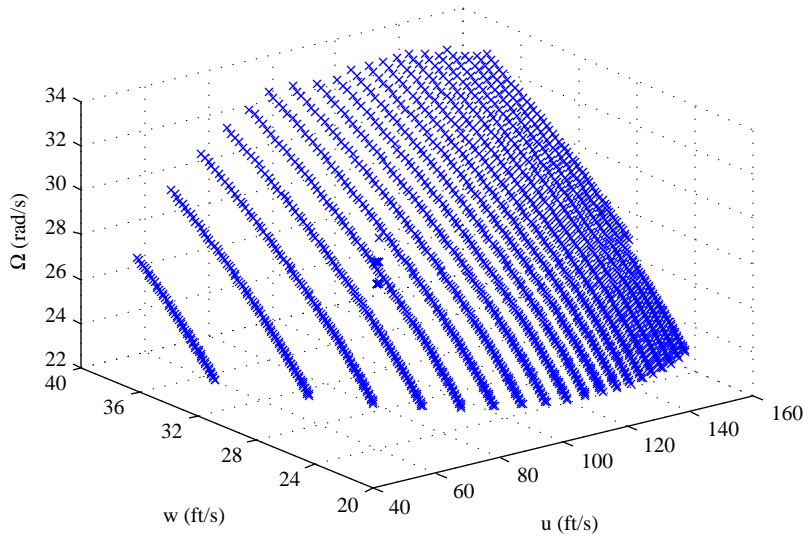
Figure 3.4. Autorotation trim states for a generic utility helicopter.

Table 3.2. Parameters for generic utility helicopter

parameter	symbol	value
blade cord	c	1.75 feet
rotor profile drag coefficient	C_{d0}	0.01
equivalent flat plate area	f_e	27.58 feet^2
rotor height	H_r	9.417 feet
main rotor polar moment of inertia	I_R	1512.6 feet^4
induced power factor	K_{ind}	1.05
number of blades	N_B	4
rotor diameter	R	26.83 feet
gross weight	W	16638 lbs
power efficiency factor	η	0.97
air density	ρ	2.134×10^{-3} slugs/foot^3

To find $\mathcal{S}$, a candidate state $\hat{\mathbf{s}}$ is selected and the feasibility of a safe trajectory to touchdown is computed. If a safe (landing is within acceptable limits),

feasible (vehicle state remains within acceptable limits throughout the maneuver) trajectory exists then $\hat{\mathbf{s}} \in \mathcal{S}$. The procedure is summarized in Algorithm 1.

Algorithm 1 Compute safe landing set.

1: $\mathcal{S} = \emptyset$, $\tilde{\mathcal{A}} = \emptyset$
2: Select candidate $\hat{\mathbf{s}}_i = \begin{bmatrix} x_{ip} & z_{ip} & \mathbf{a}_i^T \end{bmatrix}^T$
3: Compute optimal trajectory from $\hat{\mathbf{s}}_i$ to goal
4: **if** trajectory is feasible and safe **then**
5:     $\mathcal{S} = [\mathcal{S} \ \hat{\mathbf{s}}_i]$
6:     $\mathcal{A} = [\mathcal{A} \ \hat{\mathbf{a}}_i]$
7: **else if** Trajectory is feasible but not safe **then**
8:     reduce γ
9:     go to 3
10: **else if** Trajectory is safe but not feasible **then**
11:     increase γ
12:     go to 3
13: **else**
14:     discard $\hat{\mathbf{s}}$
15: **end if**
16: **if** No more candidate states **then**
17:     Return $\mathcal{S}$, $\tilde{\mathcal{A}}$
18: **else**
19:     go to 2
20: **end if**

3.3   Summary

The first section in this chapter, 3.1, describes the parameter optimization approach used to solve for safe trajectories to touchdown. The parameter optimization problem works my minimizing a cost function, C. C consists of two parts: a state cost, C_{state}, and touchdown cost, C_{td}.

Section 3.1.1 describes the state constraints. These constraints are presented as a barrier function. Costs from these functions at each discretized step are summed to find the total cost for state violation. Writing the state cost in this way leads to the cost function becoming an interior-point problem.

Section 3.1.2 gives the touchdown cost. The touchdown cost is a quadratic cost function depending on touchdown location, touchdown velocities, and helicopter

pitch angle. Rotor speed, time to touchdown, and thrust coefficient at touchdown are unimportant. This is reflected in the cost function by weights of zero for these variables in the touchdown weight matrix.

Section 3.1.3 describes the gradient based approach used to solve for optimal trajectories. The MATLAB function fmincon is used. this function finds a local minimum of the cost function. The gradient based approach is highly dependent on initial guess values. the gradient based approach is also somewhat self correcting, having a value γ which adjusts the weight of the step cost relative to the touchdown cost.

Section 3.2 describes the algorithm for calculating the safe landing set. The Safe Landing Set is a reachable set consisting of steady autorotation conditions and flare initiation points. Together these form safe states for the helicopter. To find the Safe Landing Set, steady autorotation conditions are tested at multiple flare initiation points. Using the parameter optimization described in section 3.1 a solution to touchdown is found. Safe solutions are added to the Safe Landing Set. Solutions that satisfy only limits on the vehicle states while in flight or only landing constraints have a weight on the two parts of the cost function adjusted until a solution is found, or until it is determined that no overall solution exists. Once all trim conditions have been tried with all flare initiation points, the Safe Landing Set construction is complete. The Safe Landing Set can be divided into the Probably Safe Set and the set of safe flare initiation points.

Chapter 4 contains simulation results for a generic utility helicopter using the solution method presented in this chapter.

Chapter 4

Simulation Results

The following chapter presents results of combined safe set and parameter optimization simulations.

1. Simulation approach: The algorithm for finding the Safe Landing Set is briefly discussed

2. Flight Path Examples: Flight paths from some sample initial states to safe on ground are examined. Flight paths from initial states near, but not in the safe set are also shown, with explanation for their exclusion.

3. Safe Set Visualization: Various visualizations of the Safe Landing Set, including the Probably Safe Set and safe flare initiation points are presented

4.1   Simulation Approach

The algorithm for finding the Safe Landing Set was described in Chapter 3. Briefly, a number of points in space, the flare initiation points, are combined with a number of safe trimmed autorotations consisting of forward velocity, sink rate, and main rotor angular velocity. These form the set of possible safe states. Each of these states is tested using a parameter optimization approach to see if a safe path to landing exists. The process is made somewhat faster by having the initial guess for control inputs be the control inputs for the nearest safe state. The collection of states for which a safe, feasible path to landing exists is the Safe Landing Set.

The optimizer used was the function *fmincon*, a MATLAB function which finds the minimum of a constrained nonlinear multivariable function. The function was

set up such that the variable it attempted to optimize was the control input vector **u**. **u** was optimized over the path to the ground. Limits on thrust coefficient are $1.5C_w$(upper) and 1e-5 (lower). Ideally the lower bound would be zero, however intricacies of the function required a very small, but positive, lower bound. Limits on tip-path-plane angle are $+30°$(upper) and $-30°$(lower). These values are somewhat arbitrary but are chosen to be near, but not exceeding, acceptable operational limits. The function has a maximum of 20 iterations to find a minimum value. If a minimum is not found in this time the function exits and flags the optimization as unsuccessful. However, the solution is still checked to see if it provides a safe path to touchdown. While the path may not be optimal, it may still be safe and feasible.

4.1.1   Flare Location

Chapter 1 described the bounds on where flare should exist. Flare occurs near to the ground and involves the helicopter maneuvering away from a trim condition. Collective pitch also increases noticeably. A maximum height of h=500 ft was chosen. Above this height, the helicopter far exceeds what may be considered the final portion of autorotation. Flight to the ground from this height will take at minimum 12 seconds with the maximum allowed descent rate of 40 ft/s.

As described in previous chapters, flare involves the helicopter increasing its collective pitch, and in doing so increasing its thrust and thrust coefficient. This slows the rotor due to increased drag and also arrests the descent rate. Effectively the helicopter is using energy stored in its rotor to slows itself. It is then able to be concluded that flare is a maneuver which generally benefits involves a high rotor speed.

Figures Figure 4.1, Figure 4.2, and Figure 4.3 show the relative safety of total velocity and rotor speed combinations for overlapping regions of flare initiation points. The closer to dark red (and consequently farther from blue) a point is, the greater the number of safe flare initiation points that exist for that state. All three figures have a maximum h of 500 ft. Figure 4.1 considers points between 0 and 800 feet from the horizontal landing location. Figure 4.2 has points between 550 and 1200 feet away and Figure 4.3 contains points between 800 and 2200 feet.

2200 feet is roughly the distance from the landing zone where safe points cease to exist below h=500 ft. As the start location is moved away from the landing zone horizontally a shift from high rotor speed to low rotor speed and moderately high airspeed becomes evident.
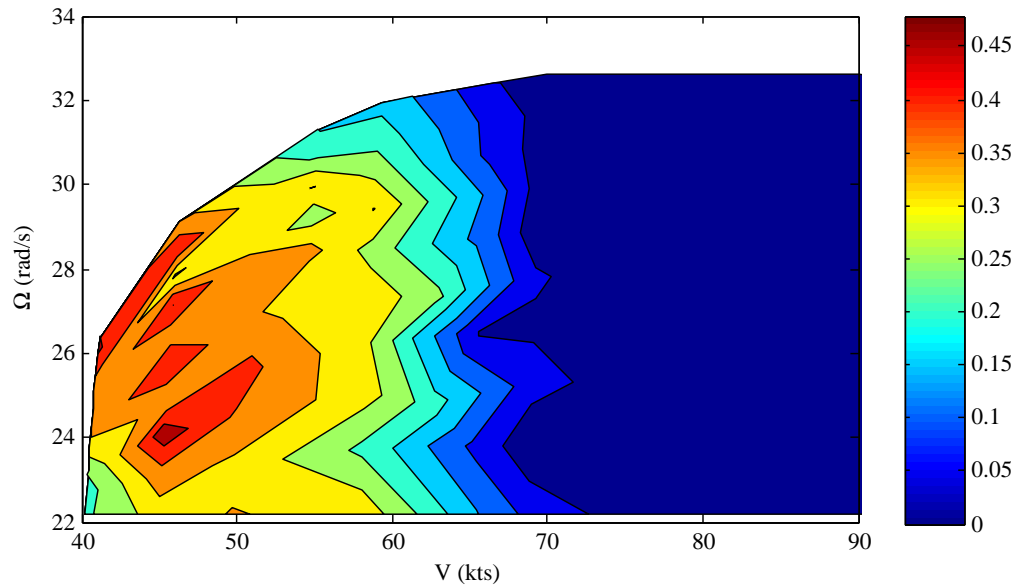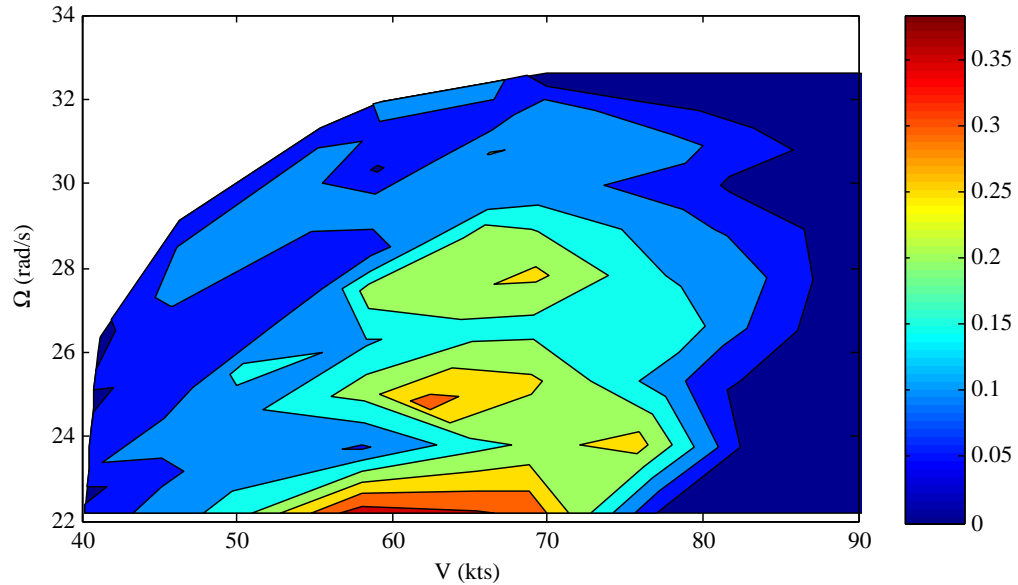

Figure 4.1. Close start results

Figure 4.4 gives insight into why this is the case. In this figure the helicopter attempts to reach the landing zone from the point (-850,350) at a low speed but high rotor speed condition. The helicopter initially decreases thrust. This increases rotor speed and decreases descent rate. The helicopter maintains this sort of maneuver until approximately 250 feet from the touchdown location. Closer than this the helicopter performs a familiar flare: a general increase in C_T which causes Ω and w to fall. Between -850 and 250 feet to touchdown the helicopter does not try to flare, but rather attempts to sprint into an area where it can flare. At these far away distances, low rotor speed is an advantage. Low initial rotor speed means the helicopter has room to increase its rotor speed and briefly slow the descent rate while the helicopter quickly flies to a closer point. Assuming the helicopter can reach the actual flare location before drag slows the rotor significantly,the helicopter is then able to use its rotor speed to manage a flare maneuver.

This maneuver, while a part of autorotation, is outside the scope of what is
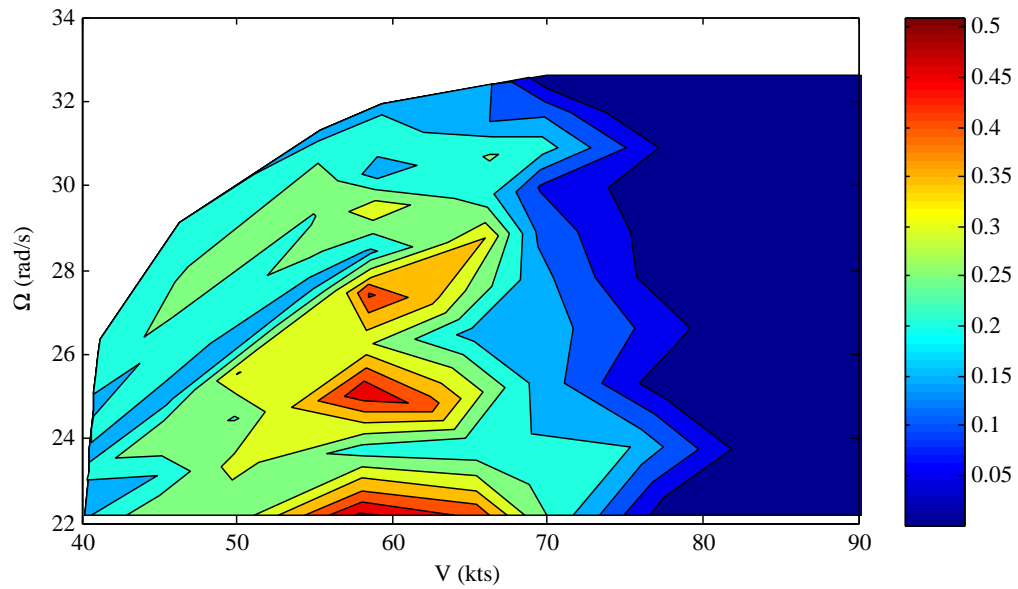
Figure 4.2. Midrange start results

Figure 4.3. long distance start results

classically considered flare. Considering points only behind approximately 800 feet from the landing zone leads to analysis of the sprint maneuver, which is outside the bounds of this thesis. Considering points both close and farther than 800 ft
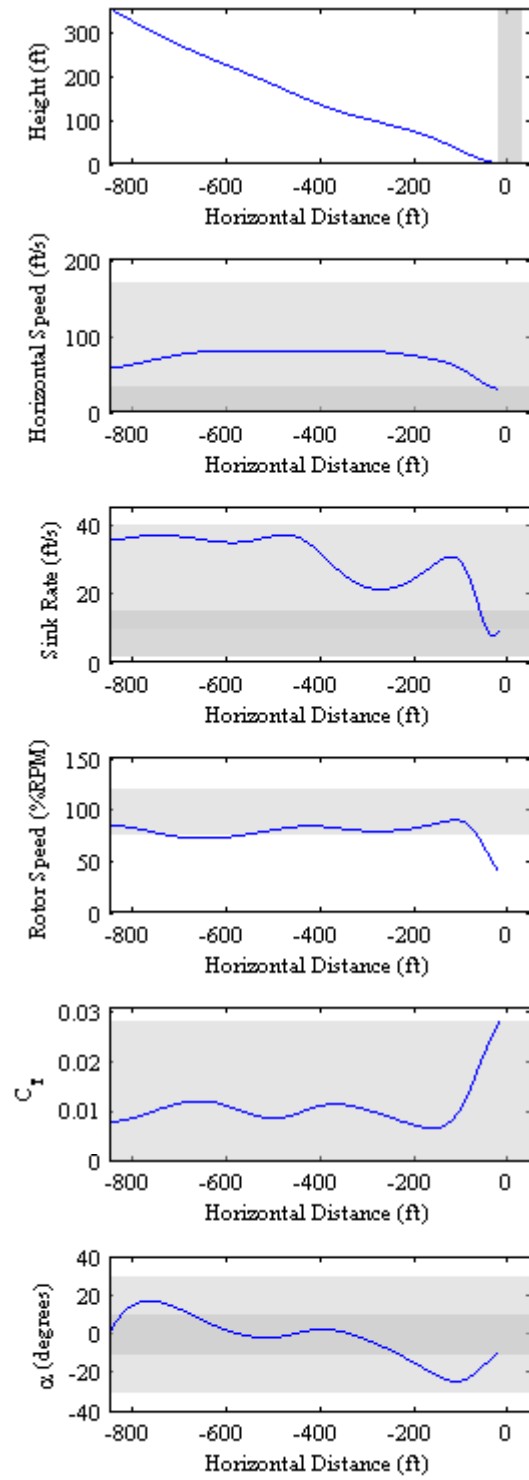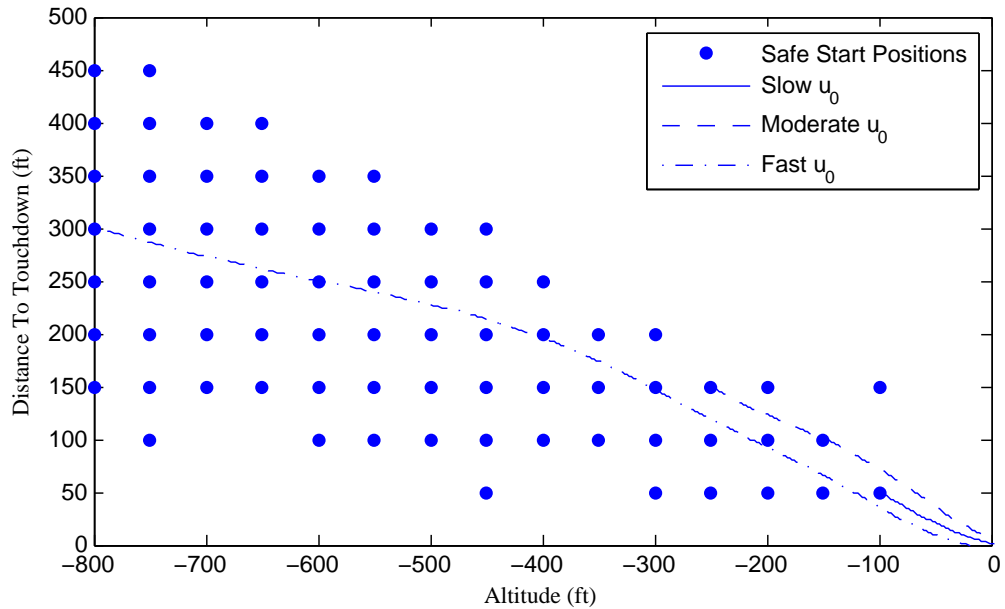
Figure 4.4. Sample Flight Paths

from the landing zone creates a mix of maneuvers whose analysis yields no insight into flare. As such the search for safe flare locations was stopped at d=-800 ft.

4.2   Flight Path Examples

4.2.1   Safe Flight Paths

For the Safe Landing Set findings to be valid, it must first be proven that the path optimization produces safe, feasible flight paths. Figure 4.5 shows flight paths for some initial states which have safe paths to landing. More detailed views that show state and control histories for these example paths are shown in Figure 4.6, Figure 4.7, and Figure 4.8. These states differ mostly in initial velocity and starting position.

Figure 4.5. Sample Flight Paths

In this first example, the helicopter begins flare very close to its goal location, and very low to the ground. It also starts with a low forward speed, but a high descent rate, and slightly below nominal rotor RPM. The tip path plane angle shows the helicopter tilts back a mild amount to gently slow the helicopter. Then just before touchdown the helicopter tips back sharply to slow itself to an accept-
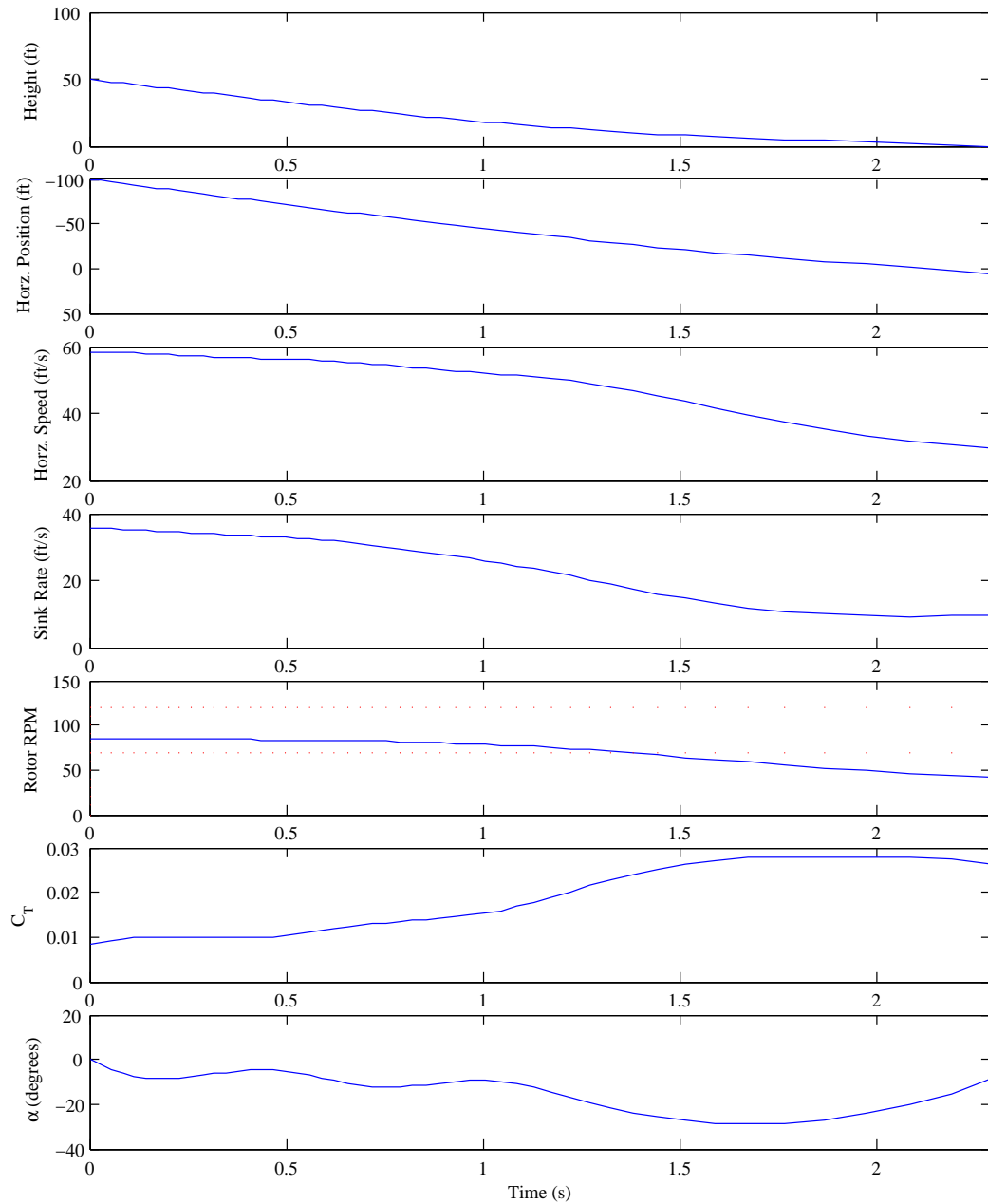
Figure 4.6. State History: Slow Initial Speed

able velocity before returning to an acceptable orientation for landing. The thrust coefficient remains low at first to bring the helicopter to the ground before it overshoots the landing site, then increases to its maximum value, quickly reducing the descent rate to an allowable value for landing. The rotor RPM dips due to the high

C_T drawing energy from the rotor to reduce the descent rate. It is worth noting that this maneuver occurs in just over 2 seconds and over a hight of only 50 feet, displaying just how intricate an optimal flare maneuver is.
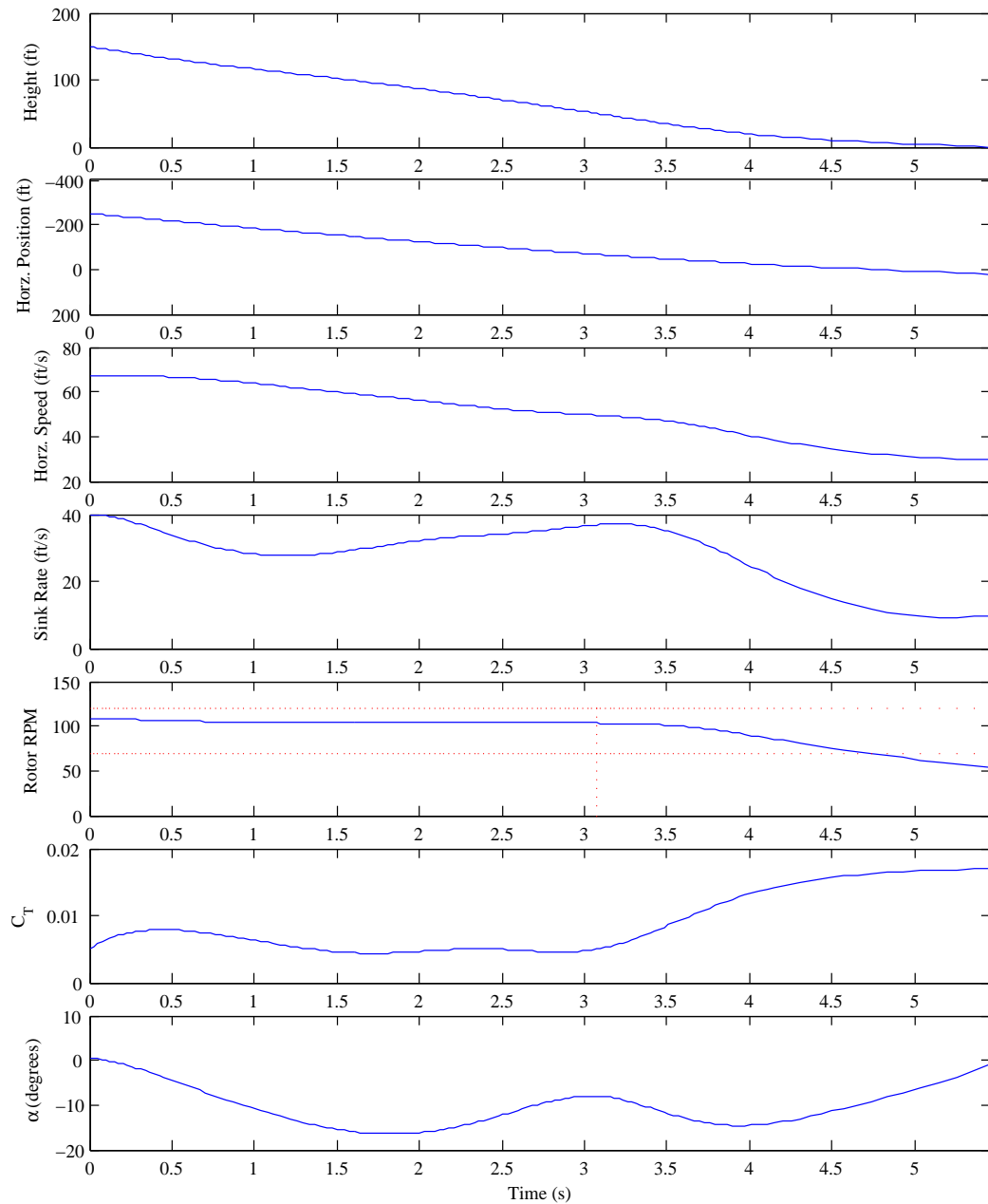
Figure 4.7. State History: Moderate Initial Speed

The second example shows a helicopter starting with a faster forward speed and

sink rate, at a higher altitude and farther from the desired landing site. The rotor is above nominal speed. The main concern during this maneuver is controlling the descent rate. The controls show this. The thrust coefficient behaves similarly to the previous example, but does not spend such a large portion of the maneuver at the maximum value. This is probably because the tip-path-plane angle maintains a more shallow tilt in this example. This means the thrust vector is directed more towards a vertical orientation, so more power goes to slowing descent. The higher initial height means that the maneuver takes longer than the first example. But the time frame is still very short, a little more than 5 seconds.

The final example presented here is a helicopter with a fast initial horizontal speed, lower sink rate than the previous examples, an under sped rotor that begins flare at a higher altitude far from the touchdown location. In this case the high forward speed is not a hindrance, but an advantage, allowing the helicopter to reach the desired horizontal position before it touches down. This is also apparent because the tip path plane angle is low, but only briefly dips near the allowed limit. Rotor speed is obviously more of a concern, the helicopter increases descent rate early in the maneuver to increase the rotor speed considerably. This allows the thrust coefficient to max out at the end, dropping the now higher rotor speed and driving the sink rate down to an acceptable level for landing. This maneuver takes the longest of the three examples presented here: over 11 seconds.

4.2.2   Safe Flights from Different Regions

The previous section showed that safe paths exist for a flare maneuver in the searched region. It is now pertinent to ask: what do these paths look like at different points within the safe set? The following examples compare the found paths to landing for many different points within the safe set to a "central" point in the the safe set. The "central" point is made of the safest trim condition (one having the most safe flare initiation points) and located physically in the center of its safe flare point set. The "central" point is shown in (Figure 4.9 and Figure 4.10).

Being that this point is in the center of the safe set, it is expected that the controls will approach their limits minimally or not at all. This proves to be the case: α_{TPP} briefly reaches its lower limit just before landing and the thrust coefficient
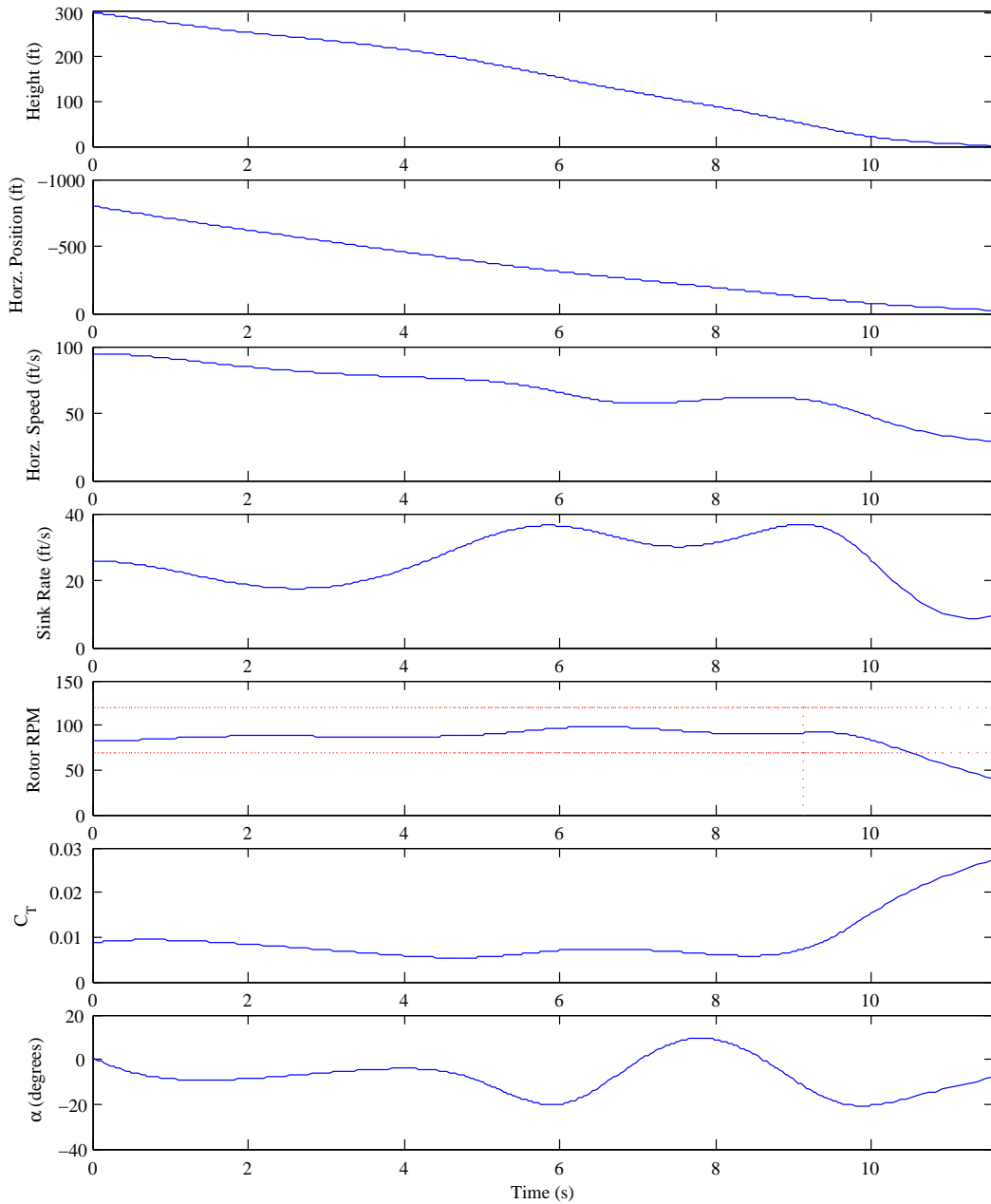
Figure 4.8. State History: Fast Initial Speed

increases to its maximum as touchdown approaches. These are exactly the inputs expected for flare. It may be noted that α oscillates during the maneuver. There is no penalty on control rates, and so this activity is allowed by the optimizer. While this is not ideal for a real helicopter, this consideration was left for future work.
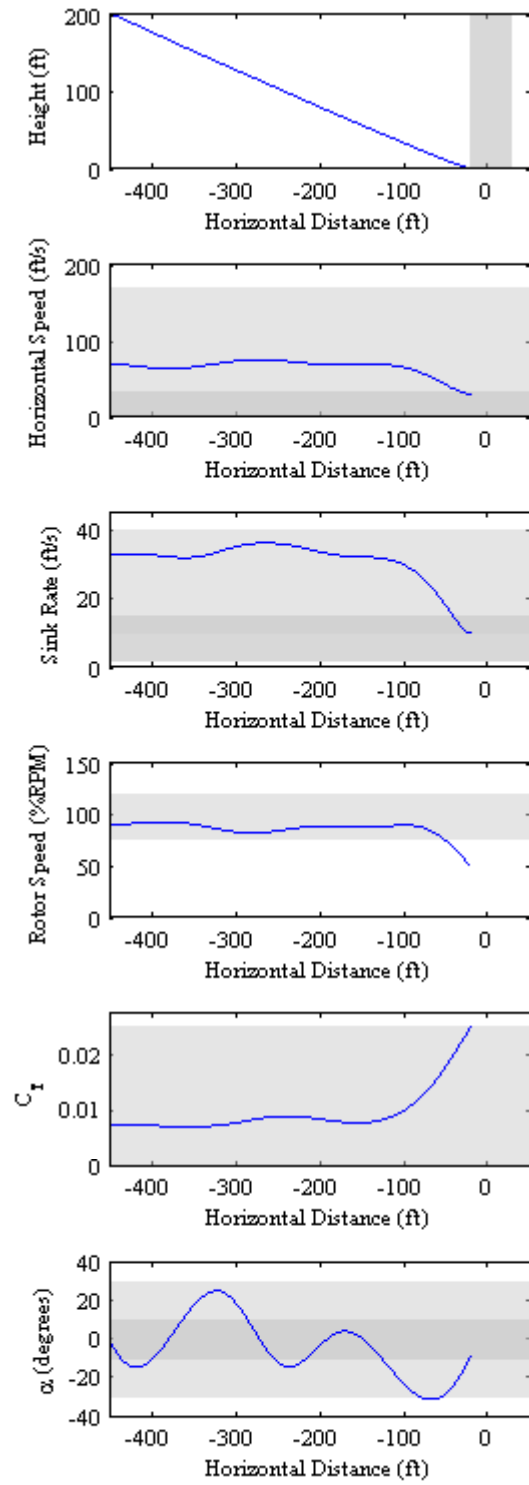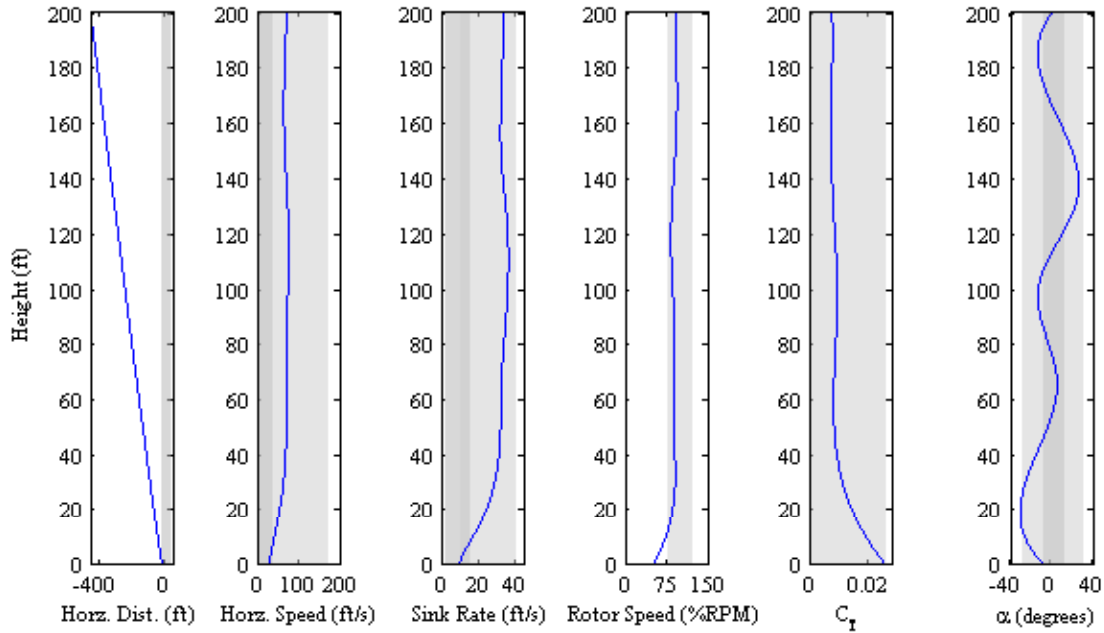
Figure 4.9. Point in the center of the safe set: state v. distance to touchdown

Figure 4.10. Point in the center of the safe set: height above touchdown v. state

The landing comes in within bounds on u and w and lands within the acceptable range for d, but close to the negative bound. The rotor speed also trends toward its nominal value. Overall this safe point has a very generic path to landing, as would be expected for a point in the center of the safe set.

The edge state here in Figure 4.11, Figure 4.12 represents the closest location from which the trim state state of the central point can reach a safe landing. Unsurprisingly this means the helicopter lands far toward the rear of the designated landing zone. The tip path plane angle reaches its allowable limit multiple times during the encounter as the helicopter attempts to quickly arrest the forward speed before the short 100 feet to the landing zone are covered. The vertical distance is very small, only 50 feet, so C_T is well above the trim value throughout the maneuver. It also remains at its upper limit for a short time before touchdown rather than only reaching this value at the instant of touchdown. The end result of this intense use of the controls is the main rotor speed rapidly falling during the maneuver. This is acceptable: Ω is allowed to go beyond its bounds below h=50 ft, as mentioned in Chapter 3.

At a different edge of the safe set, Figure 4.13 and Figure 4.14 compare a point
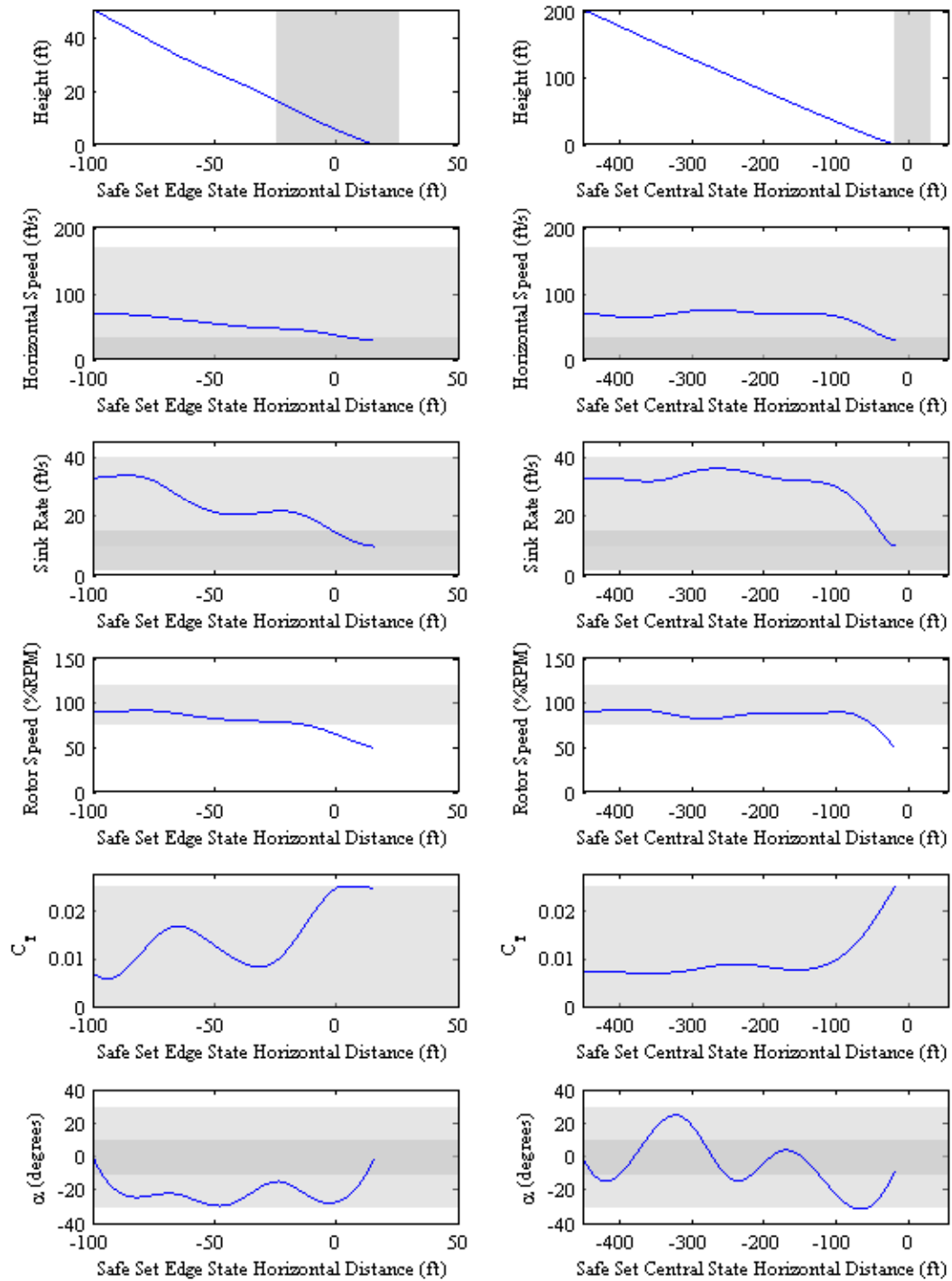
Figure 4.11. Comparison to forward and lowered start point: states v horizontal distance. Figures on the right are the same as those in Equation (4.9)
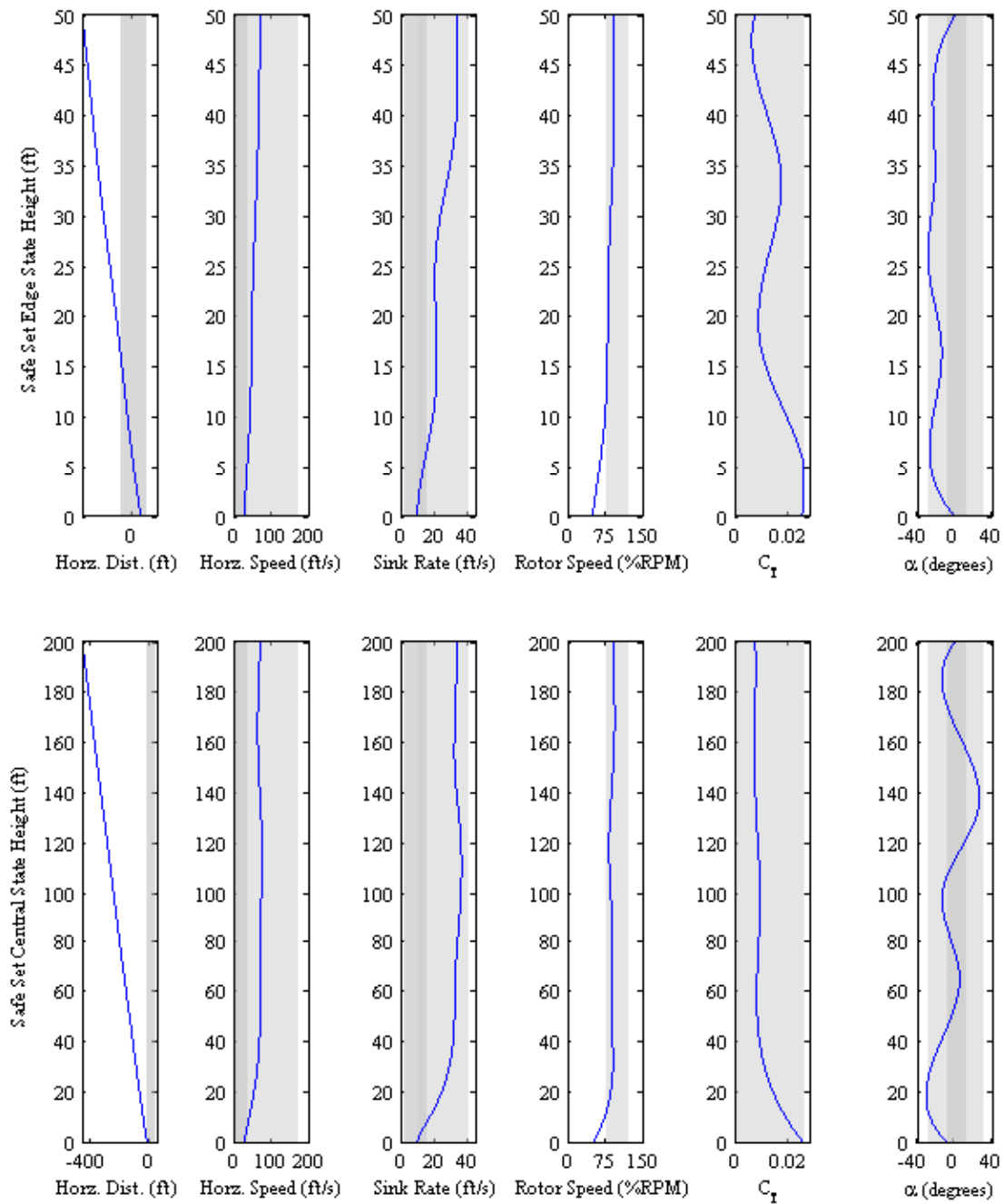
Figure 4.12. Comparison to forward and lowered start point: height v. states. Figures on the bottom are the same as those in Equation (4.10)

that shares the central start point's initial position but has the fastest velocity for which it is possible to safely reach the landing zone from that point. The reason
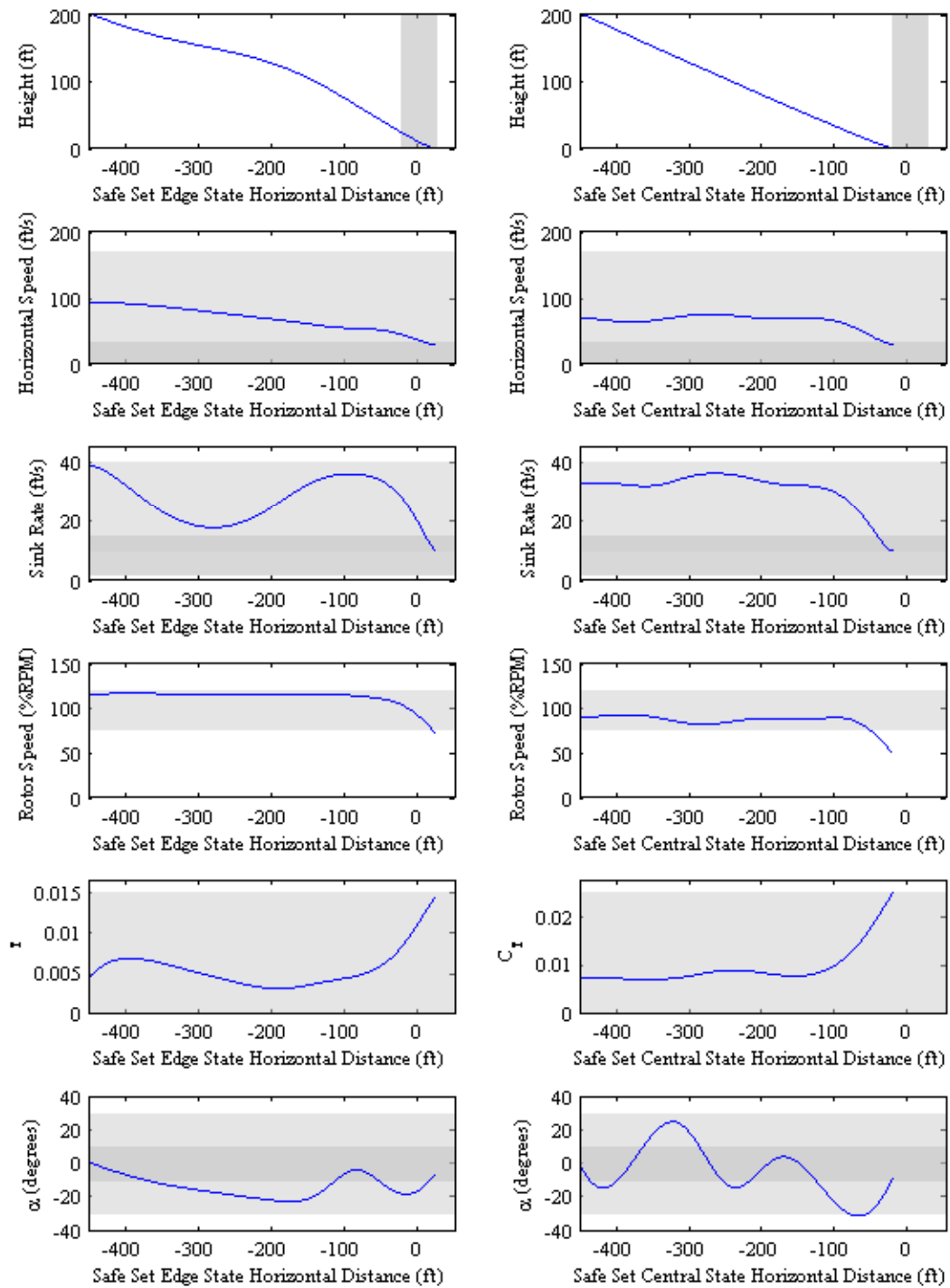
Figure 4.13. Comparison to faster start point: states v horizontal distance. Figures on the right are the same as those in Equation (4.9)
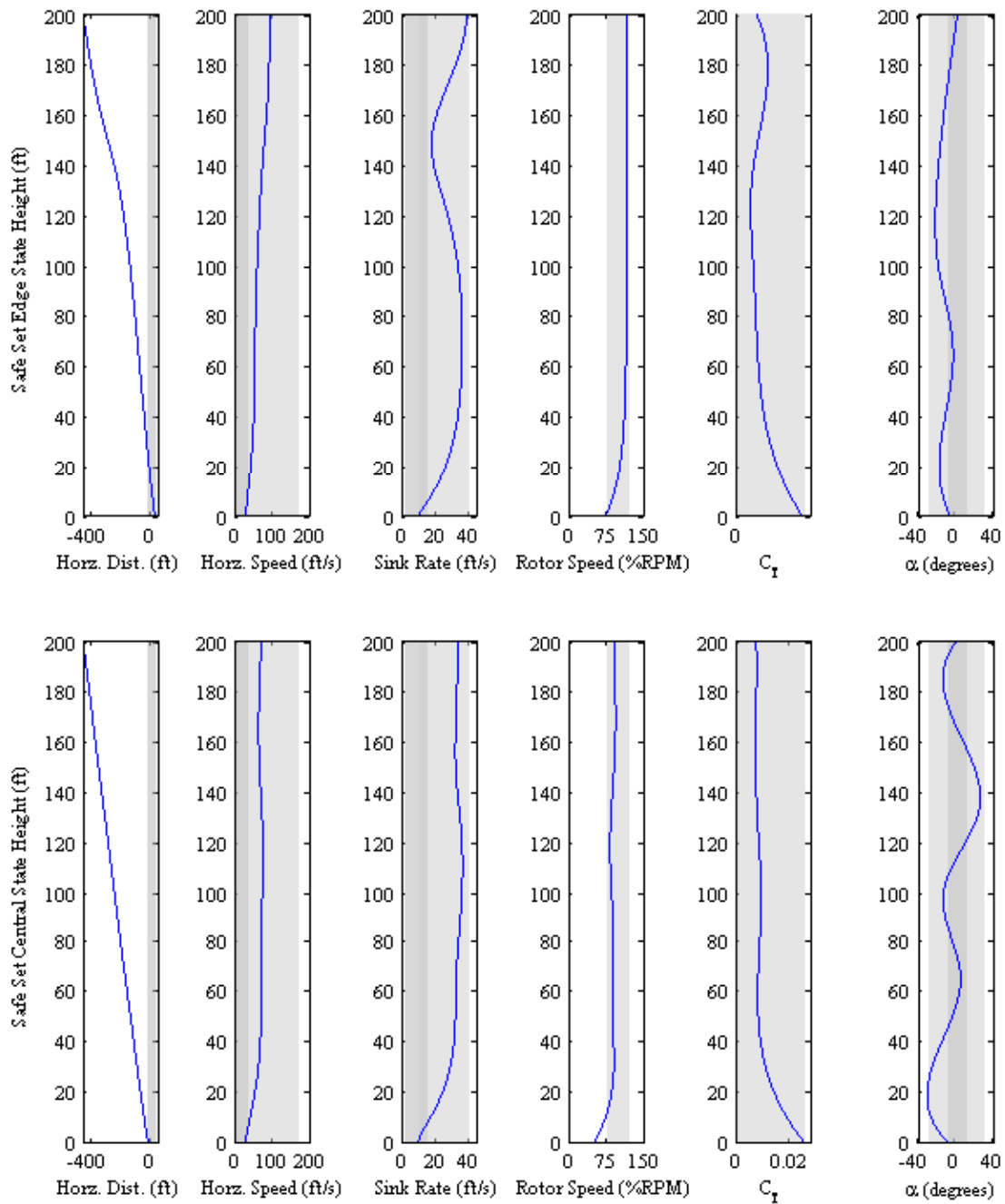
Figure 4.14. Comparison to faster start point: height v. states. Figures on the bottom are the same as those in Equation (4.10)

this is the maximum velocity for which a safe path to landing exists seems mainly due to the rotor speed. C_T and α_{TPP} approach their limits, but do not reach

them for more than an instant. w oscillates but does not break its bounds. Rotor speed, though, quickly reaches its maximum allowed value and remains there for the majority of the maneuver. It is easy to see that the rotor speed is at the limit of what can be considered a safe flight.

More examples of safe states at the edge of the safe set can be found in Appendix A.

4.2.3 Unsafe Flight Paths

Many tested initial flare point/vehicle trim state combinations fail to produce a safe path to landing. This may be due to the initial flare point, the trimmed autorotation state, or a combination of the two. Some select examples of failed states just outside the safe set compared to points just inside the edge are shown below. Figure 4.21 also shows the result of applying nearby safe state controls to an unsafe state and what use can come from this.

On the left of Figure 4.15 and Figure 4.16 is the lowest altitude from which the safest trim state can reach a safe landing at a starting distance of 200 feet from touchdown. On the right is the best attempt the path-finding algorithm could make with its alloted attempts for a point 50 feet below the original point. The sink rate quickly exceeds the upper limit, then drops briefly to a value below zero. A fundamental assumption of the height-parameterized equations of motion is that the independent variable h does not change directions, similar to how time does not reverse direction for the time-parameterized equations of motion. This means $\dot{h}_k$ must be negative. This violation of a fundamental assumption of the height discretized model has a predictable result: the equations of motion are no longer valid and results after this instant are meaningless.

Figure 4.17 and Figure 4.18 has the same safe state shown in Figure 4.11 and Figure 4.12. The unsafe start point is closer to the landing zone: it is 50 feet lower to the ground. It is obvious that the unsafe state is at its limit for possible control inputs. The tip path plane angle is at its lowest allowed value almost throughout the maneuver and the thrust coefficient spends a long portion at its maximum. Though the states u, w, and Ω behave acceptably, the helicopter overshoot the landing zone. This illustrates that not all path finding failures are catastrophic as
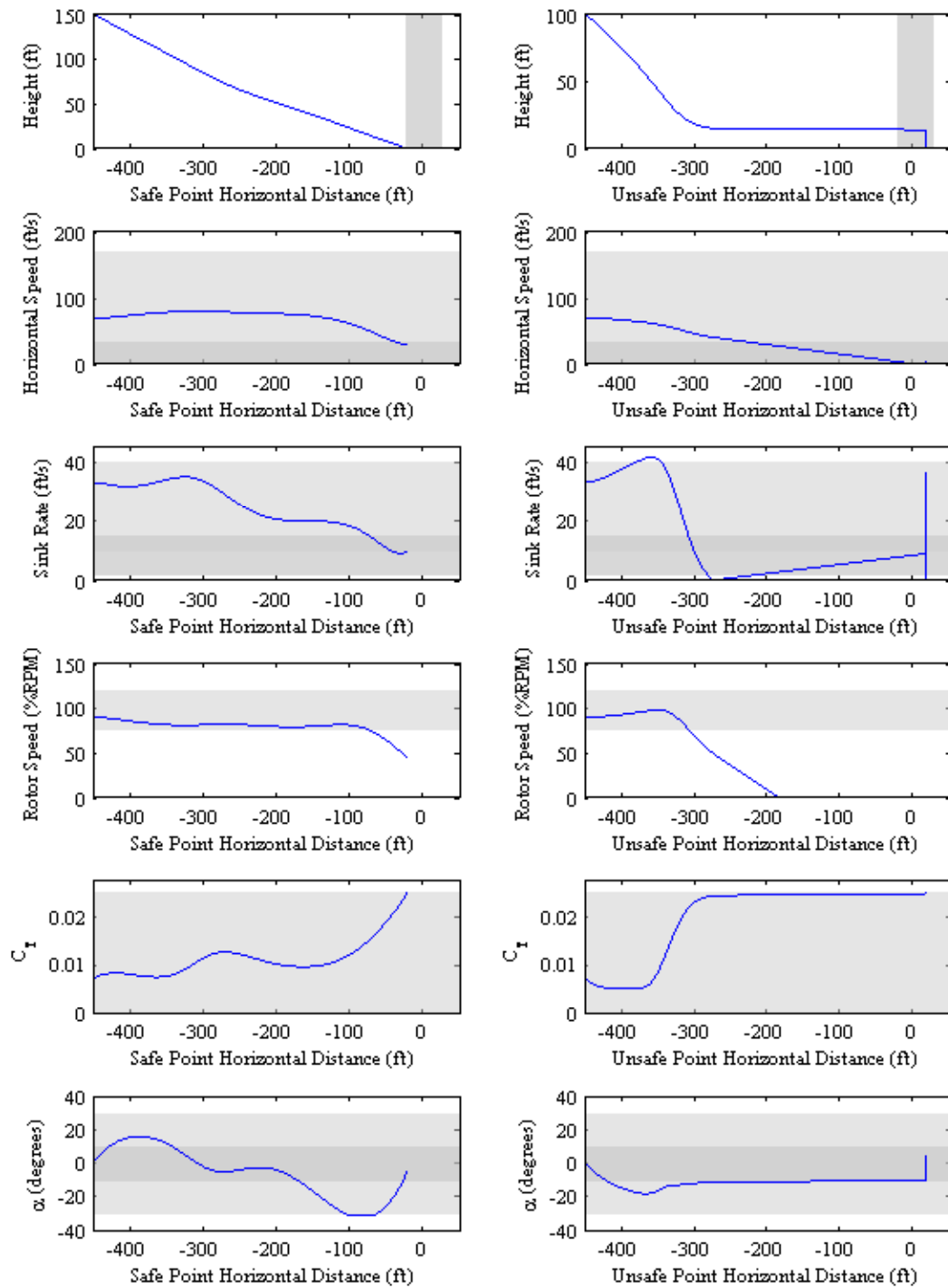
Figure 4.15. Comparison to lower start point: states v horizontal distance

in the above figures.

Figure 4.19 and Figure 4.20 compares the state with the slowest initial speed
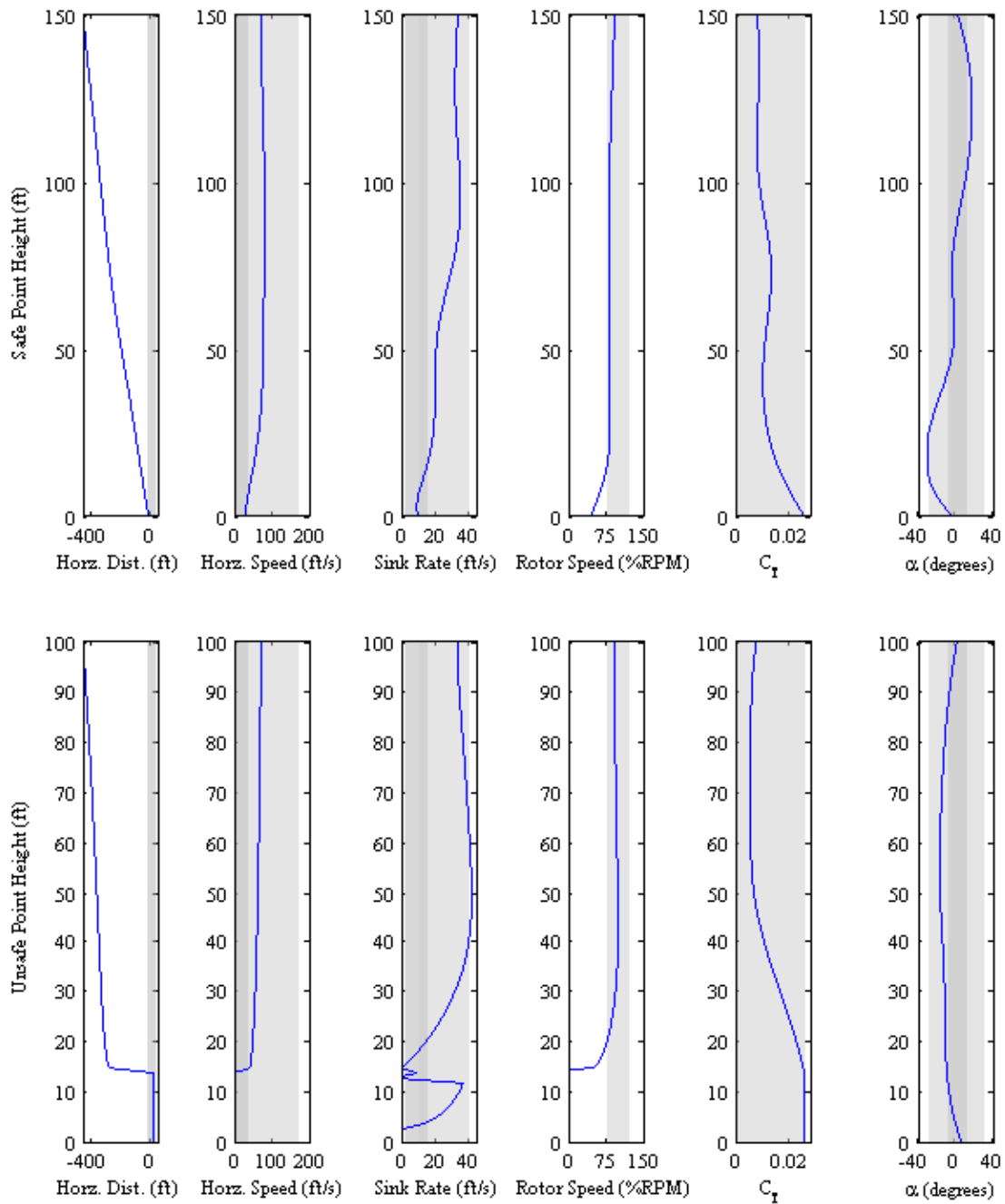
Figure 4.16. Comparison to lower start point: height v. states

that can safely land from (-450,200) to a trim state with slightly lower initial velocity. The controls continually approach and reach their limits throughout the maneuver, as seen in the other unsafe examples. The failure here is because the
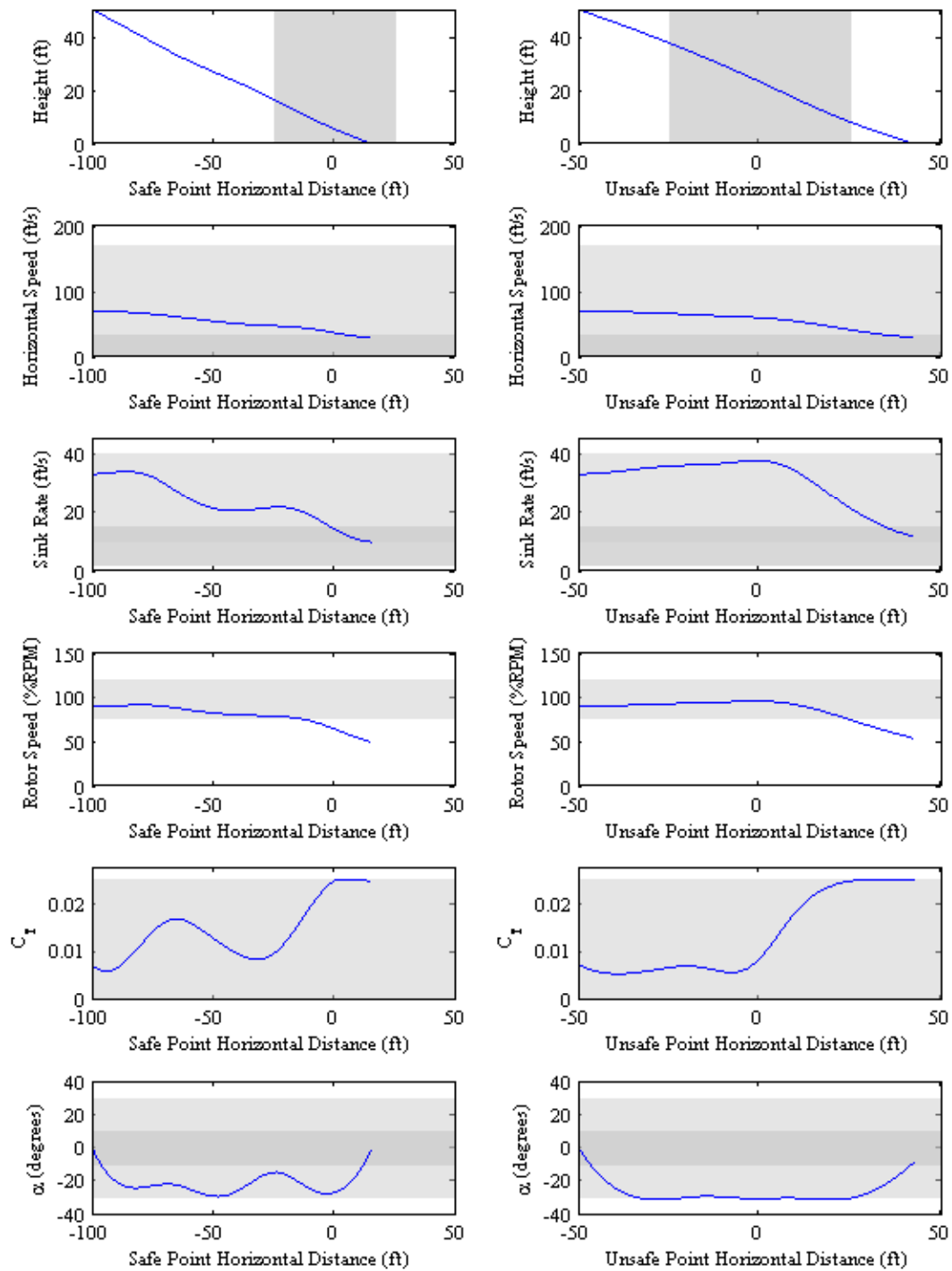
Figure 4.17. Comparison to lower start point: states v horizontal distance

sink rate exceeds the safe limit and the rotor speed drops below the allowable limit during the attempt to land.
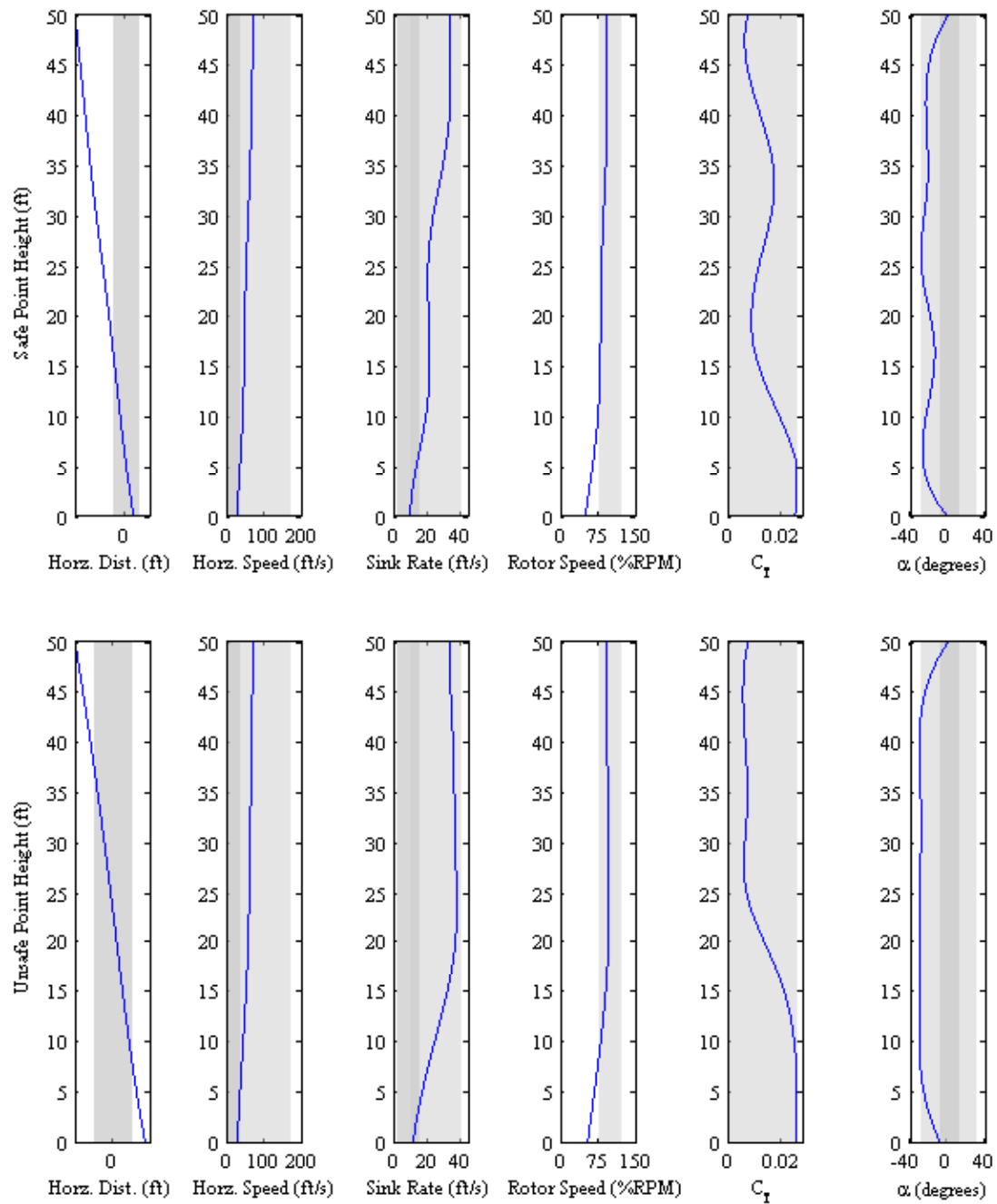
Figure 4.18. Comparison to lower start point: height v. states

For situations such as this, actions may be undertaken to find additional safe states. One method that may yield results at the expense of computing time is increasing the number of iterations the optimizer is allowed to use to find safe
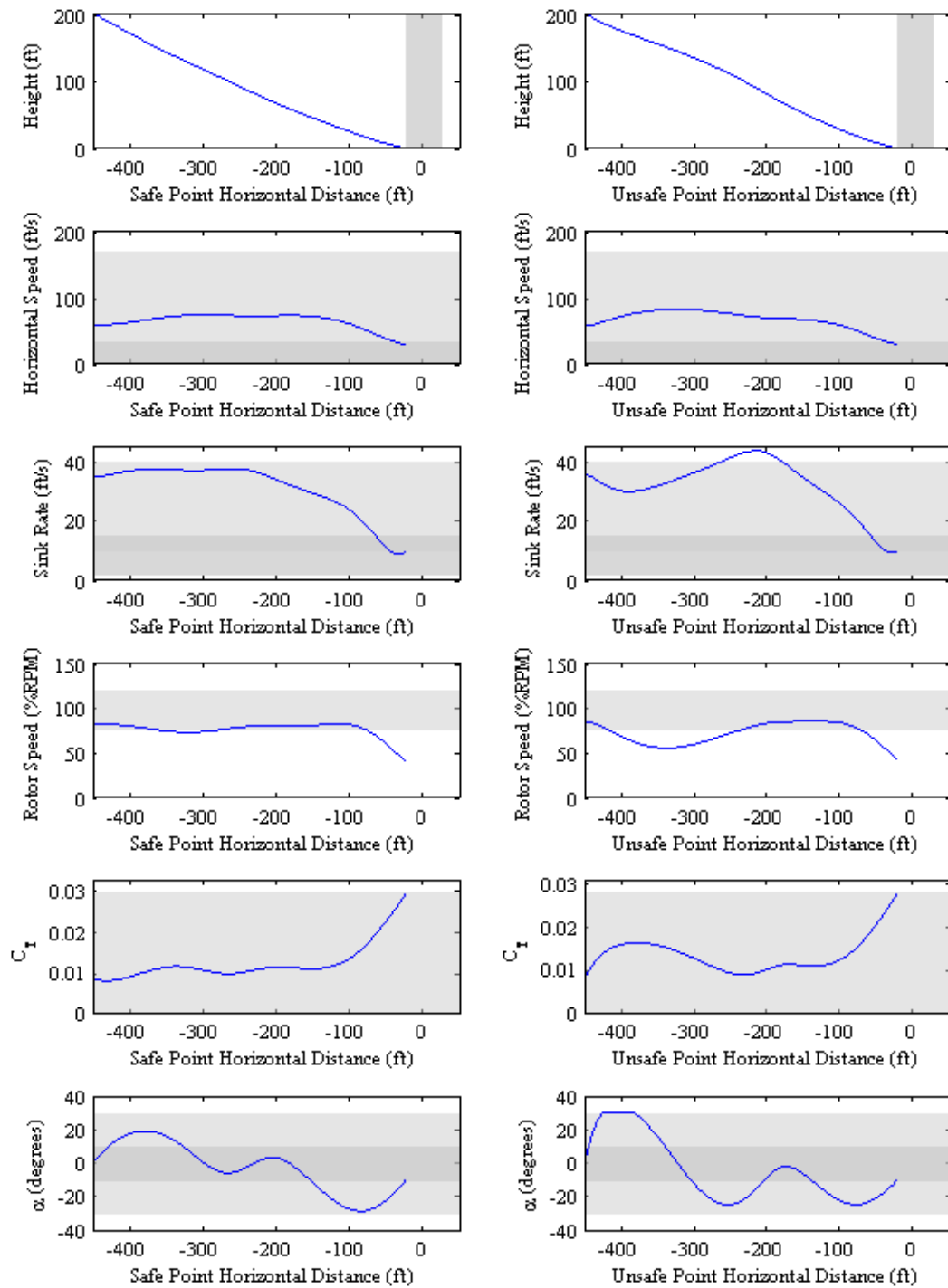
Figure 4.19. Comparison to slower start point: states v horizontal distance

states. This allows for a larger range of γ to be applied. Applying 'nearby' safe controls to unsafe states can also improve performance. Figure 4.21 applies the safe
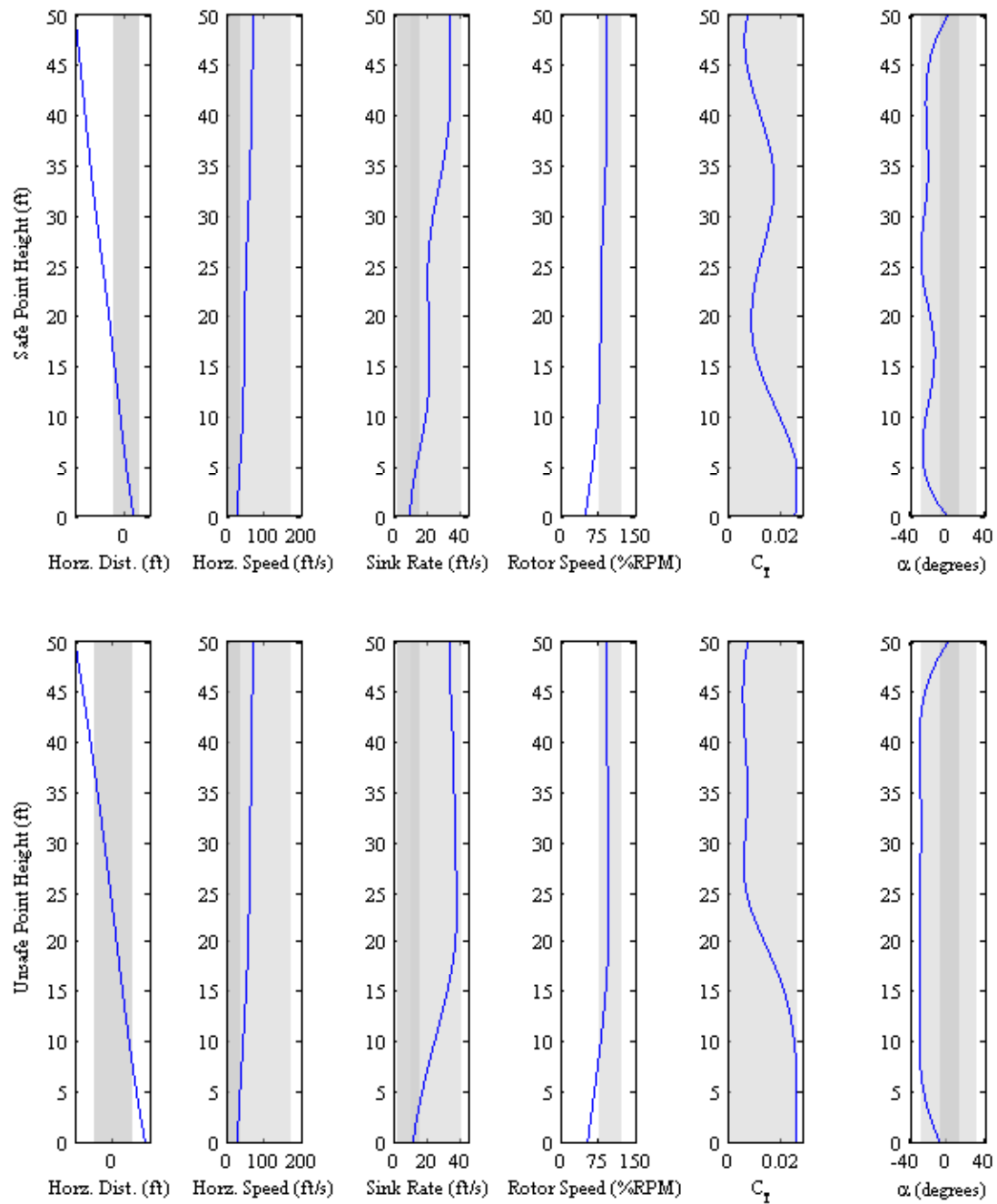
Figure 4.20. Comparison to slower start point: height v. states

state's controls from Figure 4.19 and applies them to the unsafe state. The result is
the unsafe state becomes safe, behaving almost exactly as the safe state did. Using
this method, additional safe states can be found from unsafe states. Running the

path-finding algorithm a second time using nearby safe controls as initial guesses has potential to find safe states missed on the first pass through. While this is outside the scope of this thesis, some experimentation into the technique by the author has yielded promising results.

In earlier versions of this work the controls had a tendency to show somewhat 'jagged' histories, especially in states near the boundary of the safe set or controls for failed states just outside the safe set. A solution to this was proposed and implemented by Floros [11] in which control rates were controlled rather than the controls themselves. In this work the problem is overcome by forming the control vector with a spline from a small number of controls able to be adjusted by the optimizer.

While only a few paths are presented in detail here, examining these shows that the optimizer is capable of producing safe, feasible paths for a flare to landing. Examining these states has additionally shown that the results of safe/unsafe testing produce expected results. Additional comparisons of safe/unsafe paths are available in Appendix A.

4.3 Safe Set Visualization

The safe landing set is a high dimensional space. It consists of five dimensions $[u, w, \Omega, d, h]$ and as such is difficult to visualize. This section contains several projections of the Safe Landing Set onto 2D planes and 3D surfaces.

4.3.1 The V-h diagram

The traditional means of determining safety in powered flight and autorotation is the V-h diagram. An example V-h diagram is shown in Figure 4.22. At first it may be guessed that a projection of the safe landing set onto the V-h diagram would allow comparisons between the two presentations of safe states, but there are critical differences. The V-h diagram is developed for powered straight and level flight under which a helicopter may lose power. This allows a much wider range of velocities to be taken into account. The helicopter setup studied and presented in this thesis is limited to trimmed autorotation conditions, and only the flare portion
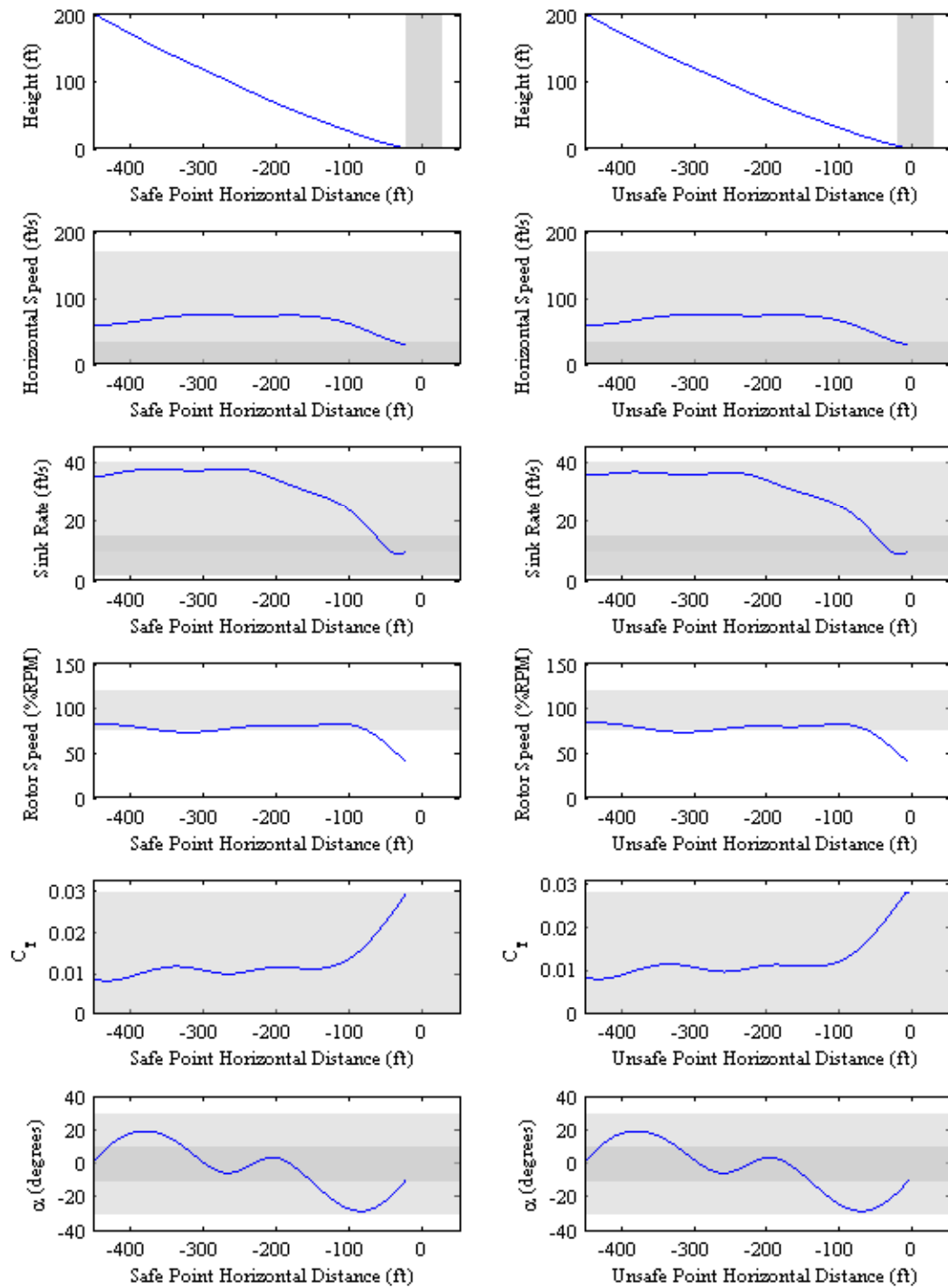
Figure 4.21. Nearby safe state's controls applied to an unsafe state: states v horizontal distance

of autorotation. The traditional V-h also assumes the helicopter will go though an autorotation maneuver, while the work presented here examines only the flare maneuver. In this case, that limits forward speed to a minimum of about 60 ft/s. In addition, a traditional V-h diagram does not account for the physical location of the landing zone, while the values generated in this simulation must account for this. This is reflected in Figure 4.23, the V-h diagram determined by the safe set simulation. High velocities produce unsafe conditions as the helicopter overshoots the landing zone or descends too rapidly to the ground. At high altitudes, low speed is preferred so the helicopter has time to to get to the ground before overshooting the landing zone. At lower altitudes, low speed means the helicopter has time to arrest its sink rate before reaching the ground. A general trend of low speeds and moderate height is evident.

For these reasons, the traditional V-h diagram can not be compared to the simulation's V-h diagram. And while the simulated V-h diagram provides some information, other outputs can give a much broader view of the results.

4.3.2   Flare Initiation Points

Figure 4.24 shows all the flare initiation points. The greater the number of vehicle states that produce a safe state when paired with the initiation point, the closer to dark red the point becomes. Matching intuition, the results show unsafe states to be located in two particular locations. When the helicopter is near the horizontal touchdown point relative to its initial altitude it cannot safely reach the ground before overshooting the desired landing site. Horizontally far from the desired landing zone and low to the ground, the helicopter cannot reach the landing zone before it sinks to $h = 0$. Even near the landing site, it is not always possible to find a safe path to touchdown from very low altitudes.

A view of what regions, rather than specific points, lead to safe flare is shown in the contour plot Figure 4.25. Again, darker red indicates a flare initiation point is very safe because many vehicle trim conditions can have a safe path to landing from the point. Darker blue indicates that few or no trim states can be paired with the flare initiation point to produce a safe state. The safe stars tend to fall along a line drawn out my the trim autorotation condition. This makes intuitive
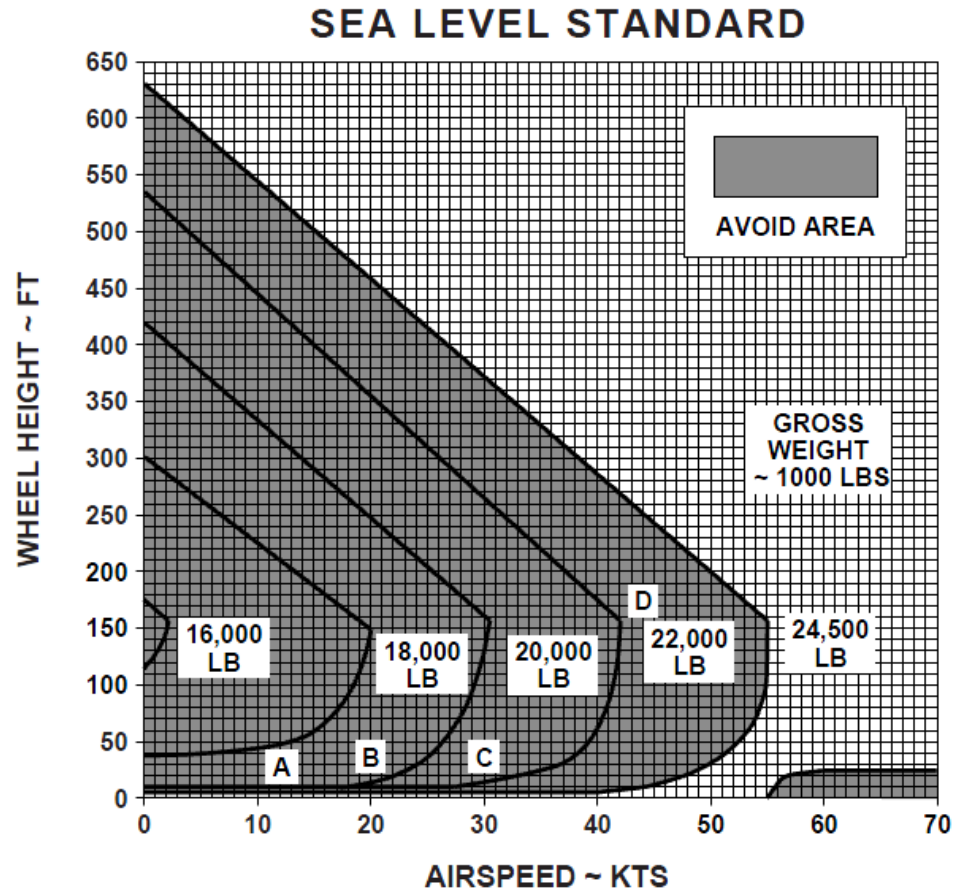
Figure 4.22. V-h diagram for a UH-60

sense: if a safe flare condition exists at some close point for a certain trim state, every point along the trimmed path to that point will be safe. The helicopter can simply travel in trim to where the safe point is. Nearby states can also follow similar paths.

Together the safe flare initiation points and the V-h diagram show the safest condition is a helicopter at low to moderate speed with a fair bit of altitude and distance to come down.

some 'islands' of safer states cna be noticed in the scatter and contour plots of Figure 4.24 and Figure 4.25. These may be due to the discretization used in testing, both for flare initiation points and vehicle trim states. These may also be the result of the optimizer design, whether due to the limited number of iterations or the discretization of the control inputs.
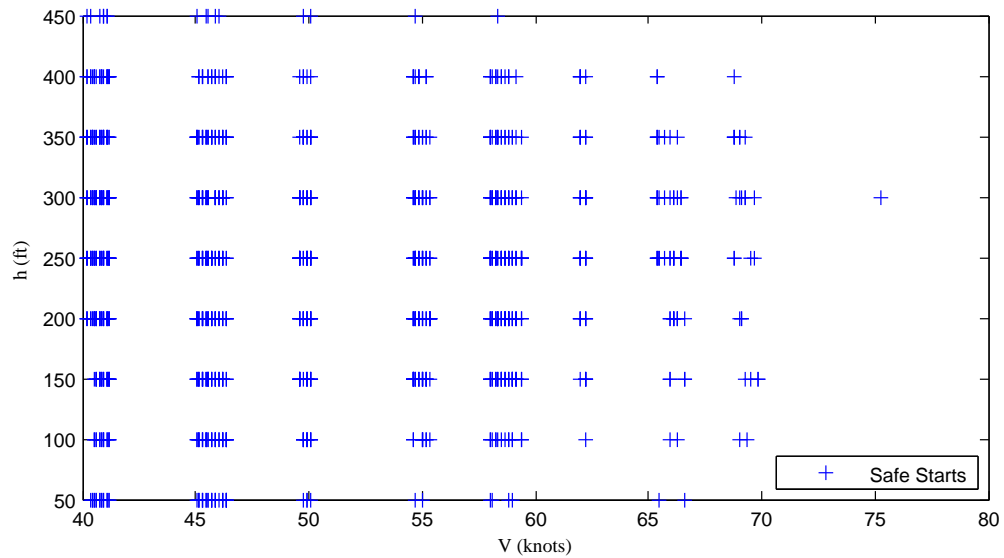
Figure 4.23. V-h diagram for Utility Helicopter Simulation
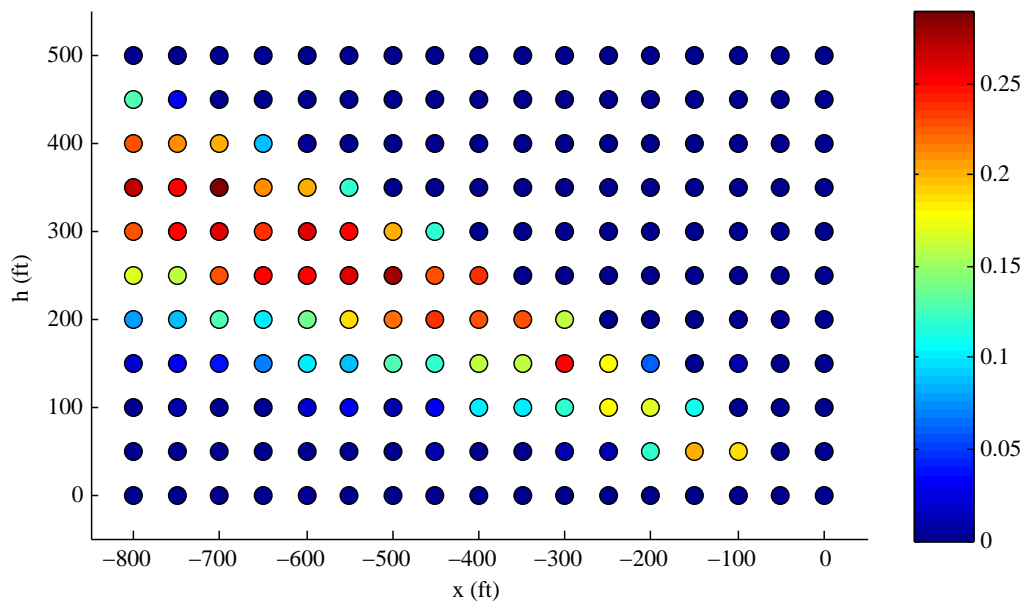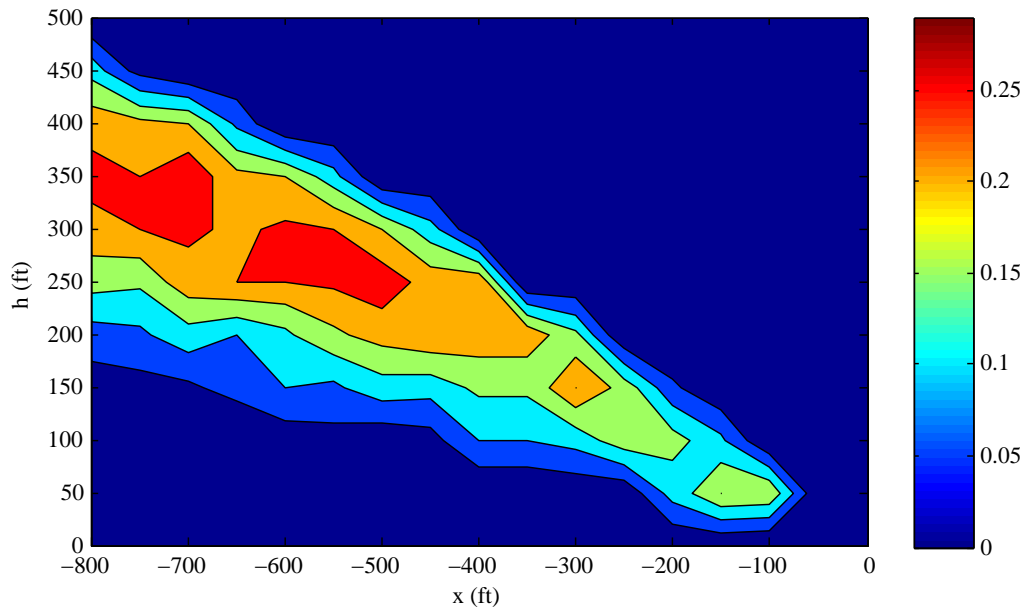

Figure 4.24. Flare Initiation Points

4.3.3 The Probably Safe Set

The Probably Safe Set was discussed previously in Chapters 2 and 3. It is the set of trimmed autorotation states for which a safe path to landing is likely to exist. The Probably Safe Set is presented in Figure 4.26. The Probably Safe

Figure 4.25. Flare Initiation Points

Set is a volume fraction of the region of flare initiation points which can result in safe landing for a particular autorotation sequence. The coloring indicates the number of safe flare initiation points normalized by the total number of safe flare initiation points. The closer to red an area is, the more safe flare initiation points exist for that particular autorotation state. A trim state with more available flare initiation points is considered safer, because it has a larger safe area in which to initiate flare. Examining Figure 4.26 leads to the conclusion that safe autorotation is likely to occur when the helicopter begins flare with low forward speed and high rotor speed. A consequence of high rotor speed is also having high initial descent rate. This turns out to be a worthwhile trade, though. The energy in the rotor can be used to manage both forward velocity and sink rate. Forward speed turn out to be the biggest limiting factor. For the area of flare that was considered states with u_0 above approximately 120 ft/s can find no safe spots from which to land.

A reason for the appearance of the probably safe set can be gleaned from Figure 4.27 and Figure 4.28. Figure 4.27 shows the helicopter's linear kinetic energy at each available trim state. Figure 4.28 gives the ratio of the rotor kinetic energy to the body kinetic energy.

Comparing these plots to the probably safe set, it becomes apparent that the
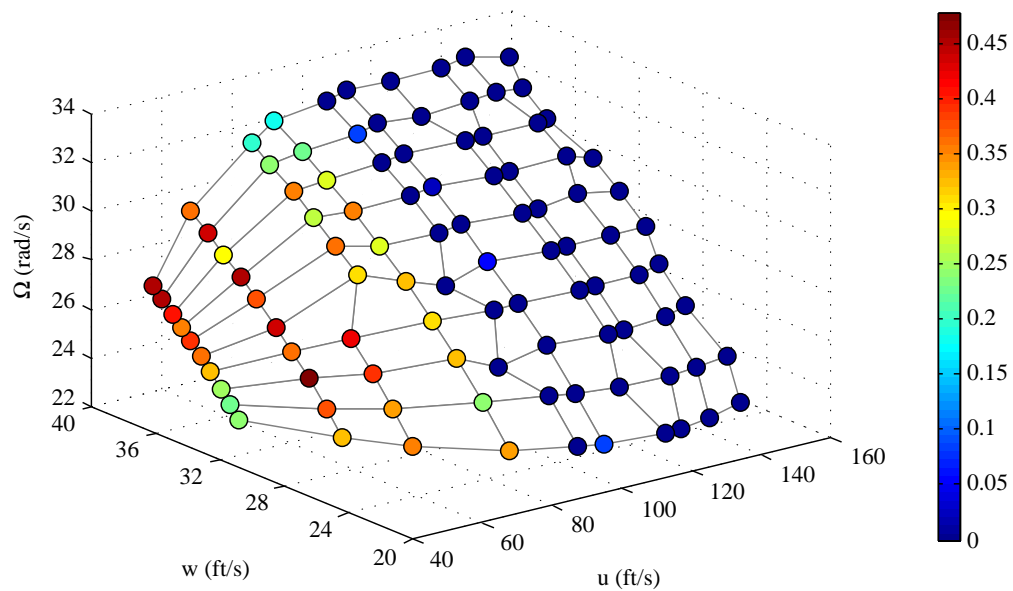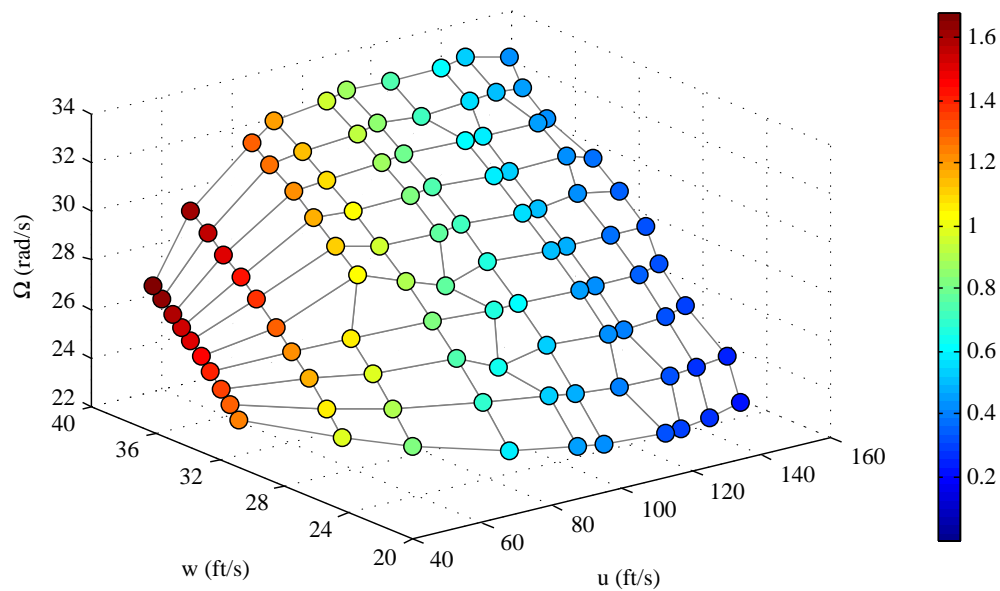
Figure 4.26. The Probably Safe Set
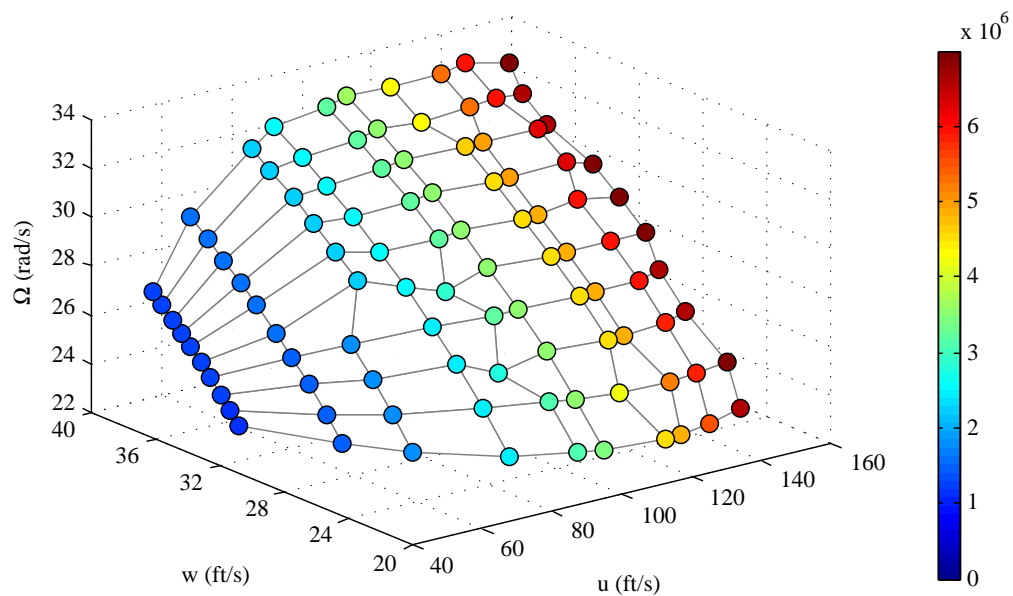

Figure 4.27. Vehicle Kinetic Energy in ft-lb

probably safe set is a mix of the two, leaning heavily toward the rotor kinetic energy fraction. As described earlier in this chapter, high rotor speed is desirable for flare. It gives the helicopter room to manage its controls. However, high rotor

Figure 4.28. Rotor Fraction of Kinetic Energy

energy is not enough to guarantee a safe landing. If the linear kinetic energy of the helicopter is too high, even large amounts of energy stored in the rotor do not allow the helicopter to and land safely. This may result from physical limits on the helicopter start point (being too close to the landing zone) or limits on the controls and states during descent. there may not be enough control authority or states may exceed their allowed limits if they start near them.

Another way to view this data is as total velocity vs. rotor speed. Figure 4.29, also shown earlier in this chapter when defining the flare area, shows that the most desirable states have low velocity and high rotor speed. This is very much an expected conclusion. High rotor speed means a much wider range of control inputs will be acceptable. Increasing C_T and adjusting alpha to slow u and w at the same time is possible if the rotor is spinning quickly. Though maneuvers tend to decrease Ω if begins with a high value then it can safely drop farther than a speed that begins near the bottom of the allowable range. Low velocity is also obviously helpful to safely reaching the landing zone. low speeds are closer to the desired landing conditions of almost zero velocity, and so need less management from the controls.
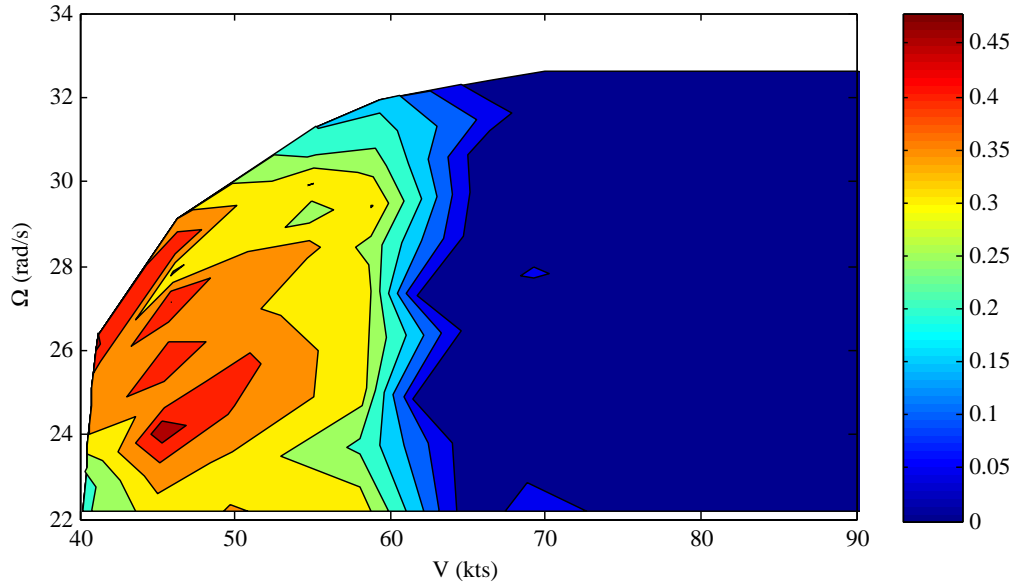
Figure 4.29. Total velocity compared to rotor speed for flare locations within the safe set

4.3.4 Safest Trim State

The trim state with the largest number of safe flare initiation points is at approximately:

$$\tilde{\mathbf{a}} = [69.1(ft/s),\ 32.87(ft/s),\ 230(RPM)]^T \tag{4.1}$$

This gives a total airspeed of 76.5 ft/s. Recommended autorotation trim for the blackhawk helicopter, which is similar tot he model used in this analysis, is an airspeed of 135 ft/s and a rotor RPM of 260 according to the manual [12]. The simulated best state is 43%(airspeed) and 11.5%(main rotor RPM) lower than the manual reccomended values. The reccomened autorotation condition exists for a few reasons. It is near the best lift/drag ratio for autrotation descent. This gives the pilot the most choices for the possible landing zone. This condition is also fairly well approximated by linearization. Linearized equations of motion near this region closely approximate the more complicated and accurate non-linear equations of motion. This makes control for this state much easier to discern. The solved

'safest state' indicates when flare should begin. This means that the pilot should use the reccomended best autorotation state to find a landing zone. Then before initiation flare, reduce airspeed and increase descent rate to the reccomended safest state.

The safe flare initiation points for the previously mentioned best autorotation trim state are shown as white circles on top of the safe flare initiation point contour in Figure 4.30. Methods to fill in the "missing" safe flare initiation points were discussed throughout this chapter.
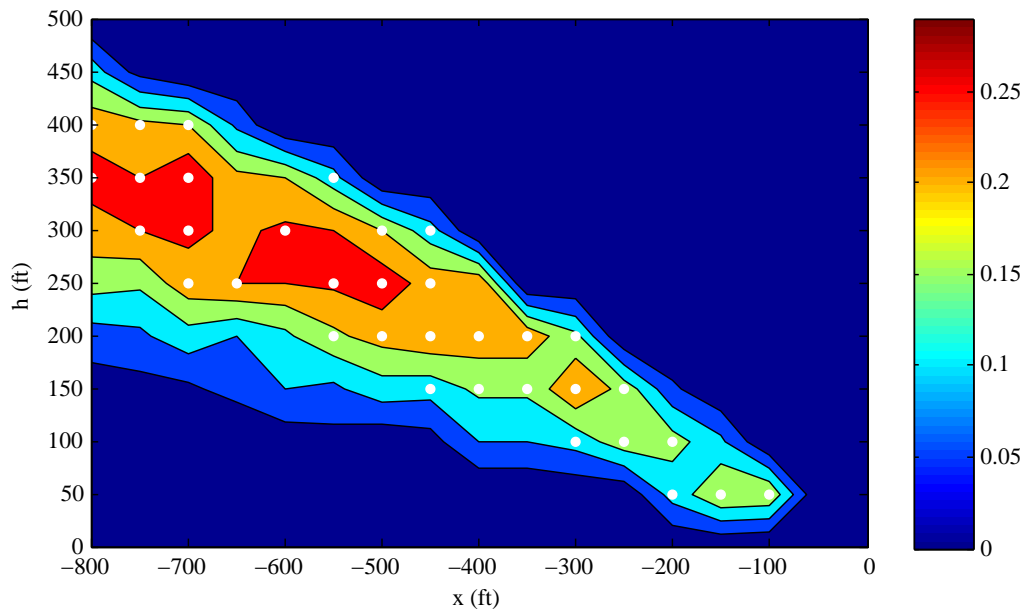
Figure 4.30. Flare Initiation for the Best Region of the Probably Safe Set

In addition to defining safe autorotation conditions, the safe landing set can be used as a goal space for mid-phase trajectory planners. A helicopter directed toward the "thickest" area of the safe landing set will have maximum robustness to errors or external disturbances when reaching the flare phase of autorotation. Also, it would be helpful to consider the Probably Safe Set as a reference during transition from engine failure to entry into trimmed steady autorotation descent.

Fast trajectory generation could be implemented with the optimal paths used in computing the Safe Landing Set. When a helicopter enters flare, thus entering the safe landing set, a path to touchdown can be decided on based on the paths from the nearest safe points. A trajectory following algorithm can be used to guide

the helicopter along this path.

4.4   Summary

Section 4.1 briefly reviews the algorithm for finding the Safe Landing Set. Many autorotation trim states and flare initiation points are tested for paths to safe landing. The testing involves attempting to find an optimal path to landing that does not violate any constraints on the vehicle's in-flight motion and also lands sufficiently close to the desired landing location and vehicle state.

The subsection 4.1.1 describes the method by which the are where flare could be considered to take place was decided on.

Section 4.2 shows example flight paths from a selection of different regions inside and outside the safe Landing Set.

The paths in section 4.2.1 show that the optimizer used in finding the Safe Landing Set is capable of producing safe paths to landing, and the vehicle dynamics behave as expected.

Section 4.2.2 shows the difference between a point in the interior of the safe set and multiple points at the limits of the safe set.

Section 4.2.3 compares points just inside the safe set to those just outside and briefly comments on how additional points might be incorperated.

Section 4.3 focuses on different ways to view the high dimensional safe landing set. Because it is a five-dimensional space, many methods of presenting the Safe Landing Set exist and each gives a different view of the overall results. This section is broken into 3 parts.

Section 4.3.1 discusses the V-h diagram, the traditional means for evaluating safe operational conditions for helicopters. The usefulness of the V-h diagram is discussed and a traditional V-h diagram and one from the simulation results are contrasted.

Section 4.3.2 examines the safe flare initiation points, the locations in space from which the helicopter may successfully reach the desired landing zone. Successful landing from any one of these points also depends on the autorotation trim state the helicopter is in when it reaches the initiation point and begins the flare maneuver.

In section 4.3.3 the Probably Safe Set is presented. It is the most informative view of the safe landing set. The Probably Safe Set is a view of all the available autorotation trim states and the relative number of safe flare initiation points that may be used in conjunction with each trim state to reach a safe on ground condition. A two dimensional view where u and w are combined to give airspeed is also shown.

Finally, section 4.3.4 compares the recommended autorotation state from the simulation with the traditionally accepted 'best' autorotation trim descent for the example helicopter model. The results are similar in rotor speed but differ considerably in airspeed. A possible explanation for this difference is presented.

Conclusion

This thesis was motivated by a need to ensure safe autorotation for unmanned aerial vehicle (UAV) helicopters. All helicopters run the risk of needing to perform an autorotation descent should their engines fail. For human pilots autorotation is a dangerous and difficult maneuver. For UAVs it is something currently beyond their capabilities. In both cases enabling a safe machine controlled or guided autorotation greatly reduces the risk of cargo and aircraft damage and pilot/passenger injury or death. Real-time autorotation trajectory planners exist for autonomous helicopters, however the final phase of autorotation, flare, happens very quickly, is near the ground, and requires precise control inputs. Because of this, real-time trajectory planners are not suitable for guiding the helicopter during flare.

Autonomous helicopters are gaining attention as systems which can be used for resupply or casualty evacuation. To enable these UAVs to perform the aforementioned tasks many are being fitted with expensive sensor suites. Medical evacuation UAV helicopters would also be carrying human cargo. Loss of payload or patient in these cases is unacceptable. This is especially true in the event of power loss, which is a condition known to be recoverable through autorotation. While this is less of a concern for multi-engine aircraft it is certainly a real risk for single-engine helicopters, which most UAV helicopters are. Additionally, guided autorotation reduces pilot workload during the maneuver, making manned flights safer as well.

Autorotation consists of five parts: (1)Engine failure causes power loss. The pilot must lower the collective pitch of the blades and (2)enter autorotation in which the air flowing up through the rotor drives the rotor and produces lift.

Entry transitions to a (3)steady descent which brings the helicopter near to the landing zone. At this point the helicopter must (4) transition from steady descent and begin the flare maneuver. During (5)flare the helicopter uses the momentum in its rotor to slow its horizontal speed and its sink rate to levels acceptable for touchdown. If flare begins too high above the ground the helicopter stalls and falls to the ground. If flare is initiated too low the helicopter crashes into the ground with too great an airspeed. The correct location for flare initiation is determined by the state of the helicopter during its steady descent.

Autonomous autorotation is an active research topic in the rotorcraft community. Optimal control has been used to find both powered and autorotation trajectories and for pilot cueing. Other novel approaches such as machine learning and model-predictive control have also been attempted. Reachable set analysis is also an active research topic. However, combining optimal control and reachable set analysis for autorotation path planning has not yet been attempted. This method is especially useful in the flare phase of autorotation. A flare law separate from the descent path planner is needed to account for differences between the simulated and actual autorotation descent paths. These differences can come as a result of wind gusts, steady wind fields, differences between the actual helicopter and the model, or changes to the landing zone terrain during descent. An improved method for flare control is also a topic recommended by other researchers in the field focused on the entry and descent phases.

5.1   Summary of Contributions

5.1.1   Safe and Probably Safe Sets

The backwards reachable set consisting of initial vehicle states for which there exists safe, feasible paths to touchdown was created. This is the Safe Landing Set. The Probably Safe Set a subset of the Safe Landing Set, is the set of all trim autorotation conditions for which a safe, feasible path to landing exists when paired with the correct flare initiation point. these sets can be used to guide the helicopter during the entry and descent phases of autorotation, and also provide robustness for the helicopter should the simulated path not match the actual path

of the vehicle. As long as the helicopter remains within the Safe Landing Set a safe path to touchdown exists. An algorithm for computing the Safe Landing Set using parameter optimization and varying relative weights of cost function variables was developed.

5.1.2 Derivation of Height-Discretized Equations of Motion

The equations of motion for a generic utility helicopter were modified such that time was replaced by height as the independent variable. This derivation removes the ambiguity of an unknown time end condition and replaces it with a known $h_f = 0$ end condition. A forward Euler method was presented as means of discretizing these equations of motion.

5.1.3 Trajectory/Parameter Optimization

Trajectory optimization was shown to be a legitimate method for solving for a safe path from flare initiation to touchdown. After introducing the height-based equations of motion, the trajectory optimization approach becomes a parameter optimization approach. The MATLAB function fmincon, which minimizes a cost function C, was used to solve the parameter optimization problem. The cost function C consists of two parts: a touchdown cost C_{td} and a vehicle state constraint cost C_{state}. The relative weight of these costs may be adjusted with the parameter γ.

5.1.4 Autorotation Analysis

The parameter optimization approach was used with a generic utility helicopter model to analyze the flare maneuver. The region that constitutes flare was defined. It was shown that trimmed autorotation states with low kinetic energy and a high fraction of rotor-to-total kinetic energy are desirable because they have a larger number of points from which it is safe to begin flare.

Points on the edge and slightly outside of the safe set were also examined. Points at the edge of the safe set show controls and states near or at their limits

for large portions of the maneuvers, as would be expected as the optimizer strains to find acceptable solutions at the edge of its limits. Various reasons for the unsafe states failure to produce a safe flare maneuver are investigated and explained.

5.2 Recommendations for Future Work

5.2.1 Control Rate Limits

For some solutions the controls oscillate in a manner that would not be acceptable when operating a helicopter. A cost should be applied to the controls or their rates to minimize this. For instance: minimizing the 1-norm of the control vectors would push the controls toward less extreme values. This would of course mean large changes in control inputs are less favorable.

5.2.2 State and Wind Estimation

This thesis assumes perfect knowledge of vehicle state and zero wind. However, this is not the case in which actual UAVs fly. While the safe set is capable of handling disturbances caused by imperfect models or wind gusts, the helicopter must be aware of how it has moved and what its current environment is. Without proper state and wind estimation the helicopter is unable to ascertain if it is within the safe set or what corrections it must make to its trajectory to remain on a safe, feasible path to landing.

5.2.3 Landing Site Selection

In order for the Safe Landing Set to have any impact the desired landing site must be known. A good estimation of location, terrain angle, and special features (e.g. sandy or dusty conditions limiting downwash to avoid brownout) is necessary. Safety of initial states is tied to their ability to reach the desired landing site. If the actual desired site differs from the estimated desired site by too wide a margin then the safe set is of little use.

In addition, in order to use the Safe Landing Set as a goal for other stages of autorotation a landing site must be selected well in advance of the helicopter

reaching the descent or flare phase of autorotation. Ideally, landing site selection would happen in real time while the helicopter was under powered flight as a precaution in case power loss should occur.

5.2.4 Flare Trajectory Generator and Follower

A helicopter attempting flare within the boundaries of the safe landing set should be able to reach the ground safely. To accomplish this for states that are not physically identical to points in the safe landing set an interpolation of the control inputs matched to nearby safe points will generate control inputs that will safely bring the helicopter to the landing zone. The helicopter may then attempt to follow the ideal trajectory produced by this method.

5.2.5 Robust Safe Landing Set

The safe landing set is likely to be affected by head and tail winds. These can be steady state winds or unsteady wind gusts. In either instance there is a possibility for the winds to change which states are safe or unsafe. Development of a landing set that is robust to both steady state head and tail winds and wind gusts will greatly improve the usefulness of the safe landing set.

Further flight path examples

A.1　Safe Flight Paths

This section provides additional comparisons between a point in the center of the safe landing set and points on the edge of this set.

Figure A.1 and Figure A.2: These compare the central point to a point on the edge of the safe set. This edge point has a identical trim state and horizontal start distance to the central point but a beginning altitude 50 feet lower. This point represented the lowest start point that matches the central point in all other aspects. The two results differ mainly in w and α. w drops quicker for the edge state and α spends a longer period at its lower limit. This makes intuitive sense. w must be lower for the edge state so that it can travel the same horizontal distance before touching down. The control α reaches its minimum threshold during the maneuver, which is to be expected as the helicopter attempts to slow itself before it reaches the ground. It is also expected that α reaches its bound because the state is at the edge of the safe set. At these edge locations the controls should be pushing against their limits. Beyond the edge points the controls can no longer create a safe flare path within acceptable bounds.

Figure A.3 and Figure A.4: The edge state is identical to the central state, except the initial horizontal distance to touchdown is as close as possible while matching all other initial conditions. The differences appear mostly in d_{final}, w, and α. The edge state landing at a d farther from the central's landing location is expected, it starts closer to the landing zone. Because the edge state is closer, it will
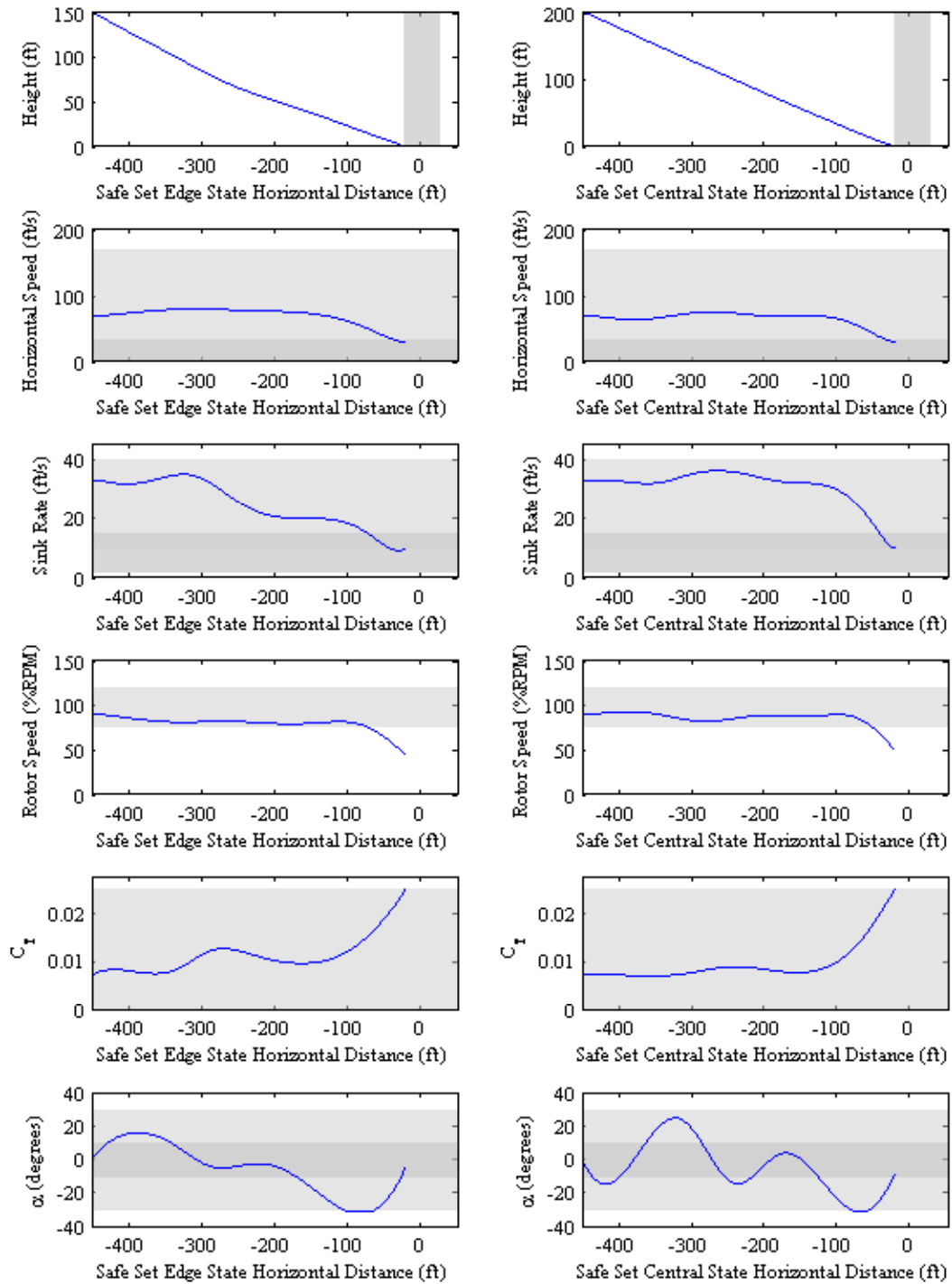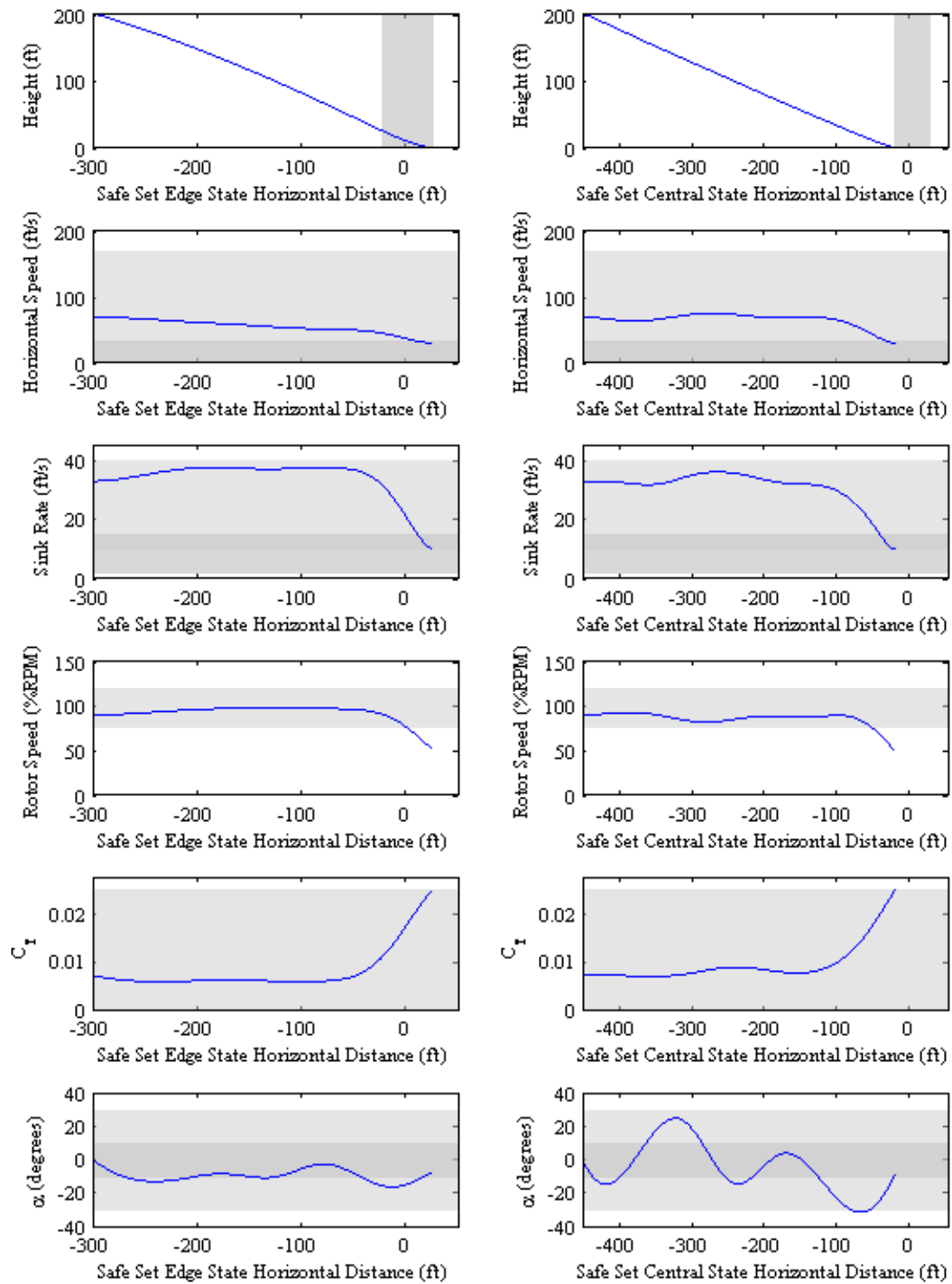
Figure A.1. Comparison to lowered start point: states v. horizontal distance

naturally overshoot the landing zone. w remains near the upper limit throughout the maneuver as the helicopter tries to drop down before overshooting the landing
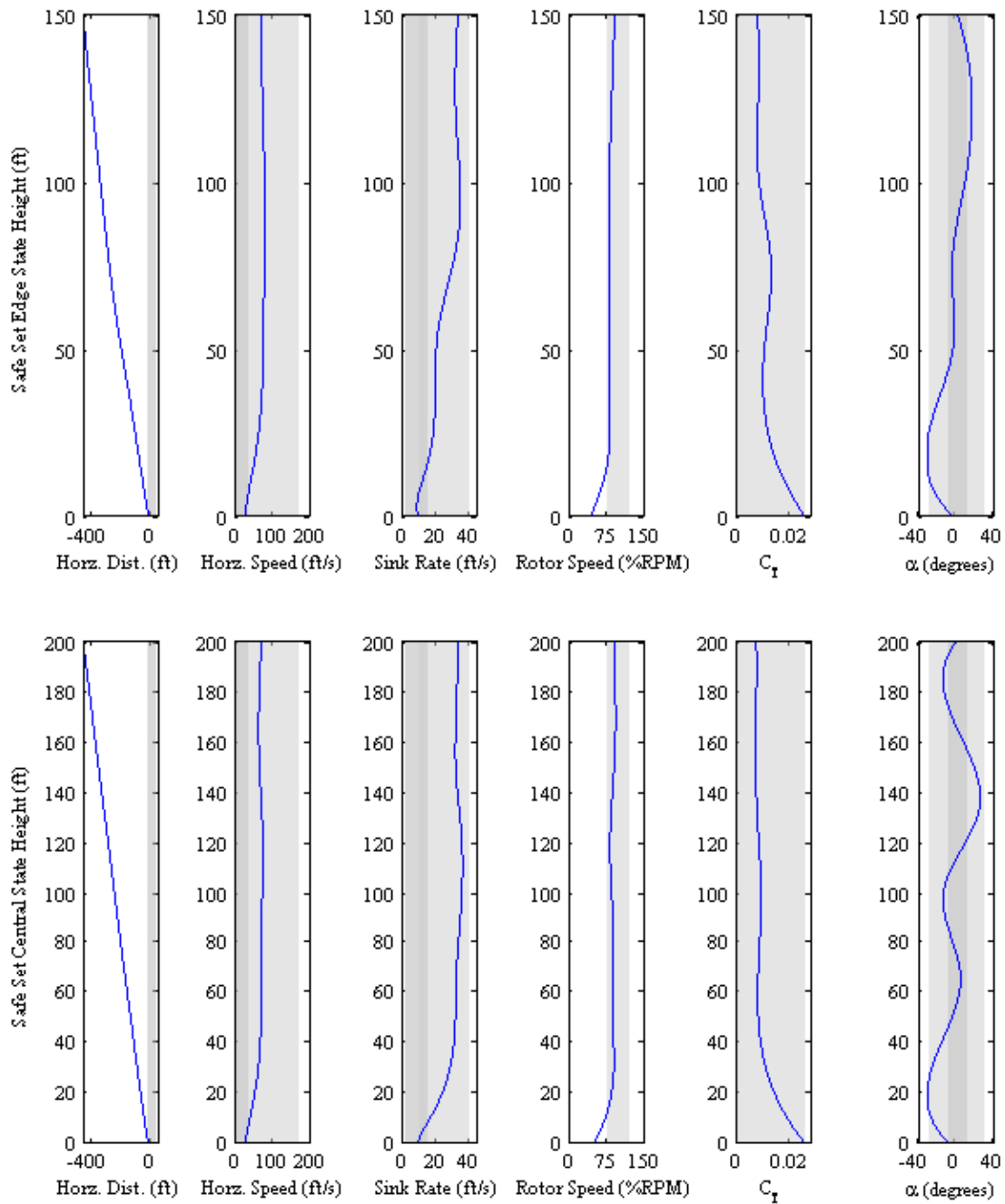
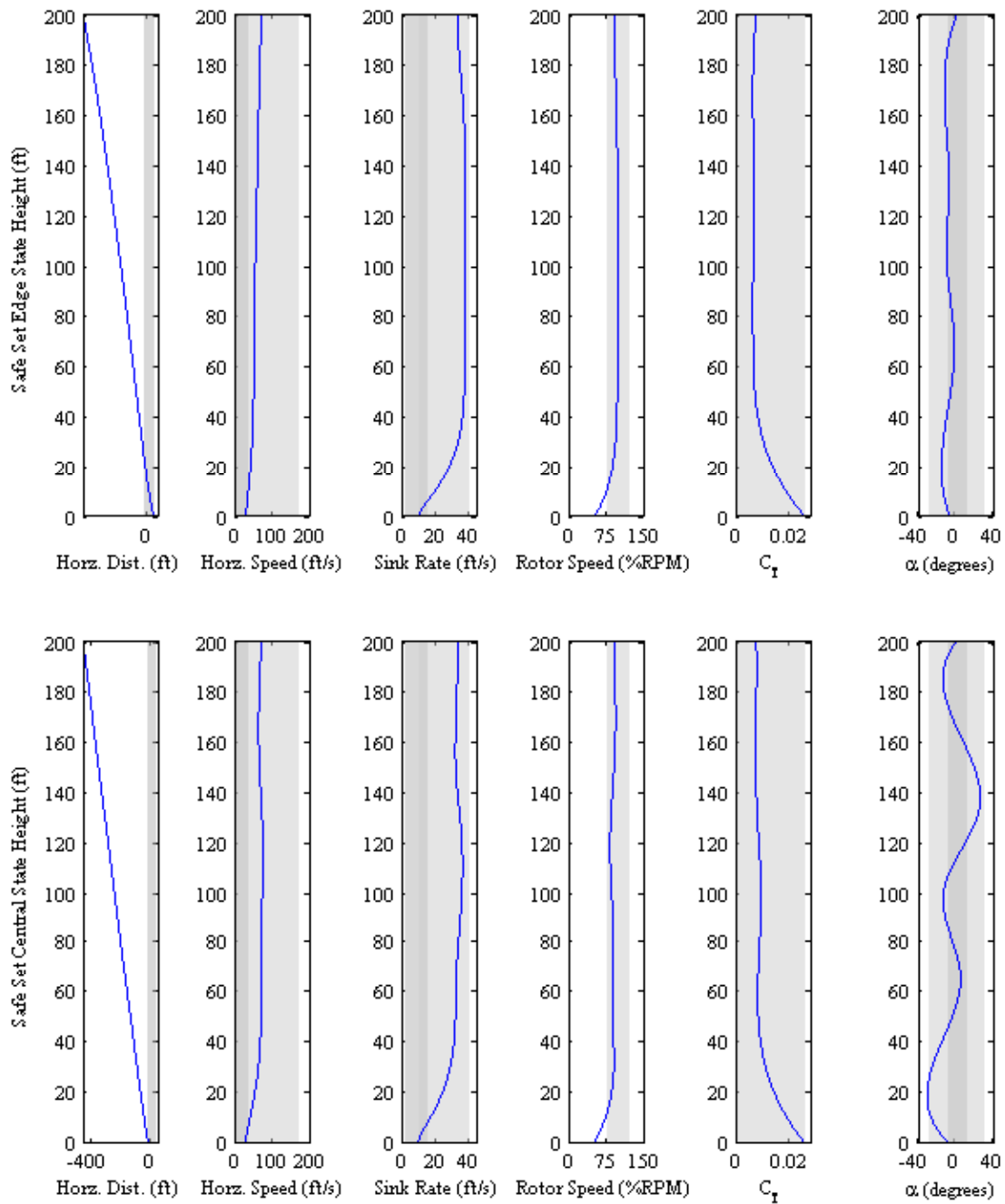**Figure A.2.** Comparison to lowered start point: height v. states

zone. The average value for α is obviously much lower than that for the central point. At a closer point it is likely the helicopter is not able to control w within the necessary bounds to reach the ground. It will either land with too great a vertical

Figure A.3. Comparison to forward start point: states v horizontal distance

velocity or will overshoot the landing zone before it can touch down.

Figure Figure A.5 and Figure A.6: A comparison is shown between the central
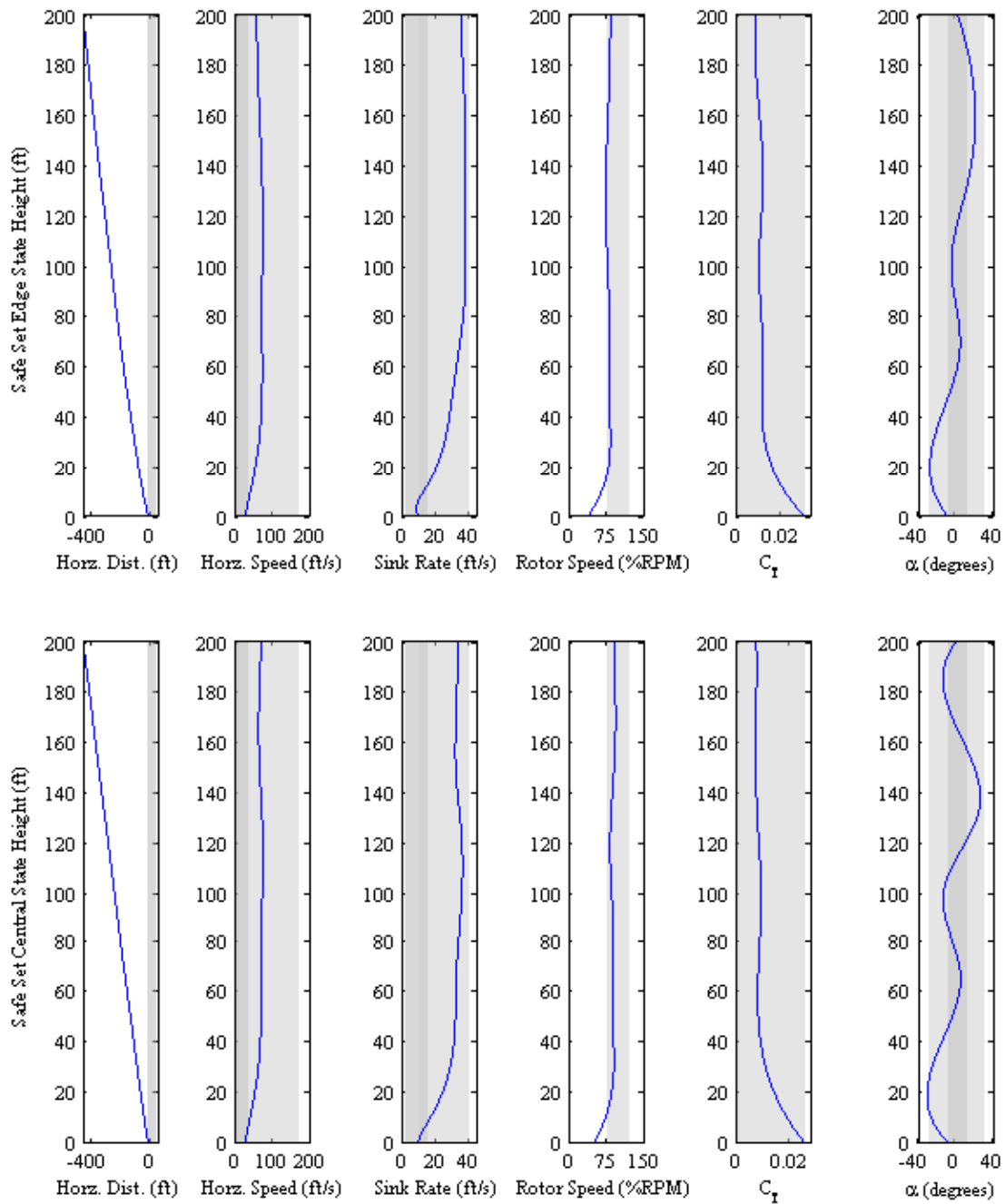
Figure A.4. Comparison to forward start point: height v. states

point in the safe set and a point sharing the flare initiation location but having the slowest velocity for which a safe landing exists at that point. This difference in velocity exists mainly in the initial horizontal velocity. The edge state also has
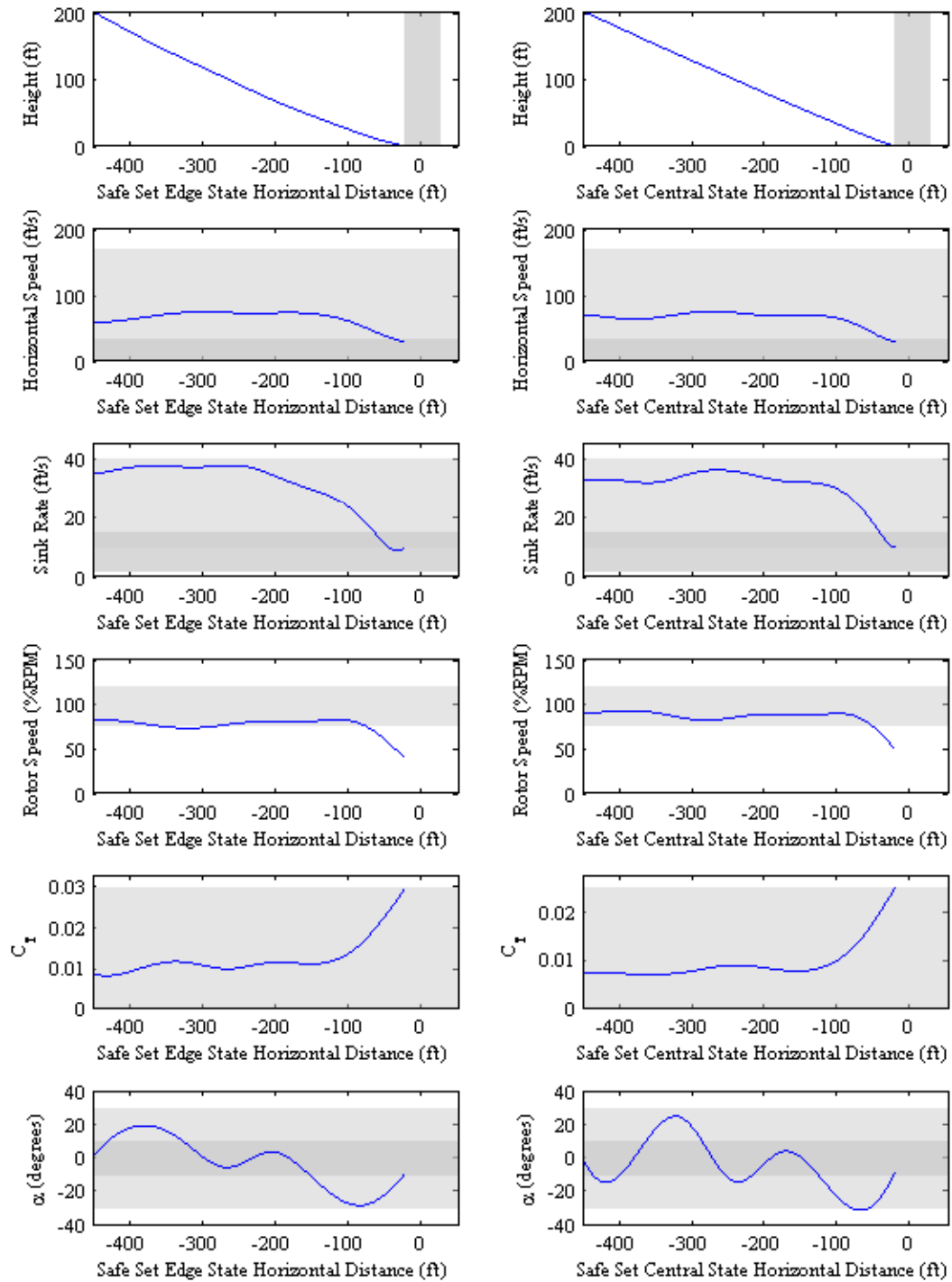
Figure A.5. Comparison to faster start point: states v horizontal distance

a lower beginning Ω. The controls behave as would be expected in this scenario:
the helicopter does not approach the limit on α because it is already moving fairly

Figure A.6. Comparison to faster start point: height v. states

slowly. The sink rate is near or at its maximum for most of the maneuver and the rotor speed is near or at its minimum. Obviously, neither of these is ideal. For slower speeds than the one presented here there is likely not sufficient energy in

the rotor to keep the other states within bounds.

A.2   Unsafe Slight Paths

This section presents more comparisons between points just inside and outside the safe landing set.

Figure A.7 and Figure A.8: The unsafe state here exists slightly closer to the horizontal landing location and matches the safe state in all other aspects. As a consequence w is made to exceed its upper limit in a bid to keep the helicopter from overshooting the landing zone. Another reason w is so large is that the helicopter spends much of the maneuver tilted as far back as is permissible trying to slow itself. Overall, it is just not feasible for this trim condition to reach the ground safely from a location as high and close as the one presented here in the unsafe condition.

Figure A.9 and Figure A.10: The unsafe state, which has a higher initial velocity than the safe state, almost immediately has its descent rate drop below zero. This breaks a fundamental rule of the height based equations of motion and results in a catastrophic failure.

As with an example in Chapter 4 Figure A.11 and Figure A.12 show that applying safe controls from a nearby state can result in improved performance. The unsafe state is still unsafe, but it appears it may be manageable with further analysis.
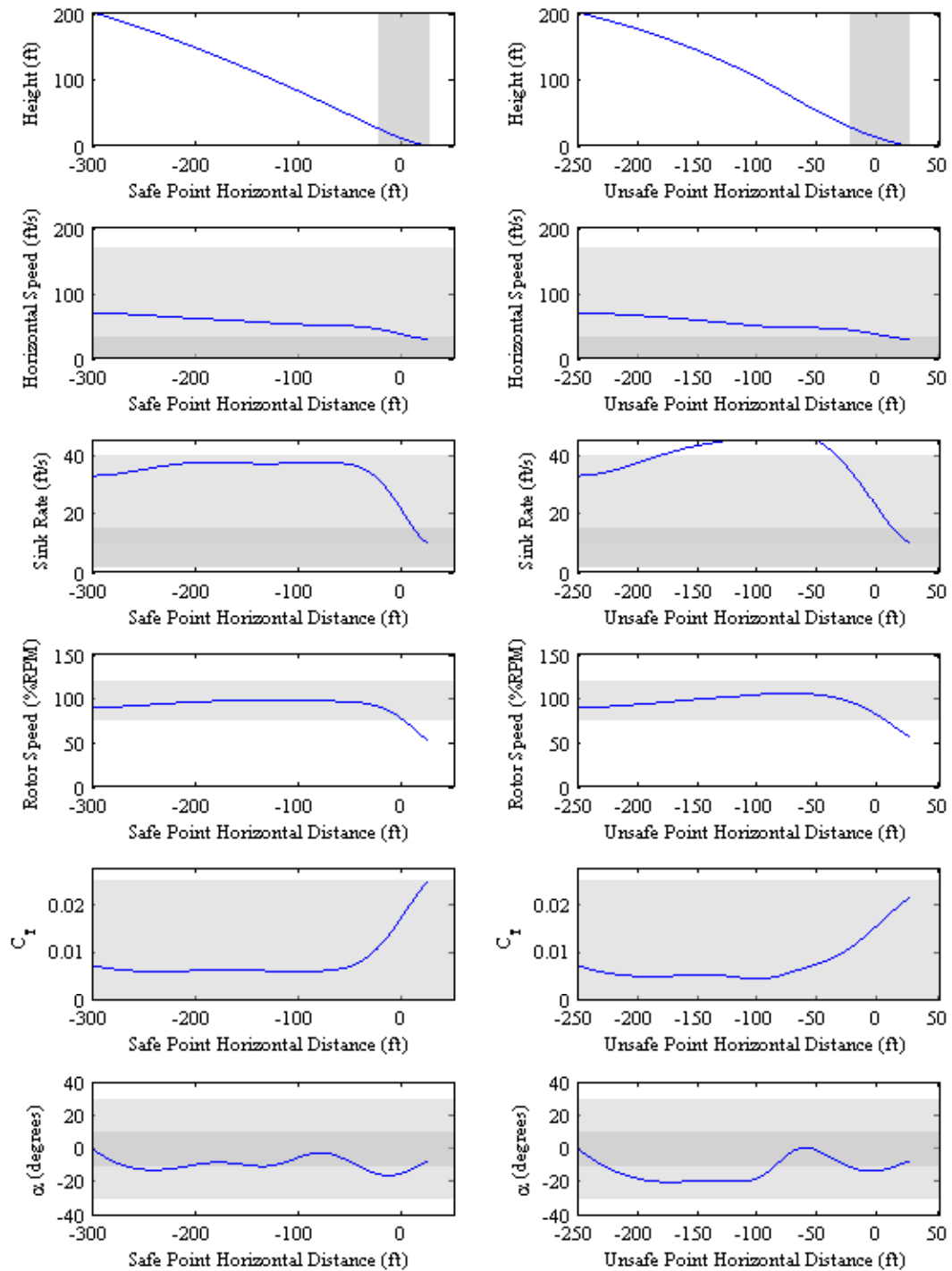
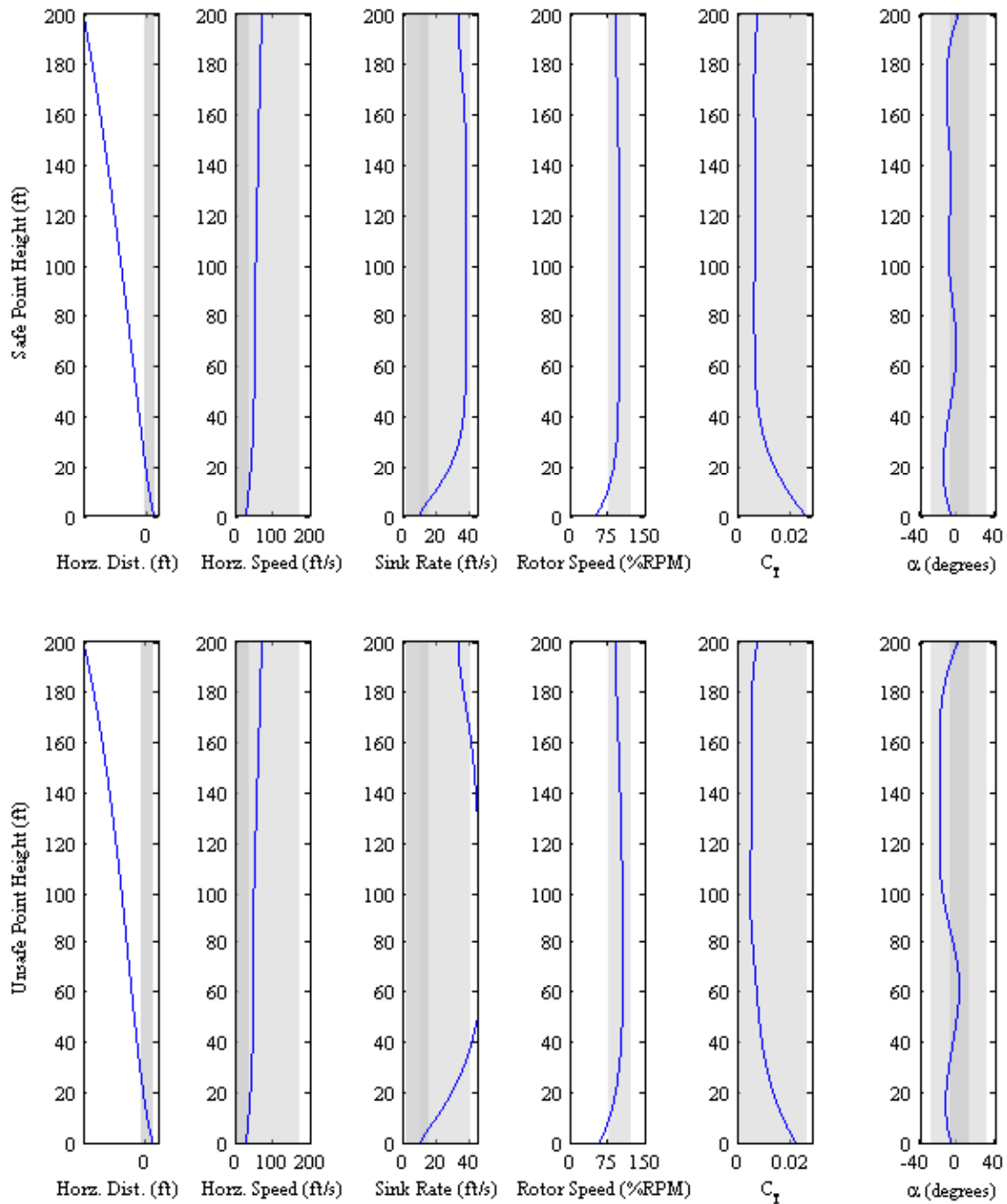**Figure A.7.** Comparison to closer start point: states v horizontal distance

Figure A.8. Comparison to closer start point: height v. states
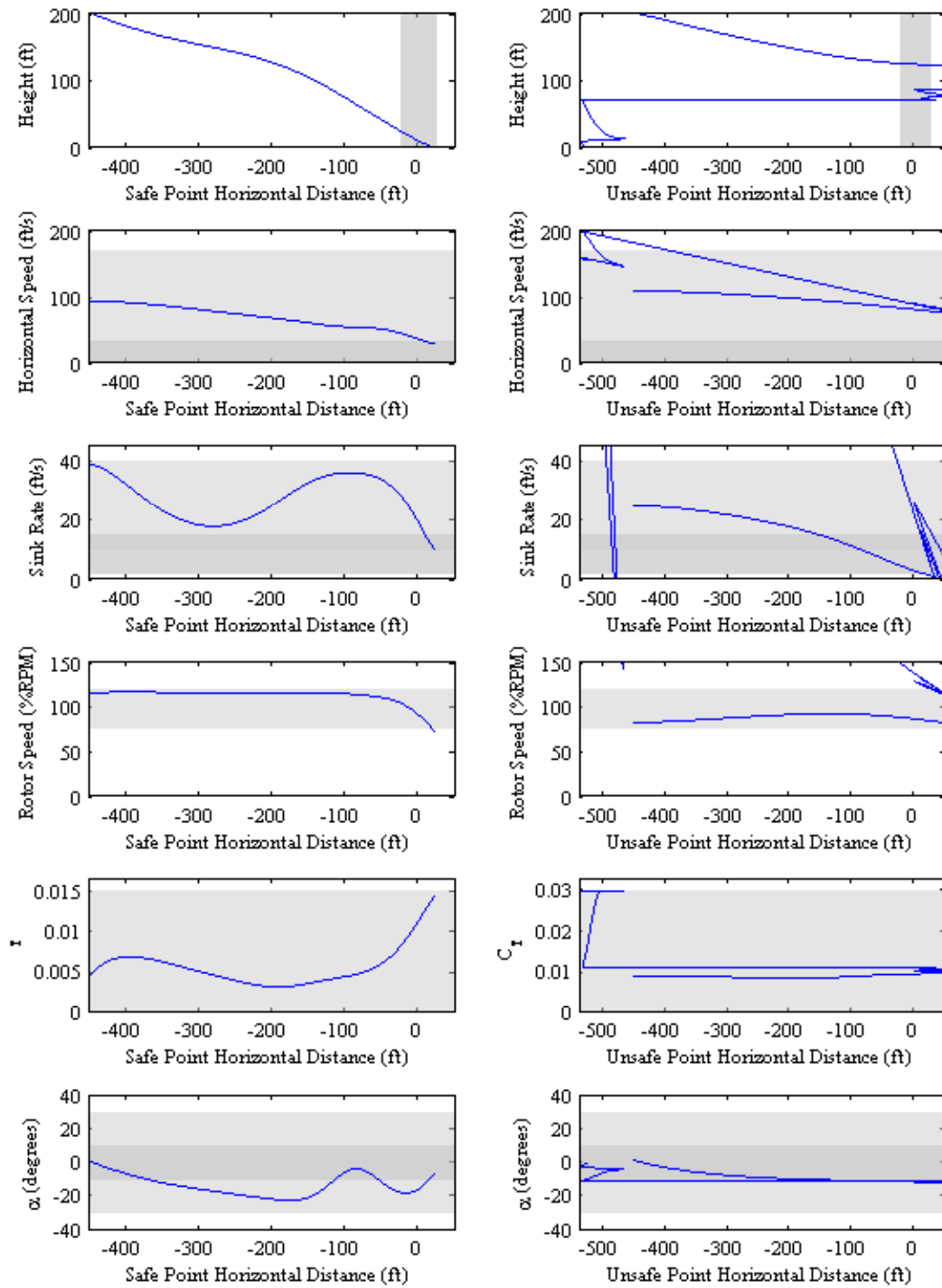
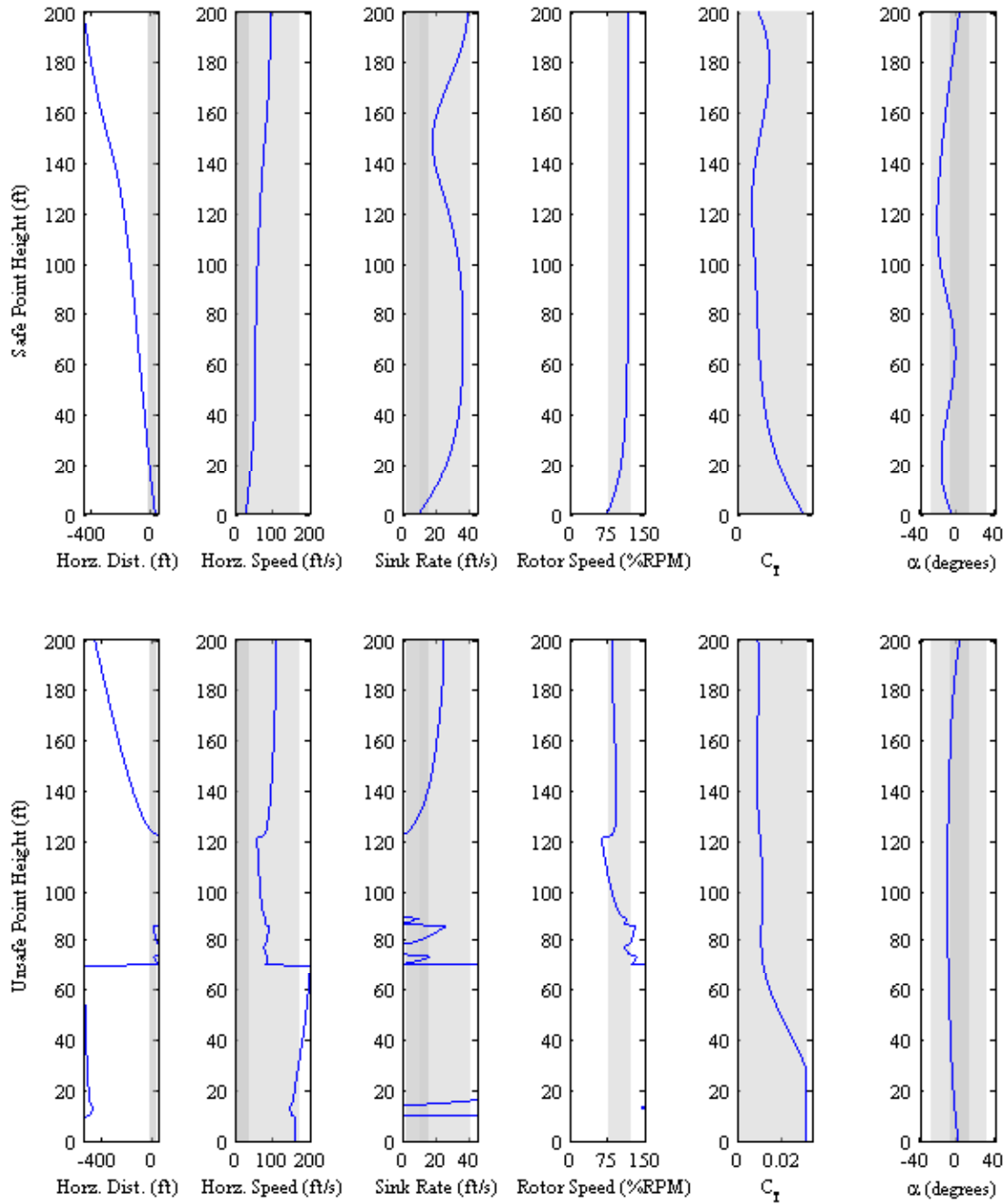**Figure A.9.** Comparison to faster start point: states v horizontal distance

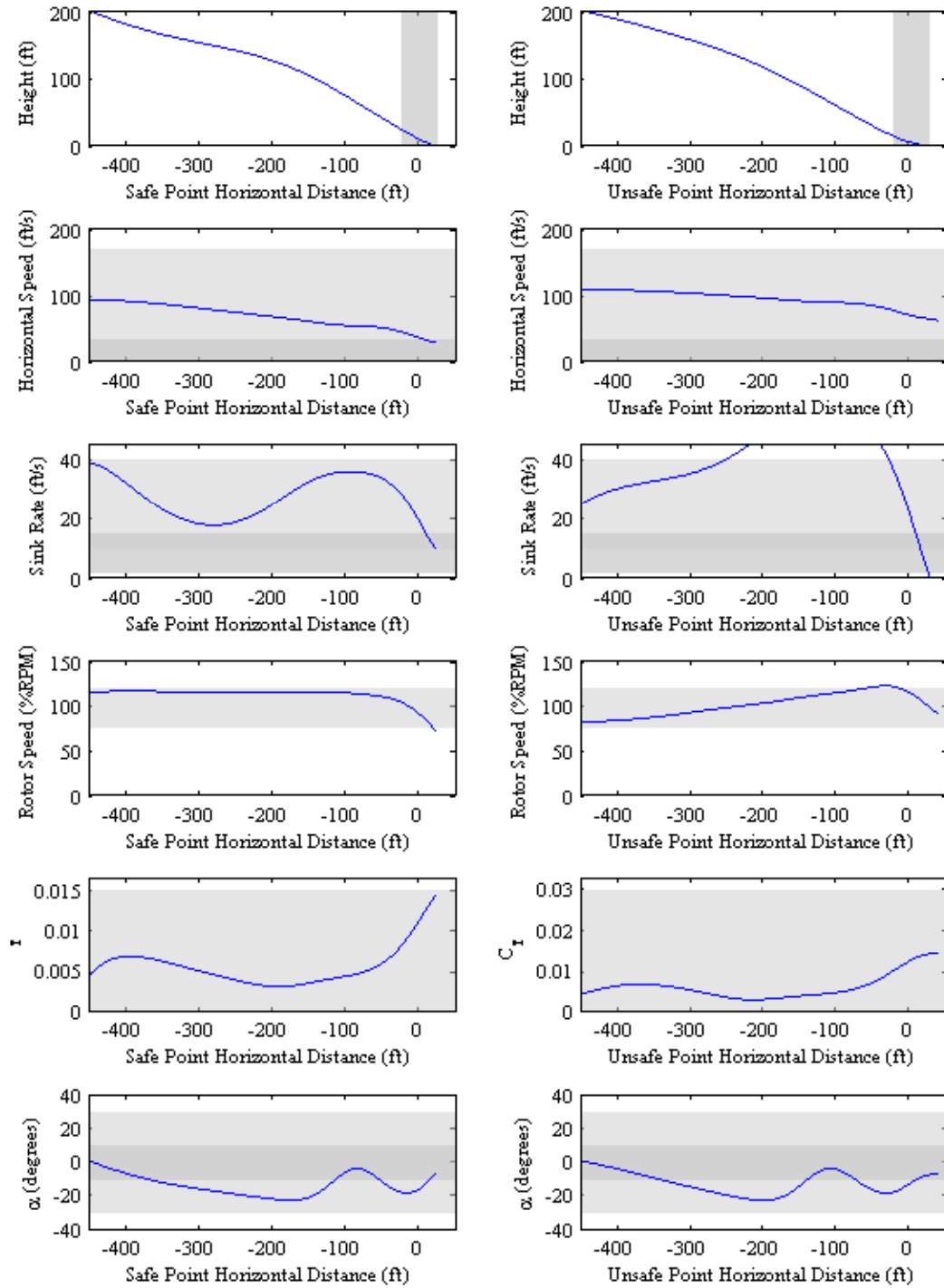**Figure A.10.** Comparison to faster start point: height v. states

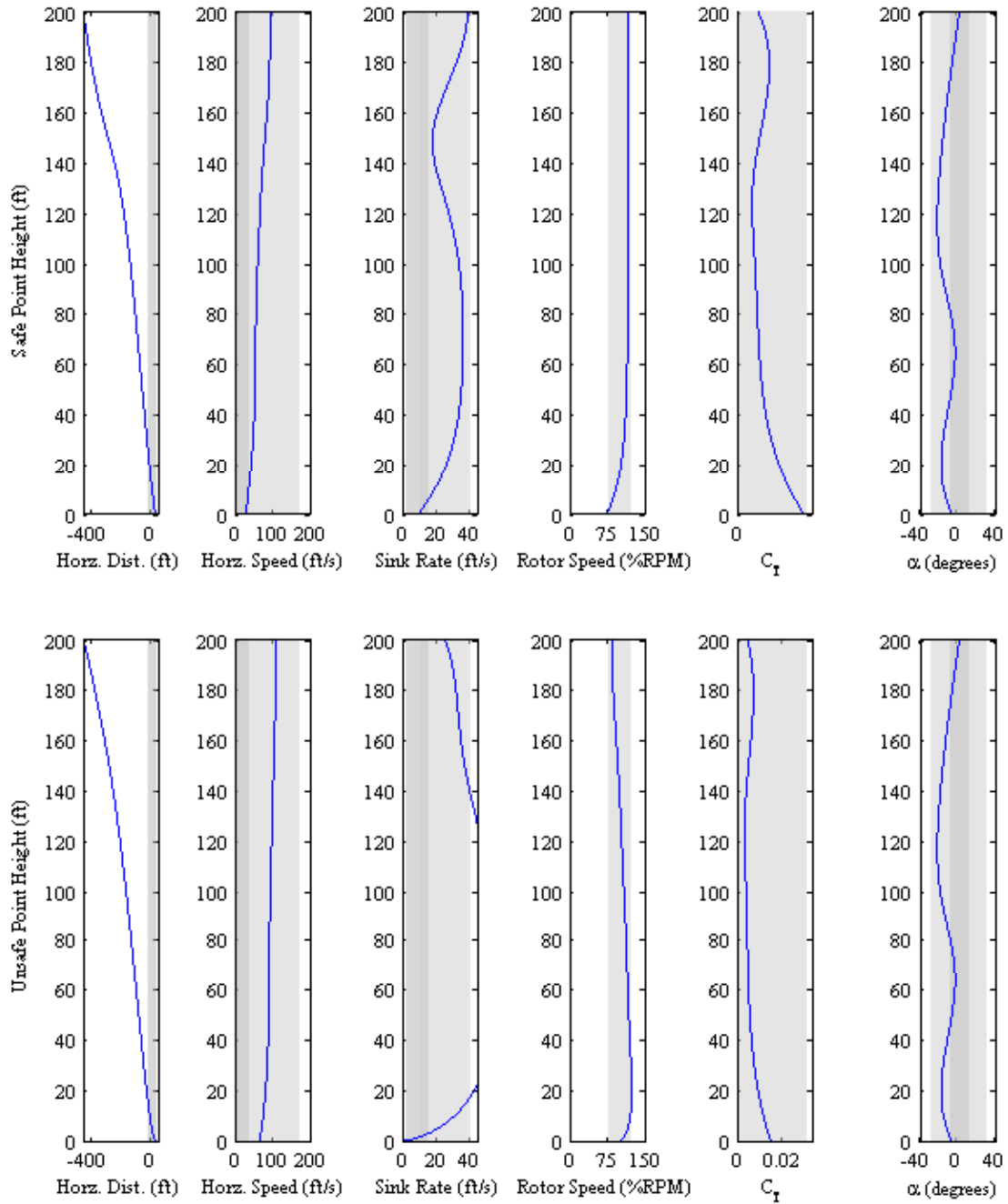**Figure A.11.** Safe controls applied to an unsafe state

Figure A.12. Safe controls applied to an unsafe state

Bibliography

[1] JOHNSON, W. (1977) *Helicopter Optimal Descent and Landing after Power Loss, Technical Memorandum TM 73244*, NASA Ames Research Center, Moffett Field, CA.

[2] APONSO, B. L., P. EDWARD N. BACHELDER, and P. DONGCHAN LEE (2005) "Automated Autorotation for Unmanned Rotorcraft Recovery," in *AHS International Specialistsí Meeting on Unmanned Rotorcraft.*

[3] LEE, A. Y., A. E. BRYSON JR., and W. S. HINDSON (1988) "Optimal Landing of a Helicopter in Autorotation," *Journal of Guidance, Control, and Dynamics*, **11**(1), pp. 7–12.

[4] BOTTASSO, C. L., A. CROCE, D. LEONELLO, and L. RIVIELLO (2008) "Rotorcraft Trajectory Optimization with Realizability Considerations," *Journal of Aerospace Engineering*, **18**(3), pp. 146–155.

[5] APONSO, B., D. LEE, and E. N. BACHELDER (2005) "Evaluation of a Rotorcraft Autorotation Training Display on a Commercial Flight Training Device," in *Proceedings of the American Helicopter Society 61st Annual Forum*, Grapevine, Texas.

[6] BACHELDER, E. N. and B. L. APONSO (2003) "Using Optimal Control for Helicopter Autorotation Training," in *Proceedings of the American Helicopter Society 59th Annual Forum*, Phoenix, AZ.

[7] ABBEEL, P., A. COATES, T. HUNTER, and A. Y. NG (2008) "Autonomous Autorotation of an RC Helicopter," in *International Symposium on Robotics.*

[8] DALAMAGKIDIS, K., K. P. VALAVANIS, and L. A. PIEGL (2009) "Autonomous Autorotation of an Unmanned Rotorcraft using Nonlinear Model Predictive Control," *Journal of Intelligent and Robotic Systems*, **57**(1-4), pp. 351–369.
URL http://www.springerlink.com/content/98w23kj142r481g1/

[9] SPRINKLE, J., J. M. EKLUND, and S. S. SASTRY (2005) "Deciding to Land a UAV Safely in Real Time," in *Americna Controls Conference*.

[10] BAYEN, A. M., I. M. MITCHELL, M. M. K. OISHI, and C. J. TOMLIN (2007) "Aircraft Autolander Safety analysis Through Optimal Control-Based Reach Set Computation," *Journal of Guidance and Control*, **30**(1), pp. 68–77.

[11] FLOROS, M. W. (2009) "DESCENT Analysis for Rotorcraft Survivability with Power Loss," in *American Helicopter society 65th Annual forum*.

[12] (1996) *Operator's Manual for UH-60A Helicopter, UH-60L Helicopter, EH-60A Helicopter, Technical Manual TM 1-1520-237-10*, Department of the Army.